Simulation of Groundwater Flow in the Regional Aquifer System on Long Island, New York, for Pumping and Recharge Conditions in 2005–15

Scientific Investigations Report 2020–5091

U.S. Department of the Interior
U.S. Geological Survey

Simulation of Groundwater Flow in the Regional Aquifer System on Long Island, New York, for Pumping and Recharge Conditions in 2005–15

By Donald A. Walter, John P. Masterson, Jason S. Finkelstein, Jack Monti, Jr., Paul E. Misut, and Michael N. Fienen

Scientific Investigations Report 2020–5091

U.S. Department of the Interior
U.S. Geological Survey

U.S. Department of the Interior
DAVID BERNHARDT, Secretary

U.S. Geological Survey
James F. Reilly II, Director

U.S. Geological Survey, Reston, Virginia: **2020**

Acknowledgments

Contents

Figures

Tables

Conversion Factors

U.S. customary units to International System of Units

Multiply	By	To obtain
Length		
inch (in.)	2.54	centimeter (cm)
foot (ft)	0.3048	meter (m)
mile (mi)	1.609	kilometer (km)
Area		
square mile (mi^2)	2.590	square kilometer (km^2)
Volume		
gallon (gal)	3.785	liter (L)
million gallons (Mgal)	3,785	cubic meter (m^3)
Flow rate		
foot per day (ft/d)	0.3048	meter per day (m/d)
cubic foot per second (ft^3/s)	0.02832	cubic meter per second (m^3/s)
gallon per day (gal/d)	0.003785	cubic meter per day (m^3/d)
million gallons per day (Mgal/d)	0.04381	cubic meter per second (m^3/s)
inch per year (in/yr)	25.4	millimeter per year (mm/yr)
Hydraulic conductivity		
foot per day (ft/d)	0.3048	meter per day (m/d)

Temperature in degrees Celsius (°C) may be converted to degrees Fahrenheit (°F) as
$$°F = (1.8 × °C) + 32.$$

Temperature in degrees Fahrenheit (°F) may be converted to degrees Celsius (°C) as
$$°C = (°F − 32) / 1.8.$$

Datum

Vertical coordinate information is referenced to the North American Vertical Datum of 1988 (NAVD 88).

Horizontal coordinate information is referenced to the North American Datum of 1983 (NAD 83).

Mean sea level, as used in this report, refers to 0 feet relative to the vertical datum.

Altitude, as used in this report, refers to distance above the vertical datum.

Supplementary Information

Concentrations of chemical constituents in water are given in milligrams per liter (mg/L).

Abbreviations

GIS	geographic information system
GWSI	Ground-Water Site Inventory
MSL	mean sea level
NWIS	National Water Information System
SVD	singular-value decomposition
SWB	soil-water balance
USGS	U.S. Geological Survey

Simulation of Groundwater Flow in the Regional Aquifer System on Long Island, New York, for Pumping and Recharge Conditions in 2005–15

By Donald A. Walter, John P. Masterson, Jason S. Finkelstein, Jack Monti, Jr., Paul E. Misut, and Michael N. Fienen

Abstract

A three-dimensional groundwater-flow model was developed for the aquifer system of Long Island, New York, to evaluate (1) responses of the hydrologic system to changes in natural and anthropogenic hydraulic stresses, (2) the subsurface distribution of groundwater age, and (3) the regional-scale distribution of groundwater travel times and the source of water to fresh surface waters and coastal receiving waters. The model also provides the groundwater flow components used to define model boundaries for possible inset models used for local-scale analyses.

The three-dimensional, groundwater flow model developed for this investigation uses the numerical code MODFLOW–NWT to represent steady-state conditions for average groundwater pumping and aquifer recharge for 2005–15. The particle-tracking algorithm MODPATH, which simulates advective transport in the aquifer, was used to estimate groundwater age, delineate the areas at the water table that contribute recharge to coastal and freshwater bodies, and estimate total travel times of water from the water table to discharge locations.

A three-dimensional, 1-meter (3.3-foot) topobathymetric model was used to determine land-surface altitudes for the island and seabed altitudes for the surrounding coastal waters. The mapped extents and surface altitudes of major geologic units were compiled and used to develop a three-dimensional hydrogeologic framework of the aquifer system, including aquifers and confining units. Lithologic data from deep boreholes and previous aquifer-test results were used to estimate the three-dimensional distribution of hydraulic conductivity in principal aquifers. Natural recharge from precipitation was estimated for 2005–15 using a modified Thornthwaite-Mather methodology as implemented in a soil-water balance model. Components of anthropogenic recharge—wastewater return flow, storm water inflow, and inflow from leaky infrastructure—also were estimated for 2005–15. Groundwater withdrawals for various sources, including public water supply, industrial, remediation, and agricultural, were compiled or estimated for the same period.

These data were incorporated into the model development to represent the aquifer system geometry, boundaries, and initial hydraulic properties of the regional aquifers and confining units within the Long Island aquifer system. Average hydraulic conditions—water levels and streamflows—for 2005–15 were estimated using existing data from the U.S. Geological Survey National Water Information System database. Model inputs were adjusted to best match average hydrologic conditions using inverse methods as implemented in the parameter-estimating software PEST. The calibrated model was used to simulate average hydrologic conditions in the aquifer system for 2005–15.

About 656 cubic feet per second of water was withdrawn on average annually for 2005–15 for water supply and an average of about 349 cubic feet per second of water recharged the aquifer annually from return flow and leaky infrastructure. Parts of New York City have drawdowns exceeding 25 feet, mostly because of urbanization and associated large decreases in recharge rates. Large areas in the western part of the island have drawdowns exceeding 10 feet, mostly from large groundwater withdrawals and sewering, which largely eliminates wastewater return flow. Water-table altitudes in eastern parts of the island increased by more than 2 feet in some areas as a result of wastewater return flow in unsewered areas and changes in land use. Changes in streamflows show a similar pattern as water-table altitudes. Streamflows generally decrease in western parts of the island where there are large drawdowns and increase in eastern parts of the island where water-table altitudes increase.

Introduction

Long Island, in southeastern New York, extends eastward from Manhattan and Staten Islands and is bordered by bays and narrows to the east and west, the Atlantic Ocean to the south, and Long Island Sound to the north (fig. 1). The island is about 120 miles (mi) long, 25 mi wide at its widest point, and about 1,400 square miles (mi²) in total area. The island is densely populated and had an estimated population of
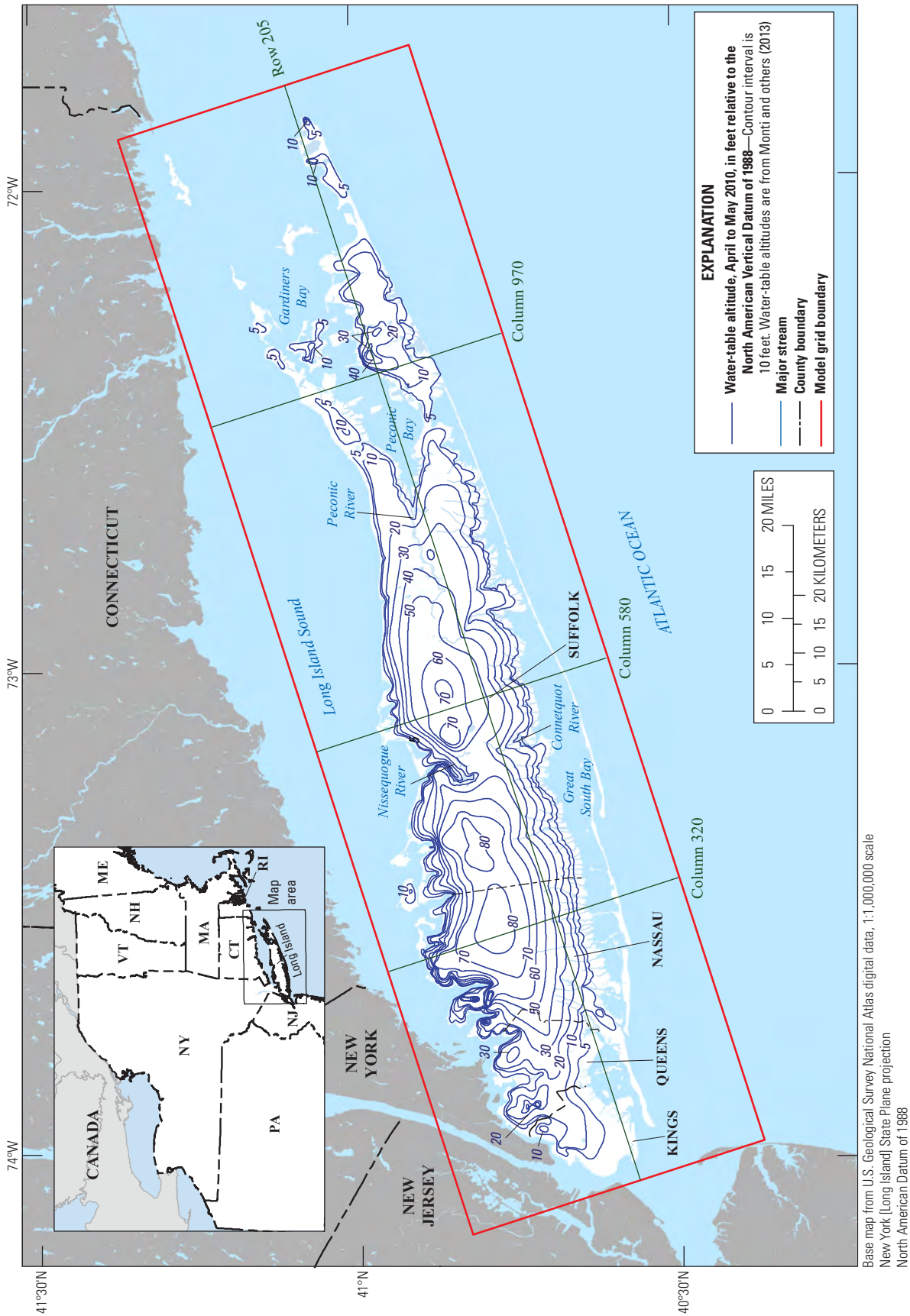
Figure 1.   Map showing the location and hydrography of Long Island and water-table altitudes in April-May 2010 on Long Island, New York. ft, foot; MSL, mean sea level; NAVD 88, North American Vertical Datum of 1988.

about 7.9 million people in 2017 (U.S. Census Bureau, 2018). Most—about 5 million people—reside in Queens and Kings Counties, which are part of the New York City metropolitan area. The remaining population resides to the east, in Nassau and Suffolk Counties. Land use generally changes from west to east from urbanized to rural, with densely urbanized landscapes in New York City and areas of undeveloped and agricultural land in eastern Suffolk County.

Unconsolidated sediments underlying the island comprise a sole-source aquifer that supplies water to about 2.9 million people in Nassau and Suffolk Counties; the aquifer also contributes groundwater discharge to freshwater and marine ecosystems that are important recreational and economic resources. Anthropogenic activities have affected both the quantity and quality of groundwater, owing to the island's large population and the generally unconfined conditions prevalent across the aquifer system. For instance, groundwater withdrawals, particularly in the western part of the island, have resulted in large declines in water-table altitude and in the landward movement of the freshwater/saltwater interface, encroaching on local water supplies (Terraciano, 1996). Additionally, subsurface contamination emanating from numerous point sources, associated with industrial sites in developed areas in western Long Island, adversely affects downgradient water supplies (Misut and others, 2020).

Nutrients emanating from nonpoint sources associated with residential development and agricultural activities also have degraded water quality in shallow parts of the aquifer. Nitrogen entrained in groundwater discharge has caused eutrophication and degradation of aquatic ecosystems in coastal waters across the island, resulting in marine-habitat degradation, harmful algal blooms, and the loss of shell fisheries.

In 2016, the U.S. Geological Survey (USGS) began development of a regional-scale numerical model of the Long Island aquifer system, as part of the National Water Quality Program to assess the vulnerability of the area's water supply to contamination from anthropogenic and natural compounds. The regional model of Long Island is a synthesis of a diverse set of data on the physiography, geology, and hydrology of the island and represents the first public domain regional model of the island since the late 1980s (Buxton and Smolensky, 1999).

The model represents steady-state (average) conditions for 2005–15 and is suitable for simulation, at a regional scale, of current hydrologic conditions, including water levels and groundwater discharge to receiving waters. The model also can be used to estimate regional-scale groundwater travel times to wells and ecological receptors and subsurface groundwater ages. The model is most suitable for analyses at the regional scale but can be used to produce boundary conditions as input into inset models more suitable for local-scale analyses.

Purpose and Scope

This report documents the development and calibration of a numerical model of the Long Island aquifer system and the use of that model to simulate hydrologic conditions for 2005–15. The report discusses the compilation and analysis of climatic, physiographic, geologic, hydrologic, and water-use data used to develop the numerical model. The use of a 1-meter (m; 3.3-foot [ft]) topobathymetric digital elevation model to estimate land-surface and seabed altitudes at the modeled scale is presented, and the incorporation of the data into representations of regional fresh and saline surface-water features are documented. The extents of surface altitudes of mapped hydrogeologic units from various sources are documented, and the methods used to develop a three-dimensional hydrogeologic framework are discussed. The three-dimensional distribution of water-transmitting properties, as represented in a grid-independent texture model, and the methods used to incorporate that data into the model are presented.

The use of a soil-water balance (SWB) model (Westenbroek and others, 2010) to estimate average recharge for 2005–15 from daily climate and spatial data—land-use, soil type, and soil-water capacity—is documented. The methods and assumptions used to estimate additional, anthropogenic components of recharge, including wastewater-return flow, recharge from urban runoff, and inflow from leaky infrastructure also are discussed. Groundwater withdrawals are presented for 2005–15 for various uses, including public supply, industrial, and remedial activities. The report also documents the hydrologic conditions in the aquifer, as indicated by observations of water levels in wells and streamflows, for 2005–15.

The model design is described in detail, including horizontal and vertical model discretization, the location and types of simulated hydrologic boundaries, the distribution of simulated recharge and the location of simulated wells. The initial values of hydraulic parameters—boundary leakances and horizontal and vertical hydraulic conductivity—are presented and the assumptions underlying them are discussed. The use of inverse-calibration methods to adjust these initial values to best match water levels and streamflows for 2005–15 also is discussed along with the parameterization of the model, the inverse techniques and assumptions used, and the fit between hydrologic observations and their simulated equivalents.

The report presents simulated hydrologic conditions of the Long Island aquifer system for 2005–15, as simulated by the calibrated model, and for hydrologic conditions approximating natural unstressed (predevelopment) conditions. A summary of the hydrologic budget, including both inflows and outflows, is discussed. Current (average) water-table altitudes and streamflows are presented as well as a summary of travel times—defined as the elapsed time of the movement of water from the water table to wells and ecological receptors. Limitations associated with the use of a numerical model to represent the aquifer system are discussed, including general limitations in the application of the numerical model and limitations specific to the regional model of Long Island.

Hydrogeologic Setting

Land-surface altitudes in Long Island range from more than 300 feet (ft) above mean sea level (MSL) relative to the North American Vertical Datum of 1988 (NAVD 88) in some areas underlain by glacial moraine to essentially sea level at the coast. The hummocky terrain associated with glacial moraines is bounded to the south by gently sloping outwash plains (fig. 2). The Long Island aquifer system comprises unconsolidated sediments that are underlain by relatively impermeable crystalline bedrock. The altitude of the bedrock surface ranges from about 2,000 ft below MSL (NAVD 88) beneath Fire Island, a barrier island along the south-central part of the island, to near sea level along the East River in northwestern Queens County, where there are small areas of bedrock outcrops (fig. 3). The overlying sediments of Late Cretaceous age (prior to about 66 million years before present) are part of the Northern Atlantic Coastal Plain regional aquifer system (Masterson and others, 2016) and are, in turn, generally overlain by Pleistocene glacial sediments deposited largely during the Wisconsin glaciation, when periods of ice advance and retreat formed morainal ridges that trend east-west along the spine of Long Island and associated outwash plains, generally to the south (Cadwell and Muller, 1986; Fuller, 1914). Pleistocene clays underlie the Wisconsin glacial sediments and overlie Cretaceous sediments along the northern and southern shores of the island.

Long Island is bifurcated at the eastern end where two morainal ridges diverge to form the North and South Forks. The glacial moraines are bounded to the south by glacial outwash deposits and, generally, to the north by ice-contact deposits. The Pleistocene—glacial and preglacial—sediments and the underlying Cretaceous units compose a series of aquifers and confining units that are as thick as 2,000 ft on the southeastern-dipping bedrock surface. The Cretaceous sediments are absent in some areas near the northern shore of the island (fig. 3); Wisconsin glacial sediments in these areas are either underlain by bedrock or by older (pre-Wisconsin) Pleistocene glacial sediments.

The seven major hydrogeologic units (fig. 4; table 1; Smolensky and others, 1989), in descending order, are the upper glacial aquifer (upper Pleistocene deposits), the Gardiners Clay (Gardiners Clay), the Jameco aquifer (Jameco Gravel), Monmouth greensand (Monmouth Group), the Magothy aquifer (Magothy Formation and Matawan Group, undifferentiated), the Raritan confining unit (clay member of the Raritan Formation), and the Lloyd aquifer (Lloyd Sand Member of the Raritan Formation). In addition to these major units, other Pleistocene units—the North Shore aquifer and North Shore confining unit—underlie Wisconsin glacial sediments in some areas where Cretaceous units are absent (Stumm, 2001), and local confining units occur within the upper glacial aquifer (Doriski and Wilde-Katz, 1982; Krulikas and Koszalka, 1982; Schubert and others, 2004).

Recharge from precipitation is the sole source of natural water to the aquifer system. Long Island received an average of about 48 inches per year (in/yr) from 1900 to 2015;

on average about half (23 in/yr) recharges the aquifer at the water table. Groundwater flows away from regional groundwater divides towards discharge in streams, coastal waters, and wells; some deep groundwater discharges upward through confining units into salty groundwater, referred to as subsea discharge (fig. 4). Water-table altitudes exceed 60 ft in two areas, to the east and west of major surface-water drainages in the central part of the island (fig. 1). Water-table altitudes are also high locally in parts of New York City, on necks and peninsulas in northern Nassau County, and on the North and South Forks in eastern Suffolk County.

The major aquifers are extensive, unconsolidated formations that yield large quantities of water to wells. The most permeable units within this multilayered aquifer system consist predominantly of either sand or sand and gravel. The two extensive clayey formations (the Gardiners Clay and Raritan confining units) have been estimated to have a vertical hydraulic conductivity several orders of magnitude lower than that of the aquifers and strongly influence groundwater flow between the adjacent aquifers (Franke and Cohen, 1972). Where present, the two formations separate the groundwater flow system into three major aquifer units: the Lloyd, the Jameco-Magothy, and the upper glacial aquifers (fig. 4). The Gardiners Clay restricts vertical flow between the upper glacial aquifer and the Jameco and Magothy aquifers, predominately along the southern shore of the island; the Raritan confining unit restricts vertical flow between the Jameco and Magothy aquifers and the Lloyd aquifer in most areas of the island. The crystalline bedrock underlying the unconsolidated deposits is much less permeable than the overlying deposits, and the bedrock surface is considered the lower extent of the aquifer system.

This multilayered aquifer system is known for abundant water resources and the groundwater-fed surface waters that harbor unique ecosystems. Surface runoff is negligible and most precipitation recharges the aquifer at the water table. Precipitation-derived groundwater is essentially the sole source of drinking water for the residents of Nassau and Suffolk Counties and is the primary source of freshwater discharge to the numerous kettle-hole ponds, streams, and wetlands throughout the region (fig. 1). Groundwater discharge also helps to maintain the biological diversity and productivity of estuaries and salt marshes. Rapid population growth, however, has resulted in increased competition among agricultural, commercial, ecological, and residential demands for water resources. As land development and water demand increase and as wastewater continues to be returned to these coastal aquifer systems through onsite, domestic septic systems and decentralized wastewater treatment facilities, water resources managers are becoming concerned about possible long-term effects of these activities on the water resources of the region. Possible effects include the (1) depletion of streamflow and the drying of headwaters, (2) lowering of surface-water levels in ponds and wetlands, (3) decrease in freshwater flow to coastal waters, (4) increase in the risk for saltwater intrusion, and (5) degradation of water quality owing to upland disposal of wastewater.

Base map from U.S. Geological Survey National Atlas digital data, scale 1:1,000,000
New York [Long Island], State Plane projection
North American Datum of 1988
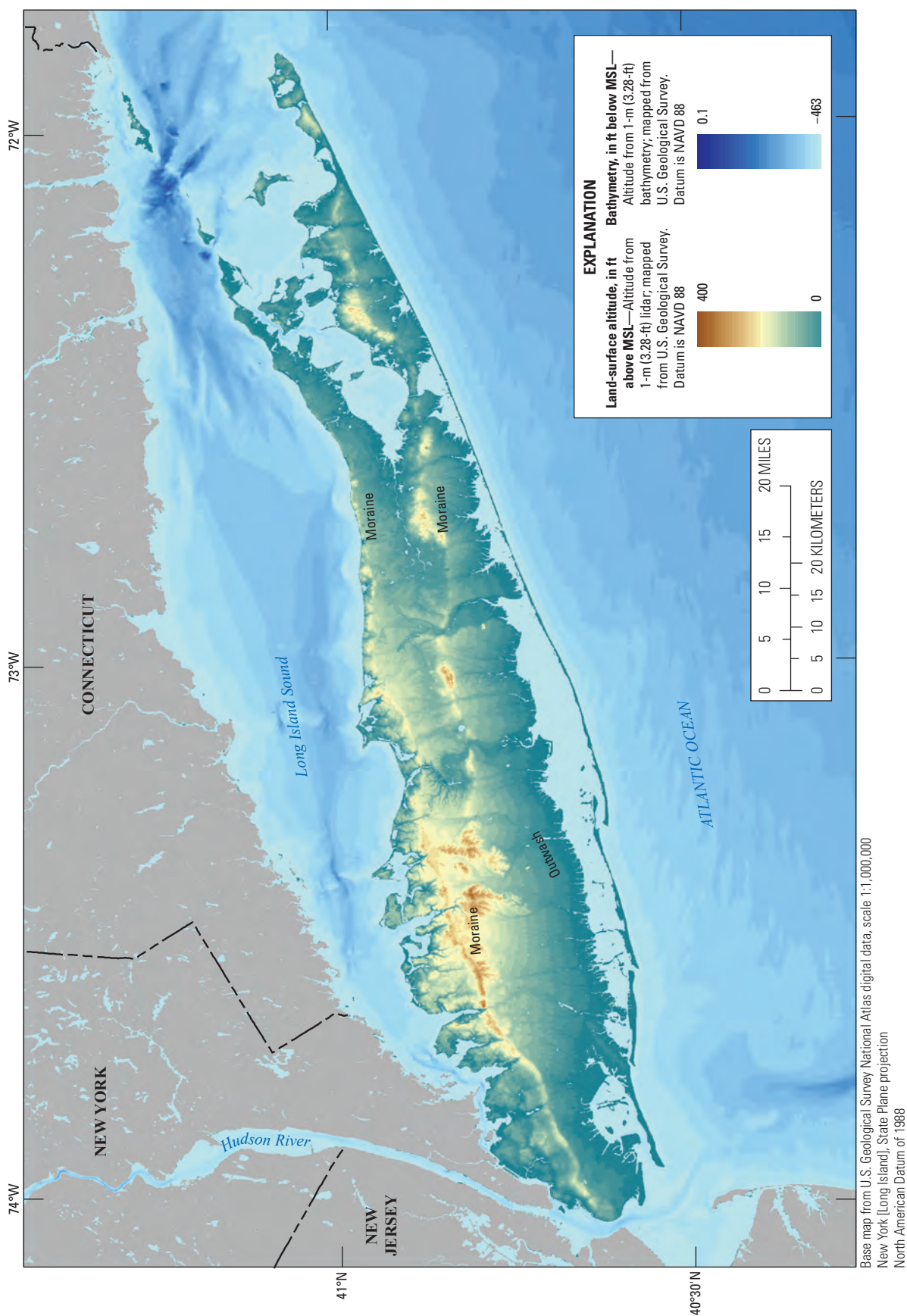
Figure 2.   Map showing land-surface and bathymetry on Long Island, New York. m, meter; ft, foot; MSL, mean sea level; NAVD 88, North American Vertical Datum of 1988.
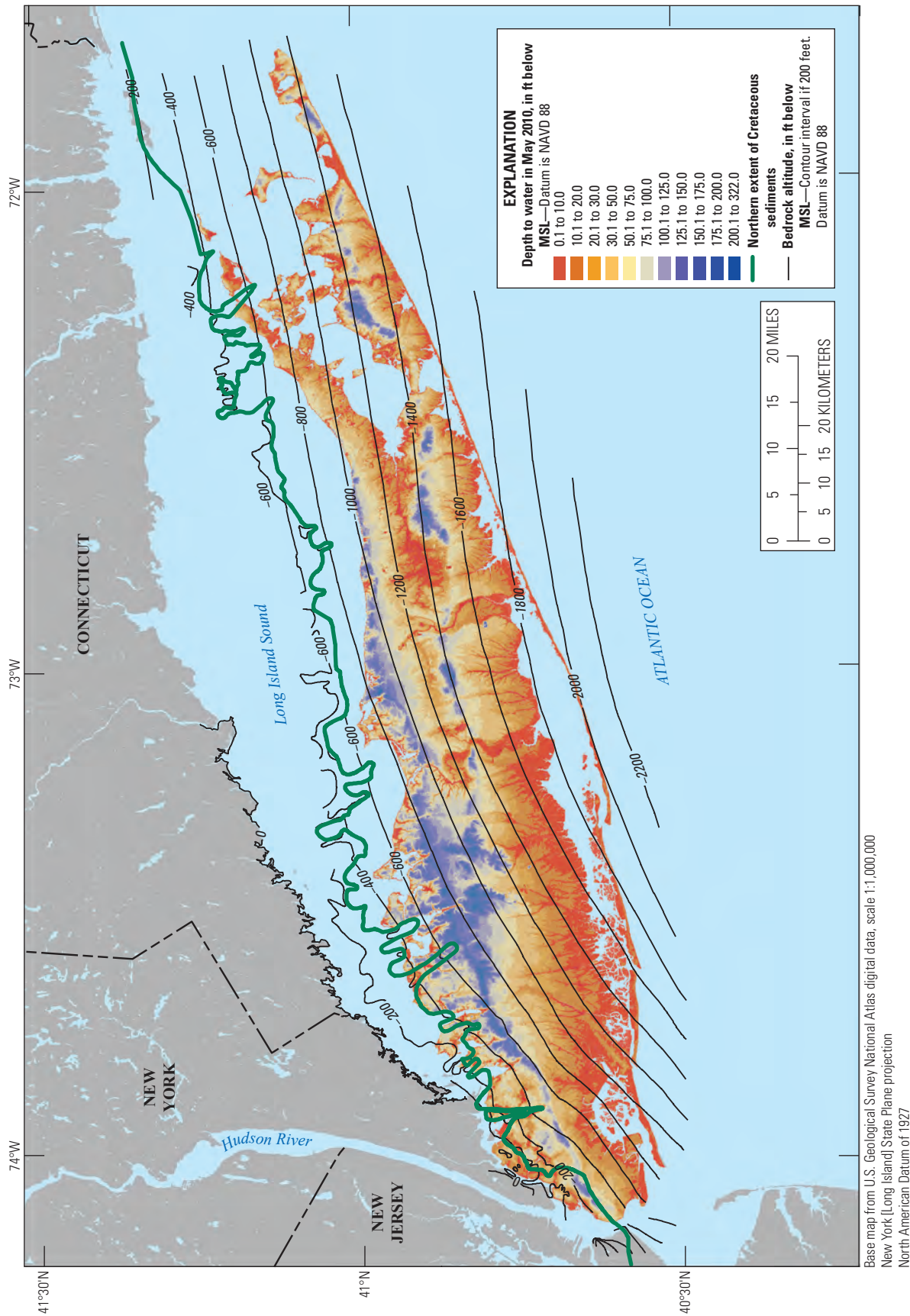
Figure 3.   Map showing the extent of Cretaceous sediments, altitude of bedrock surface, and depth to water on Long Island, New York, in 2010. ft, foot; MSL, mean sea level; NAVD 88, North American Vertical Datum of 1988.
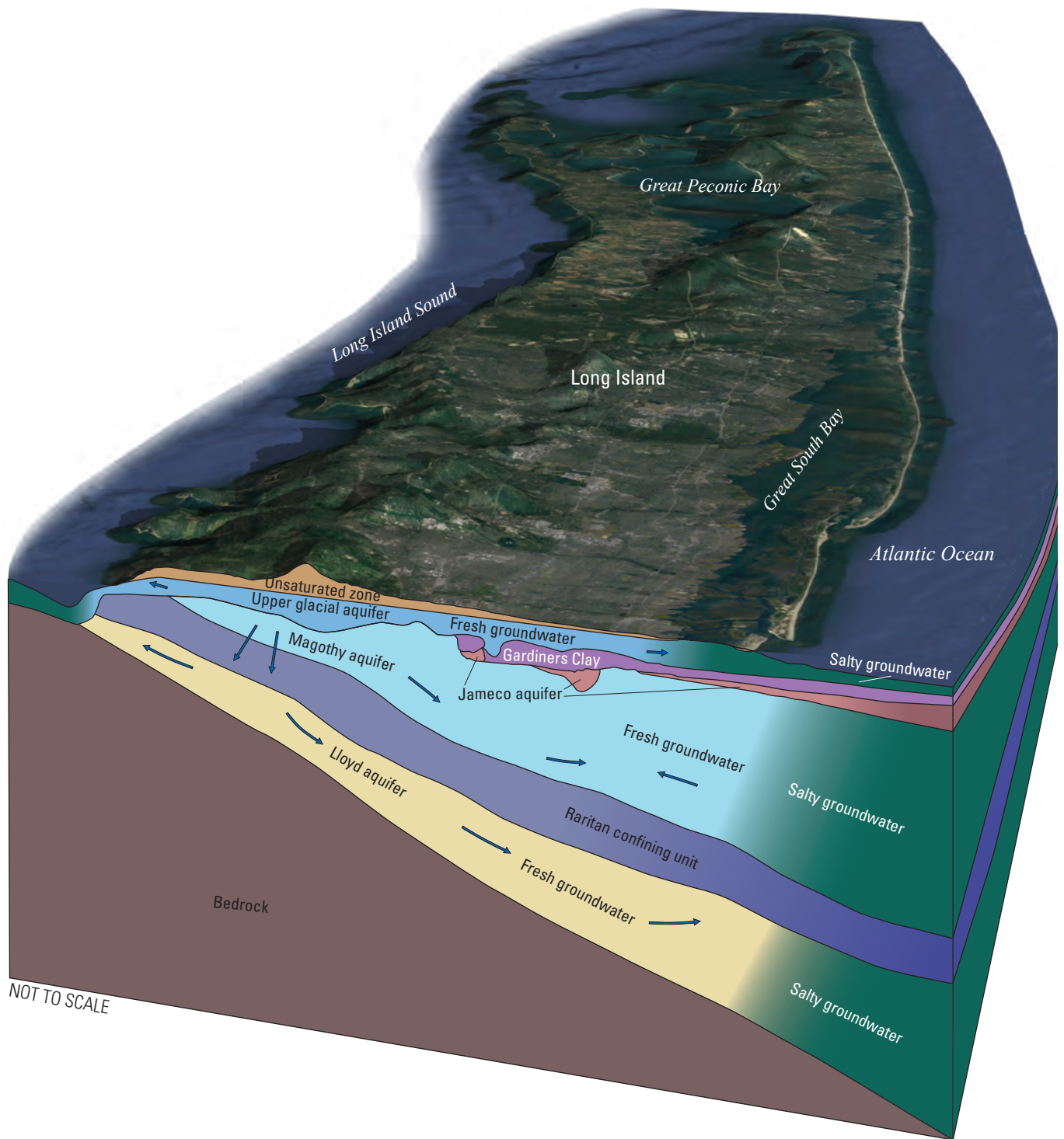
Figure 4.   Three dimensional schematic diagram showing the major hydrogeologic units, generalized groundwater flow directions (arrows), and general position of the freshwater/saltwater interface on Long Island, New York.

Table 1.   Stratigraphy of major hydrogeologic units in the Long Island aquifer system, New York.

[Modified from Smolensky and others (1989, sheet 1)]

Age	Hydrogeologic unit		Description
Pleistocene	Upper glacial aquifer	Ice-contact	Clay, silt, sand, gravel, and boulders associated with ice-marginal deposition. Includes crudely to well-sorted and stratified glaciofluvial deposits.
		Moraine	Clay, silt, sand, gravel, and boulders. Associated with terminal moraines. Deposits are commonly unsorted and unstratified.
		Smithtown clay and 20-foot clay	Local units of lacustrine or marine clay and silt. Lacustrine deposits consist of brown clay and silt and occur in inland areas. Marine deposits consist of gray-green clay and silt at shallow depths in shoreline areas.
		Outwash	Stratified fine- to coarse-grained sand and gravel associated with glaciofluvial deposition. Deposits are well sorted. Silt lenses occur in some areas.
	North Fork clay		Marine and lacustrine deposits. Clay and silt deposits with minor lenses containing shells. The clay is olive brown and olive gray and poorly permeable.
	North Shore confining unit		Marine and proglacial lake deposits. Clay and silt deposits with minor lenses containing shells. The clay is olive brown and olive gray and poorly permeable.
	North Shore aquifer [unconformity]		Sand, silt, and gravel; brown and olive gray, poor to moderate sorting. Moderately permeable.
	Gardiners Clay [unconformity]		Marine deposits of clay and silt with some interbedded sand and gravel, greenish gray in color.
Tertiary	Jameco aquifer		Stratified fine- to coarse-grained sand and gravel associated with fluvial deposition. Deposits are well sorted. Silt lenses occur in some areas.
Late Cretaceous	Monmouth greensand [unconformity]		Interbedded marine deposits of clay, silt, and sand, dark-greenish-gray. Contains glauconite and lignite. Geologic equivalent: Monmouth Group.
	Magothy aquifer		Deposits consist of gray to white, fine- to coarse-grained sand with interstitial clay, silt, and lignite interbedded with lenses of thin to thick beds of clayey and silty sand and laminae and thin beds of lignite and pyrite. The basal part of the unit is generally composed of coarse-grained sand and gravel with interstitial clay and silt. Deposited in deltaic environments, including fluvial and overbank marsh deposition. Geologic equivalent: Matawan Group and Magothy Formation.
	Raritan confining unit [unconformity]		Clay, silty clay, and clayey and silty fine-grained sand. Beds of lignite, lenses of pyrite, and sand are common and thin beds of gravel occur locally. Geologic equivalent: unnamed clay member of the Raritan Formation.
	Lloyd aquifer		Deposits of fine- to coarse-grained sand and gravel with intercalated beds and lenses of clay, silt, clayey and silty sand and lignite and pyrite. Geologic equivalent: Lloyd Sand member and Raritan Formation.
Precambrian	Bedrock		Gneiss and schist. Surface of bedrock commonly highly weathered to a greenish-white residual clay.

Data Compilation and Analysis

A variety of data were compiled and analyzed for synthesis into the regional model of the Long Island aquifer system. These datasets include (1) topographic and bathymetric altitudes, (2) the spatial extent, surface altitudes, and thicknesses of mapped hydrogeologic units, (3) estimates of horizontal and vertical hydraulic conductivity, (4) estimates of recharge from spatial and climate data, and (5) water use and the distribution of associated wastewater return flow. Water level and stream flow data for 2005–15 were used to estimate average hydrologic conditions for the period.

Physiography

The surface-water hydrography and geometry of the coast were determined from geographic information system (GIS) linework digitized from USGS 1:24,000-scale topographic quadrangles (U.S. Geological Survey, 2020). The mainland of the island encompasses the area to the west of the North and South Forks. The forks are separated by the Peconic estuary system. Most surface drainages are along the southern shore of the island, and many of those streams have artificial impoundments. The largest surface drainages—the Connetquot, Nissequogue, and Peconic Rivers—are in the central and eastern parts of the island. There are few natural ponds on the island.

The altitudes of land surface and the seabed were derived from a 1-m (3.3-ft) topobathymetric digital elevation model of the coastal regions of Massachusetts, Rhode Island, Connecticut, and New York (Danielson and Haines, 2017). The dataset is a collaboration between the U.S. Geological Survey and the National Oceanic and Atmospheric Administration and combines data from 321 sources to create a seamless, internally consistent representation of land and seabed altitudes at a spatial resolution of 1 m (3.3 ft). These data were upscaled and mapped to the regional model grid; model cells have a horizontal discretization of 500 ft, and there are about 23,100 individual measurements within each model cell. The mean and minimum values of these measurements were computed for each model cell to a distance 3 mi seaward of the coast (fig. 2). Mean land-surface altitudes range from sea level to more than 370 ft above sea level and exceed 200 ft above sea level in the north-central part of the island, in isolated areas in the eastern part of the mainland, and on the South Fork. Land-surface altitudes are highest in areas underlain by glacial moraines that have an east-west trend in the northern part of the Long Island mainland and extend onto the North and South Forks. The topography to the south of the moraines generally is gently sloping to the southern shore of the island. Topography along the northern shore of the island generally is steep, particularly in areas where moraines are adjacent to the shore. Mean seabed altitudes range from sea level to more than 350 ft below sea level. The lowest seabed altitudes (deepest water) are in offshore areas of Long Island

Sound, along the North Fork. The highest seabed altitudes (shallowest water) generally are in estuaries and bays along the southern shore of the island.

The highest water-table altitudes in 2010 exceeded 70 ft in two areas on the mainland of the island (fig. 1; Monti and others, 2013). Unsaturated (or vadose) zone thickness, defined as the difference between land surface and the water table, had a mean thickness of about 47 ft, and was as thick as 300 ft in some areas underlain by moraines. The thickness of the unsaturated zone for about 110 mi² of the island, or about 8 percent, was 10 ft or less. These areas generally are along streams and in coastal areas, particularly along the southern shore of the island (fig. 3).

Hydrogeology

The data compilation and analysis associated with the hydrogeology of the Long Island aquifer system includes the hydrogeologic framework, hydraulic properties, and lithologic texture model of unconsolidated sediments. This hydrogeologic information was used to assign model layers and hydraulic properties in the groundwater flow model developed for this investigation.

Hydrogeologic Framework

A three-dimensional hydrogeologic framework of the major hydrogeologic units underlying Long Island (table 1) was developed from published extents, surface altitudes, and thicknesses of each unit. The thickness of the aquifer system ranges from essentially zero in parts of northwest Queens County to nearly 2,000 ft in south-central Suffolk County. Surficial geology was used to determine the extent of late-Wisconsin glacial units, including moraines, outwash, and ice contact deposits (fig. 5A; Cadwell and Muller, 1986; Cadwell, 1989). Glacial moraines generally are in a narrow east-west-trending band on the northern part of the mainland of the island and extend onto the North and South Forks. Glacial outwash extends southward from the moraines; ice contact deposits extend northward, particularly in the northwestern part of the island (fig. 5A).

Extensive clays within the generally sandy Wisconsinan glacial units include the 20-foot clay and Smithtown clay units. The 20-foot clay unit occurs within glacial outwash along the southern shore between 20 and 40 ft below sea level, primarily in Nassau County (fig. 5A; Doriski and Wilde-Katz, 1982). The Smithtown clay unit in north-central Suffolk County is areally extensive and ranges in thickness between 50 and 100 ft; the surface altitude of the unit is between 75 ft above seas level to 50 ft below sea level (Krulikas and Koszalka, 1982). These clays likely are glaciolacustrine in origin.

The surficial Wisconsinan glacial sediments are underlain by older Pleistocene deposits along parts of the northern and southern shores of the island, including confining units along

A. **Intraglacial (Wisconsinan) confining units and surficial geology**

Base map from U.S. Geological Survey National Atlas digital data, scale 1:1,000,000
New York [Long Island] State Plane projection
North American Datum of 1988

B. **Pleistocene (pre-Wisoncinan) confining units**

Base map from U.S. Geological Survey National Atlas digital data, scale 1:1,000,000
New York [Long Island] State Plane projection
North American Datum of 1988
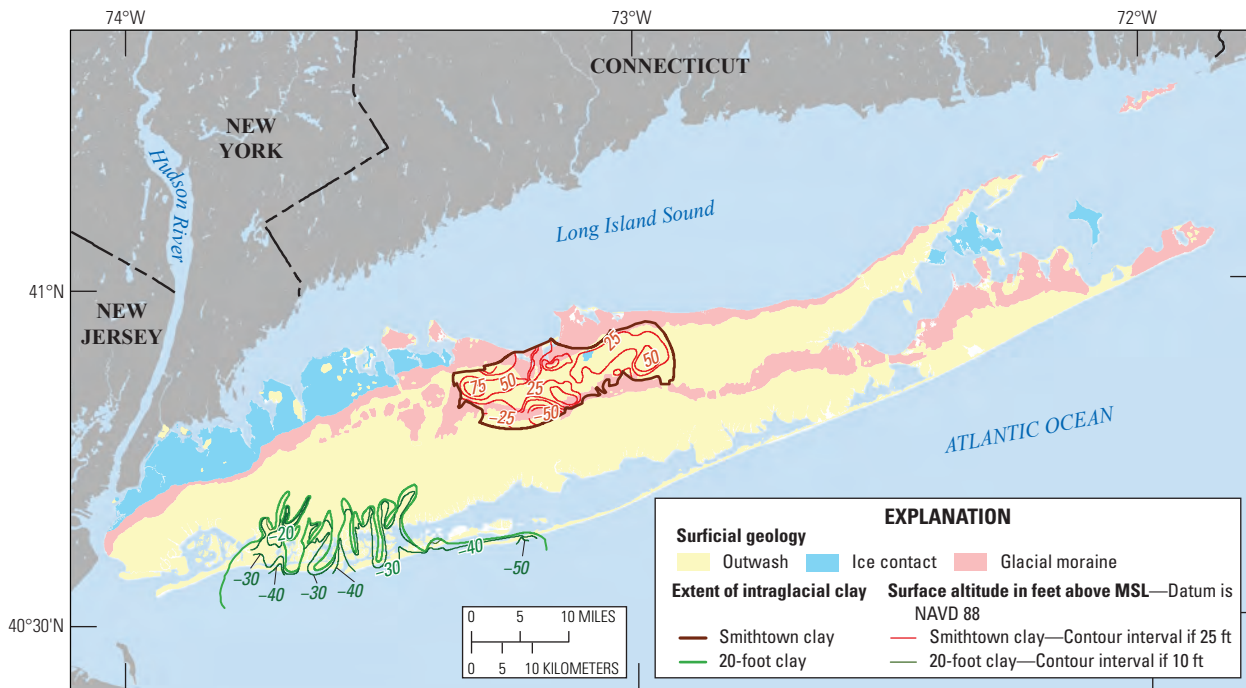
Figure 5. Maps showing surface altitudes and the extents of *A,* intraglacial (Wisconsin) and *B,* Pleistocene confining units on Long Island, New York. ft, foot; MSL, mean sea level; NAVD 88, North American Vertical Datum of 1988.

the northern shore and on the North Fork and surrounding areas. Glacial sediments along parts of the northern shore of Nassau County are underlain by the North Shore confining unit (Stumm, 2001). The unit generally occurs beneath peninsulas and estuaries where Cretaceous deposits are absent and has a surface altitude of between sea level and 100 ft below sea level. The unit is underlain by the North Shore aquifer in some areas (fig. 5B); elsewhere the North Shore confining unit is underlain by bedrock. The North Shore aquifer is a discontinuous unit that occurs in isolated areas beneath peninsulas and estuaries and is underlain by bedrock. This aquifer has a surface altitude between 100 and 500 ft below sea level and generally is contiguous with the Lloyd aquifer. The North Fork clay is an extensive clay unit that underlies most of the North Fork and parts of the South Fork and is as thick as 400 ft in some areas. The surface of the unit generally is between 50 and 150 ft below sea level (Schubert and others, 2004). This unit represents a lower preglacial confining unit.

Wisconsinan glacial sediments are underlain by the Gardiners Clay along most of the southern shore of the island (fig. 5B). The Gardiners clay occurs primarily along the southern shore and extends well inland beneath New York City; the presence of the clay unit in inland areas likely decreases the overall transmissivity of the aquifer system. The Gardiners clay generally is absent in the easternmost parts of the island. The clay is underlain by the Jameco aquifer, generally in Kings and Queens County and in Nassau County and by the Monmouth greensand in parts of Suffolk County (fig. 6A).

The geometry of the four Cretaceous hydrogeologic units—the Lloyd aquifer, the Raritan confining unit, the Magothy aquifer, and the Monmouth greensand—were determined from previously reported extents and surface altitudes (Smolensky and others, 1989; Schubert and others, 2004). The lower Pleistocene Gardiners clay has a surface altitude of between 100 and 200 ft below sea level (fig 5B; Buxton and Smolensky, 1999). The extents and surface altitudes of the Magothy aquifer (fig. 6A), the Raritan confining unit (fig. 6B), and the Lloyd aquifer (fig. 6C) were modified along their northern extents using additional borehole and geophysical data, primarily in northern Nassau and northwestern Suffolk Counties (Stumm, 2001) and in the North Fork and surrounding areas (Schubert and others, 2004). The surface altitude of the Raritan confining unit and Lloyd aquifer (fig. 6B and C) also were modified in central Nassau County using borehole and geophysical data collected in 2017 as part of remedial investigations near Bethpage, New York.

The mapped extents and surface altitudes were used to develop a three-dimensional hydrogeologic framework. The spatial data were used to develop raster images representing each unit that were combined into a full three-dimensional volume representing the aquifer system (fig. 7). A total of 14 hydrogeologic units are represented in the framework. Six Wisconsinan (glacial) units are represented: moraine, outwash, ice contact, the Smithtown clay, the 20-foot clay, and the North Fork clay. Three Pleistocene preglacial units—the North Shore aquifer, North Shore confining unit, and North

Fork clay—also are represented in the framework. Additional preglacial Pleistocene units include the Jameco aquifer and the Gardiners clay. Four Cretaceous units are included in the framework: the Monmouth greensand, Magothy aquifer, Raritan clay, and the Lloyd aquifer. The Wisconsinan glacial sediments, preglacial Pleistocene deposits, and Cretaceous units compose a hydrogeologic system that overlies the southeast-dipping bedrock surface and generally becomes thicker to the south and east. The aquifer system beneath New York City (fig. 7A) on the westernmost part of the island ranges in thickness from zero to about 1,200 ft and has an average thickness of about 510 ft.

Freshwater/Saltwater Interface

The position of the freshwater/saltwater interface is a function of natural hydrologic conditions and pumping stresses and represents the subsurface extent of the freshwater aquifer system. Where the aquifer system is unconfined, the altitude of the freshwater/saltwater interface is determined by the hydraulic head in the aquifer and differences between the density of fresh groundwater and th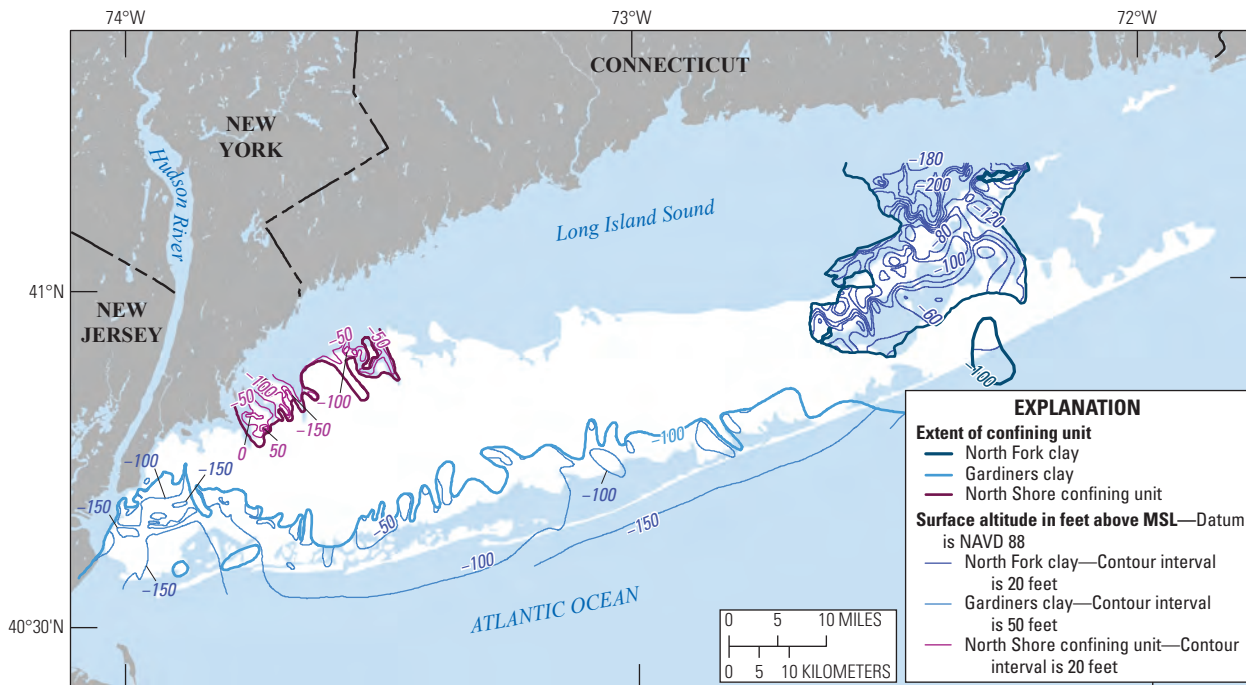at of salty groundwater. The extent of freshwater in these areas is determined by the altitudes of the interface and the seabed. The freshwater/saltwater interface in Cretaceous units is displaced offshore in areas where those aquifers are confined. The seaward extent of freshwater in the Cretaceous aquifers—as estimated from borehole and surface geophysical data (Stumm and others, 2020)—is thought to be offshore in most areas of Nassau and Suffolk Counties, but the interface between fresh and salty groundwater has moved inland beneath parts of King and Queens Counties due largely to historically large groundwater withdrawals in New York City (Terraciano, 1996).

The upper glacial aquifer and most of the Magothy aquifer generally are unconfined; the altitude of the interface in these areas was estimated from water-table altitude as measured in April to May 2010 (Monti and others, 2013) and assuming a ratio of fresh-to-salty groundwater of 40:1 (the Ghyben-Herzberg ratio). The estimated altitude of the interface in unconfined areas ranges from about 5 ft below MSL to more than 900 ft below MSL, where the interface is at the top of the Raritan confining unit (fig. 8A). The extent of freshwater in unconfined parts of the aquifer is a function of the altitudes of the interface and the seabed and generally is close to shore. The Magothy aquifer is confined along the southern shore by the Gardiners clay; the interface under confined conditions is displaced seaward, and freshwater likely extends to or near the top of the Raritan confining unit in these areas.

The location of the regional freshwater/saltwater interface within Cretaceous and Tertiary sediments of the Northern Atlantic Coastal Plain, which includes Long Island at its northern extent, was mapped using published historical chloride data as part of a study of the system in 2016 (Charles, 2016; Masterson and others, 2016). The seaward extent of fresh groundwater in the Magothy aquifer, as defined by the 10,000-milligram per liter (mg/L) isochlor, was mapped to be

A. **Magothy aquifer and associated units**

Base map from U.S. Geological Survey National Atlas digital data, scale 1:1,000,000
New York [Long Island] State Plane projection
North American Datum of 1988

B. **Raritan confining unit**

Base map from U.S. Geological Survey National Atlas digital data, scale 1:1,000,000
New York [Long Island] State Plane projection
North American Datum of 1988
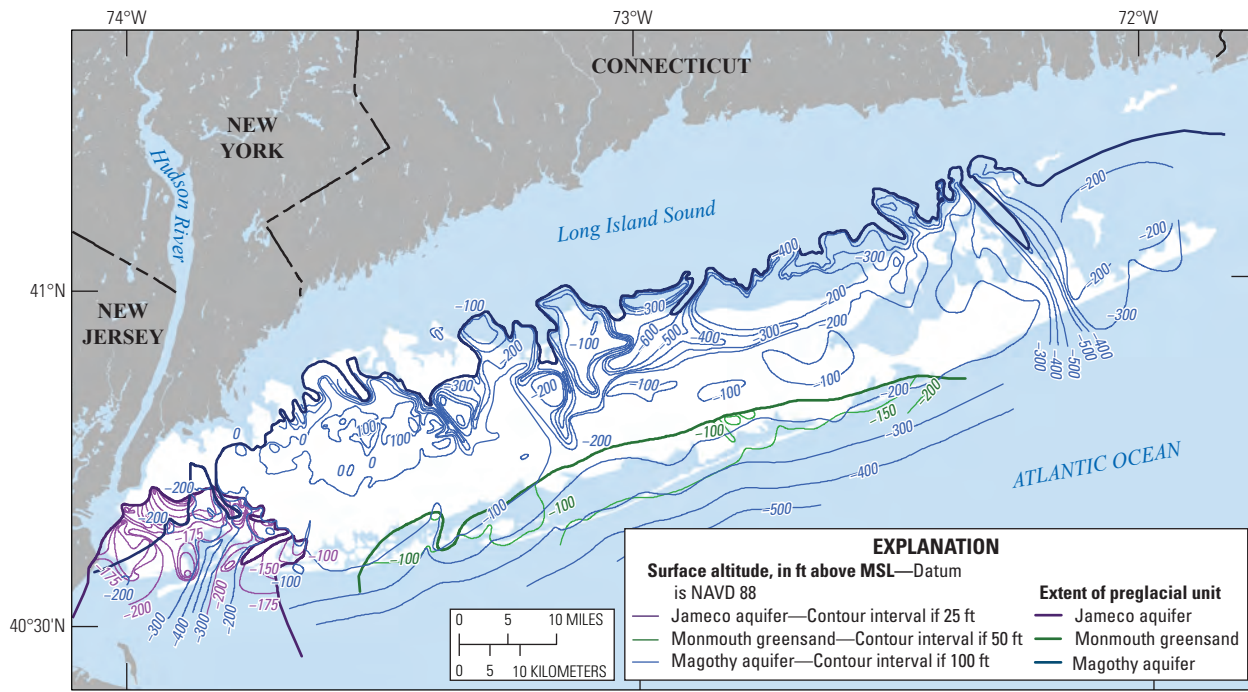
Figure 6. Maps showing extents and surface altitudes of major preglacial hydrogeologic units on Long Island, New York: *A*, Magothy aquifer and associated units, *B*, Raritan confining unit, and *C*, Lloyd and North Shore aquifers, and *D*, surface altitude of the bedrock surface. ft, foot; MSL, mean sea level; NAVD 88, North American Vertical Datum of 1988.

C. **Lloyd and North Shore aquifers**

Base map from U.S. Geological Survey National Atlas digital data, scale 1:1,000,000
North American Datum of 1988

D. **Bedrock surface**

Base map from U.S. Geological Survey National Atlas digital data, scale 1:1,000,000
New York [Long Island] State Plane projection
North American Datum of 1988
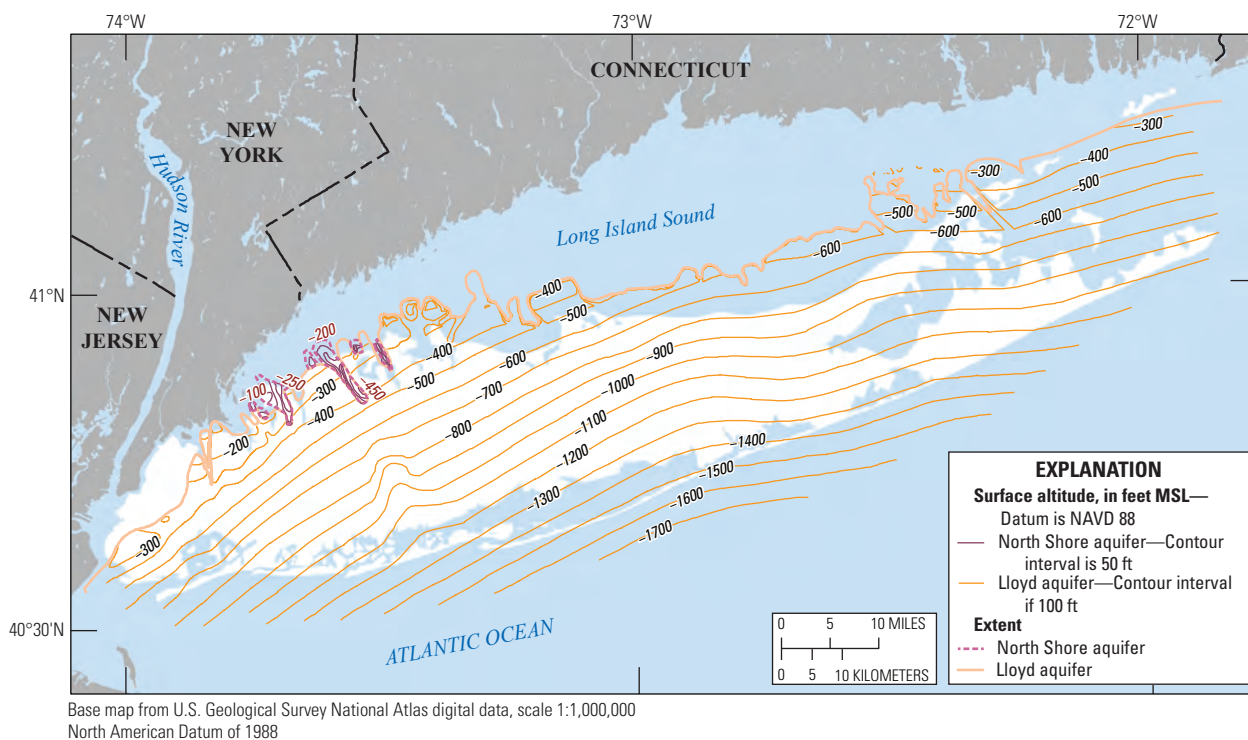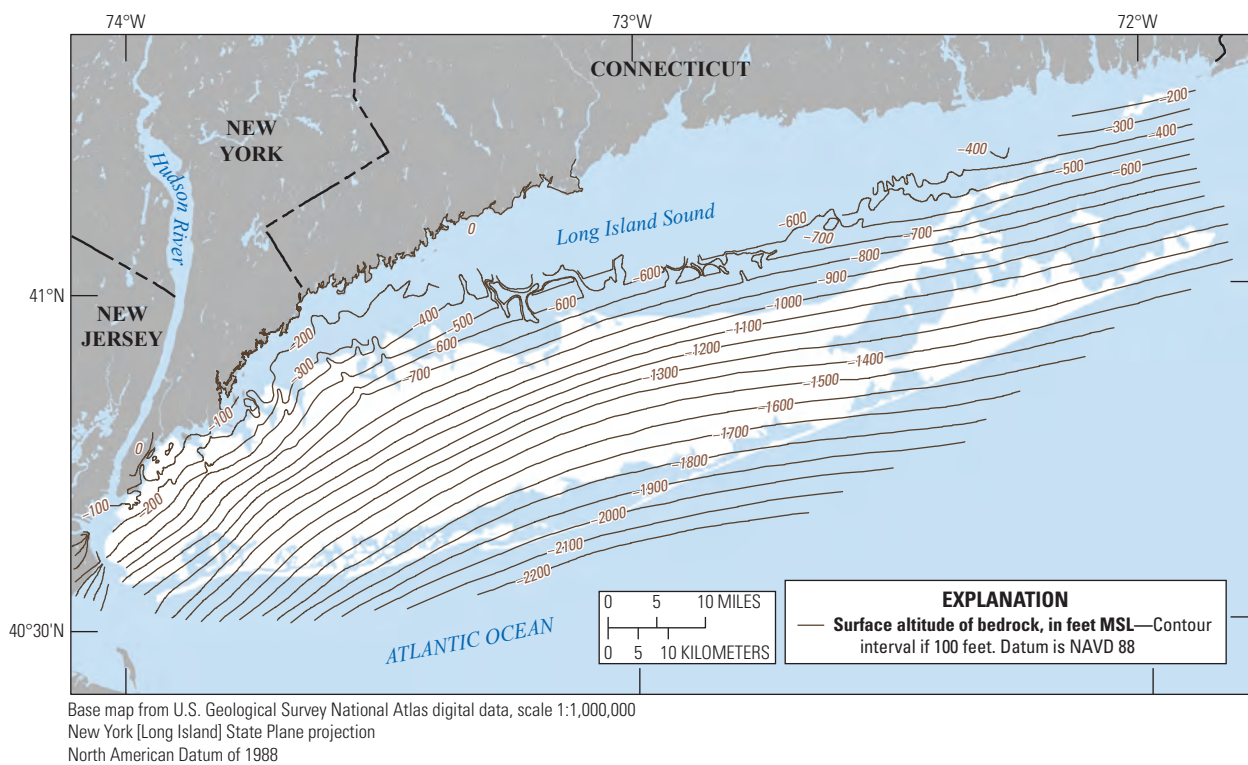
Figure 6. —Continued

A. **Column 320**
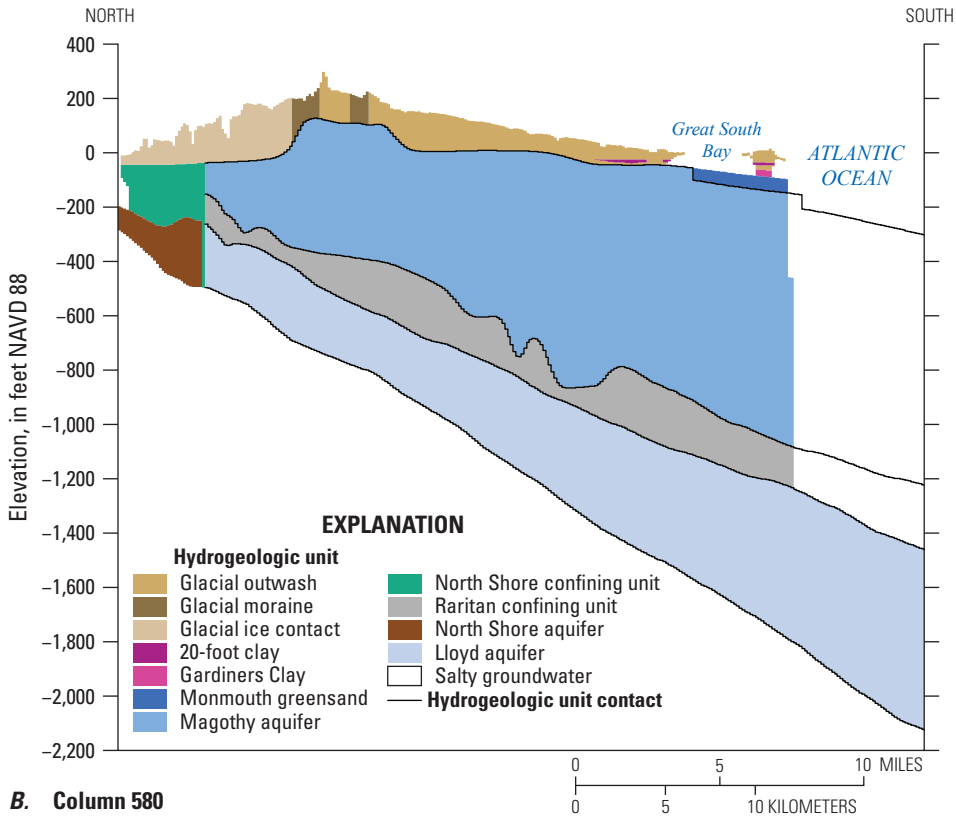
B. **Column 580**
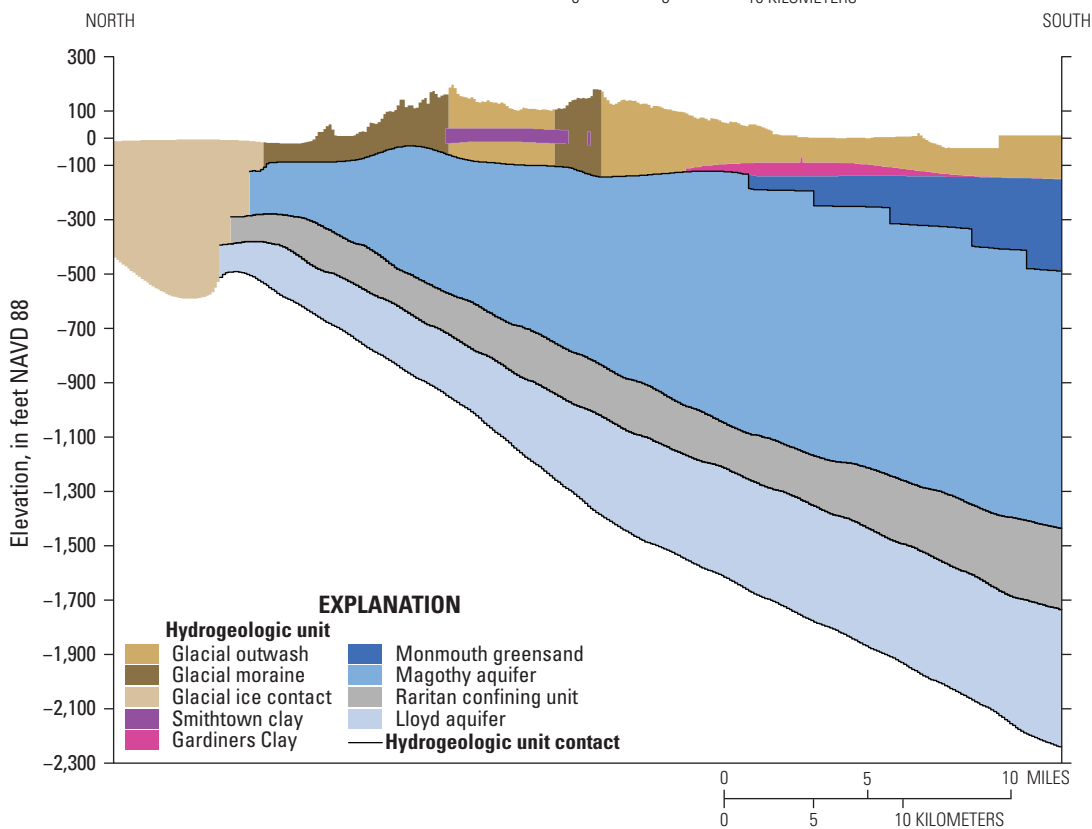
Figure 7. Sections showing hydrogeologic units along *A–C*, north-south (downdip) and *D*, east-west sections.

C. Column 970

EXPLANATION

Hydrogeologic unit
Glacial outwash
Glacial moraine
Glacial ice contact
North Fork clay
Magothy aquifer
Raritan confining unit
Lloyd aquifer
Salty groundwater
Hydrogeologic unit contact

D. Row 205

EXPLANATION

Hydrogeologic unit
Glacial outwash
Glacial moraine
20-foot clay
North Fork clay
Gardiners Clay
Jameco aquifer
Magothy aquifer
Raritan confining unit
Lloyd aquifer
Salty groundwater
Hydrogeologic unit contact

Figure 7. —Continued

A.   **Upper glacial, Jameco, and Magothy aquifers**

Base map from U.S. Geological Survey National Atlas digital data, scale 1:1,000,000
New York [Long Island] State Plane projection
North American Datum of 1988

B.   **Lloyd and North Shore aquifers**

Base map from U.S. Geological Survey National Atlas digital data, scale 1:1,000,000
New York [Long Island] State Plane projection
North American Datum of 1988
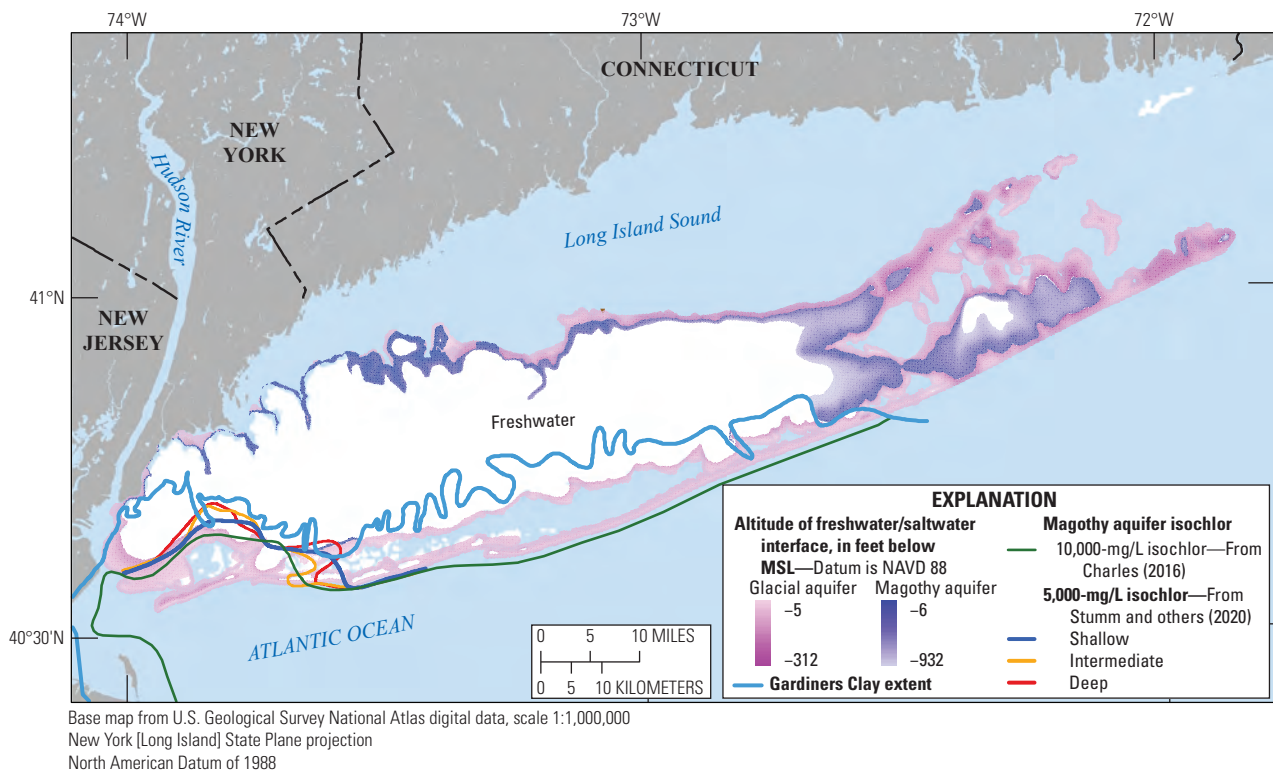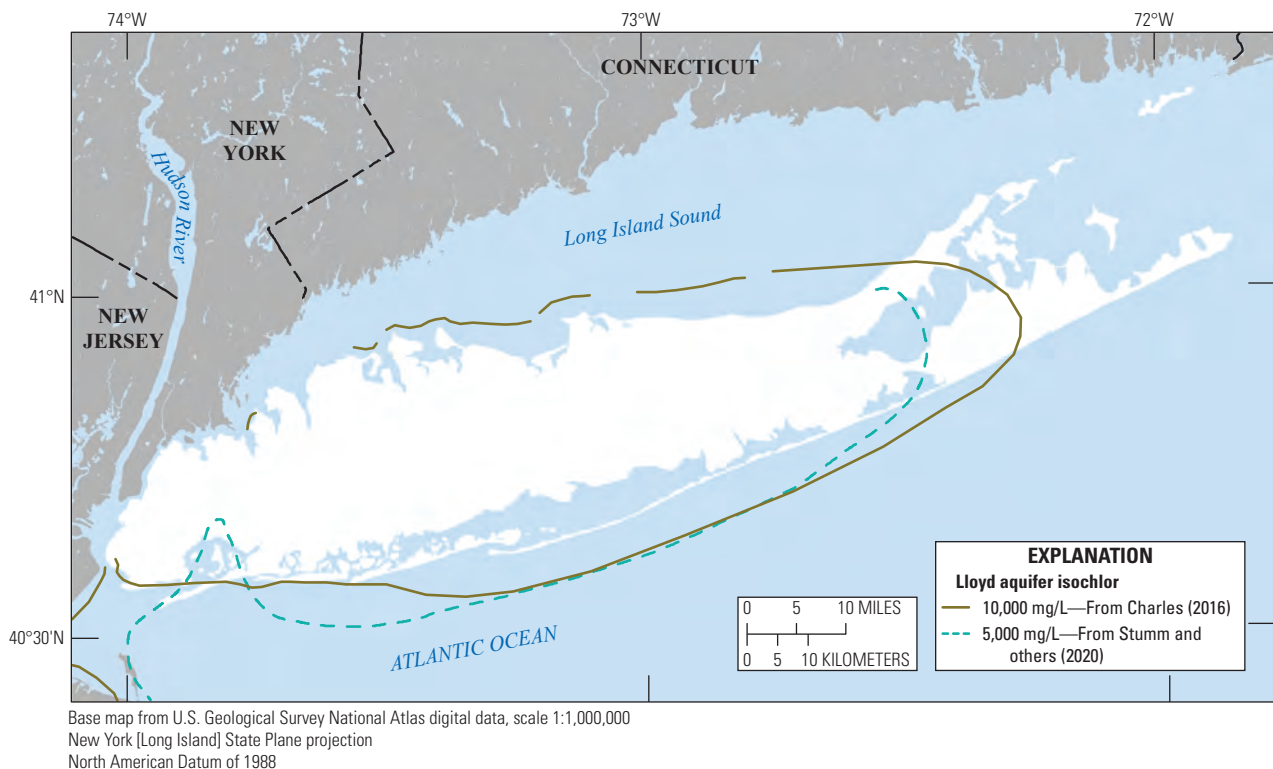
Figure 8.   Maps showing *A*, the estimated altitude of the freshwater/saltwater interface in unconfined parts of the Magothy aquifer and the extent of salty groundwater in the confined parts of the aquifer and *B*, the estimated altitude of the freshwater/saltwater interface in the Lloyd and North Shore aquifers on Long Island, New York (modified from Charles (2016) and Stumm and others (2020). ft, foot; MSL, mean sea level; NAVD 88, North American Vertical Datum of 1988.

close to but seaward of the southern shore of the island (fig. 8*A*; Charles, 2016). Borehole and surface geophysical data from 2015 to 2017 indicate that salty groundwater—delineated by the 5,000-mg/L isochlor, extends inland in parts of Kings, Queens, and Nassau Counties (Como and others, 2020; Stumm and others, 2020), likely in response to large historical groundwater withdrawals. The landward extent of salty groundwater in the Magothy aquifer in this area varies with depth and differs between shallow, intermediate, and deep parts of the aquifer.

The seaward extent of fresh groundwater in the Lloyd aquifer, as delineated by the 10,000-mg/L isochlor (Charles, 2016), extends further east and further seaward along the southern shore than that in the overlying Magothy aquifer (fig. 8*B*). Freshwater in the Lloyd aquifer may underlie western parts of the North and South Forks. Recent [2015–17] data suggest that salty groundwater extends further inland in the southwestern parts of the island and that salty groundwater underlies Jamaica Bay and the southern shore of central Queens County (fig. 8*B*; Stumm and others, 2020).

Hydraulic Properties

Limited data exist on the hydraulic properties of the aquifers and confining units within the Long Island aquifer system, and these data are relatively sparse for the apparent heterogeneity of the hydrogeologic units. The spatial distribution of measurements is focused primarily around major pumping centers. Consequently, field measurements of hydraulic properties are more readily available in areas of large groundwater use and for those particular aquifer units with the most use (McClymonds and Franke, 1972; Franke and Getzen, 1976; Lindner and Reilly, 1983; Prince and Schneider, 1989; Stumm, 2001; Stumm and others, 2002, 2004). Estimates of hydraulic properties made in numerical model investigations include Buxton and Smolensky (1999), Kontis (1999), Misut and Monti (1999), Misut and others (2004), Schubert and others (2004), and Monti and others (2009).

Buxton and Smolensky (1999) provided a summary of the previous investigations of the hydraulic properties of the aquifer system. That synthesis of previous work represents the most comprehensive summary to date of the existing information on hydraulic properties of the major hydrogeologic units of the Long Island aquifer system.

The upper glacial aquifer has a range of horizontal hydraulic conductivity from 20 to 270 feet per day (ft/d). Hydraulic conductivity in glacial sediments differs for outwash, moraine, and ice-contact deposits. Values for the outwash deposits south of the moraines generally range from 200 to 270 ft/d; hydraulic conductivity within the moraine deposits is less than 135 ft/d. The average hydraulic conductivity of the upper glacial aquifer is less than 25 ft/d where the Smithtown clay is present. The anisotropy (ratio of horizontal over vertical hydraulic conductivity) of the upper glacial aquifer is estimated to be 10:1; but local values could be as low as 3:1.

Horizontal hydraulic conductivity of the Jameco aquifer ranges from 200 ft/d to 300 ft/d, and its anisotropy is estimated to be about 10:1; the aquifer generally has the highest hydraulic conductivity of any aquifer on Long Island. The hydraulic conductivity of the Magothy aquifer varies with depth; values for the upper part range from 35 ft/d to 90 ft/d; values for the coarser basal zone were estimated to be about 50 percent higher. Hydraulic conductivity of the Lloyd aquifer ranges from 30 ft/d to 80 ft/d and generally is greatest in Nassau County. The anisotropy of these aquifers is estimated to be 100:1 because of their highly stratified character.

Although data on hydraulic conductivity of the confining units are scant, the high clay and silt content indicates values several orders of magnitude lower than in the aquifers. Franke and Cohen (1972) estimated the average vertical hydraulic conductivity of the confining units to be 0.001 ft/d; Reilly and others (1983) estimated a value of 0.0029 ft/d for the Gardiners clay. A vertical hydraulic conductivity value of 0.001 ft/d was used for major pre-Wisconsinan confining units—Gardiners clay—including, the Raritan confining unit, and the North Shore confining unit. A value of 0.01 ft/d was assumed for Pleistocene clay units, including the Smithtown clay, the 20-foot clay, and the North Fork clay.

Lithologic Texture Model

The water-transmitting properties of the upper glacial and Magothy aquifers were estimated using borehole lithologic and geophysical log data from a set of 1,769 boreholes, representing the deepest borehole within each cell of a regular 1-mi² grid of the Long Island aquifer system (Finkelstein and Walter, 2020; Walter and Finkelstein, 2020). Standardized lithologic codes from the USGS Ground-Water Site Inventory (GWSI) System (U.S. Geological Survey, 2004) were assigned to each depth interval in each borehole. In total, 36,369 lithologic descriptions were included in the analysis. The descriptions were described by 45 GWSI codes that were subsequently aggregated into 14 sediment codes: 7 codes for sediments of the upper glacial aquifer sediments and 7 codes for the sediments of the Magothy and Jameco aquifers and Monmouth greensand (Walter and Finkelstein, 2020). Each code was assigned corresponding horizontal and vertical hydraulic conductivities derived from published field tests in the Long Island aquifer system (McClymonds and Franke, 1972; Franke and Getzen, 1976; Lindner and Reilly, 1983; Smolensky and others, 1989) and similar hydrogeologic environments on the coastal plain of Massachusetts (Guswa and Londquist, 1976; Guswa and LeBlanc, 1985; LeBlanc and others, 1986; Barlow, 1989; Barlow and Hess, 1993; Masterson and Barlow, 1997; Moench and others, 1996; Walter and others, 1996; Masterson and others, 1998).

The compiled data were used to create quasi-three-dimensional textural models of the upper glacial and Magothy aquifers—the principal aquifers of the Long Island aquifer system. The Lloyd aquifer was not explicitly included in the texture model owing to a paucity of data for the unit.

The hydraulic conductivities assigned to each depth interval were used to estimate thickness-weighted mean hydraulic conductivities in regular 10-ft intervals over the depth of each borehole; horizontal and vertical hydraulic conductivity values were computed using arithmetic and geometric means, respectively. These were combined to develop a database of X, Y, and Z coordinates and associated estimates of horizontal and vertical hydraulic conductivities; this database was sequentially queried to extract the X and Y coordinates of boreholes that extend to or beyond each layer in the textural model, and these point values then were used to develop an interpolated field of horizontal and vertical hydraulic conductivities for each altitude range by use of ordinary, spherical kriging (Walter and Finkelstein, 2020).

The result of this process is a two-dimensional data raster of horizontal and vertical hydraulic conductivity (fig. 9) for each 10-ft interval for the vertical thickness of each aquifer. These individual data raster images, when aggregated, created a quasi-three-dimensional array of values. Two sets of quasi-three-dimensional models were produced: a set of grids each with a thickness of 10 ft and uniform altitude between land surface and the top of the Magothy aquifer (representing the upper glacial aquifer) and a set of grids between the top of the Magothy aquifer and the top of the underlying Raritan confining unit representing the Magothy aquifer. Each of the grids representing the Magothy aquifer has a thickness of 10 ft and a variable altitude based on the altitude of the underlying surface of the Raritan confining unit, such that each grid is a given multiple of 10 ft added to that surface (Walter and Finkelstein, 2020). These two models, when combined, fully define the distribution of estimated hydraulic conductivity for the upper glacial and Magothy aquifers (figs. 9 and 10).

The spatial distribution of hydraulic conductivity, as represented in the texture model, generally is consistent with the regional geology of the aquifer system. Glacial sediments show a distribution of estimated hydraulic conductivity that is consistent with their depositional history and mapped surficial geology. Estimated hydraulic conductivity generally is highest in the shallow parts of the upper glacial aquifer, in association with coarse-grained outwash (figs. 9A and 10A). Estimated hydraulic conductivity of glacial sediments at an altitude of 5 ft below MSL generally is lower in inland areas of eastern Nassau and western Suffolk County where these sediments underlie hummocky terrain, suggesting an association with glacial moraines (fig. 2); this association also is consistent with the mapped surficial geology (Cadwell and Muller, 1986; Cadwell, 1989). Areas of low estimated hydraulic conductivity in the north-central part of Long Island also may represent glaciolacustrine sediments, which were deposited in proglacial lakes between moraines. Extensive clays, likely glaciolacustrine in origin, have been mapped in north-central and northeastern Suffolk County (Krulikas and Koszalka, 1982; Schubert and others, 2004). Estimated hydraulic conductivities to the south, within outwash sediments, generally are substantially higher than those of inland areas (fig. 9A). Estimated hydraulic conductivity for morainal and glaciolacustrine

sediments generally are lower than in outwash sediments owing to a finer grain size and more sorting. The vertical distribution of horizontal hydraulic conductivity also generally reflects geologic trends in and the depositional history of the glacial aquifer sediments (fig. 10). Glacial sediments generally become finer with depth, with lower values of hydraulic conductivity in interior parts of the island, in association with morainal and glaciolacustrine sediments. Hydraulic conductivity generally is higher in the shallow parts of the glacial aquifer in association with coarse-grained outwash sediment.

The Cretaceous sediments are deltaic in origin and were deposited in a variety of depositional environments. Hydraulic conductivity values in the Magothy aquifer generally show a large degree of spatial heterogeneity (fig. 9B). Deposition of coarse-grained, sandy sediments occur in fluvial environments within stream channels and fine-grained sediments generally were deposited in overbank-marsh environments. The variety of depositional environments resulted in the highly heterogenous hydraulic conductivity patterns.

The Magothy aquifer also shows a distribution of estimated hydraulic conductivity that is consistent with its depositional history (figs. 9B and 10B). The Magothy sediments were deposited in sedimentary environments dominated by streams and coalescing deltas (Smolensky and others, 1989). Hydraulic conductivity values generally are highest in the basal part of the Magothy aquifer where the presence of coarse-grained sediments indicate deposition in high-energy fluvial environments, such as stream channels. Hydraulic conductivity generally is lower in the middle part of the aquifer where presence of finer-grained sediments suggests deposition in low-energy environments, such as overbank marsh deposits.

Natural and Artificial Recharge

Long Island has a temperate climate typified by warm, often humid summers and cold winters; the temperate climate is moderated by the proximity to ocean waters, compared with interior parts of the northeastern United States. Precipitation on Long Island is the sole natural source of water to the aquifer system and varies annually (fig. 11); average precipitation from 1900 to 2015 was about 48 in/yr. About half of the precipitation recharges the aquifer system at the water table; the remainder is lost to evapotranspiration and, to a lesser extent, surface runoff. Aquifer recharge is a function of climatological conditions (precipitation and temperature) and landscape characteristics (vegetation, soil properties, and land use); variations in these factors affect the rates and distribution of recharge. Total recharge to the aquifer includes recharge from precipitation and from anthropogenic sources, such as wastewater return flow and leakage from water infrastructure.

An SWB model (Westenbroek and others, 2010) was used to estimate annual recharge on Long Island from 2005 to 2015. The SWB model accounts for processes that occur as water moves through unsaturated soils and sediments to the water table and is based on a modified version of the Thornthwaite-Mather approach (Thornthwaite and Mather,

A. **Upper glacial aquifer**
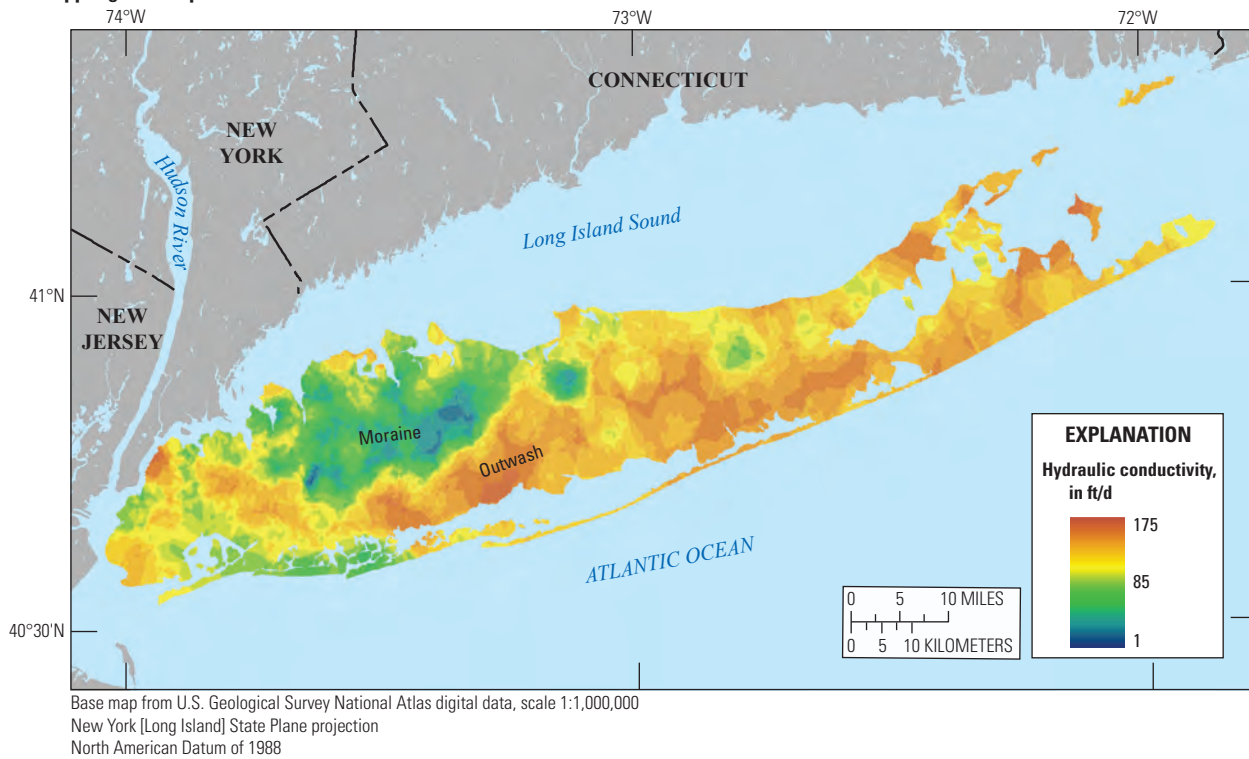
B. **Basal Magothy aquifer**
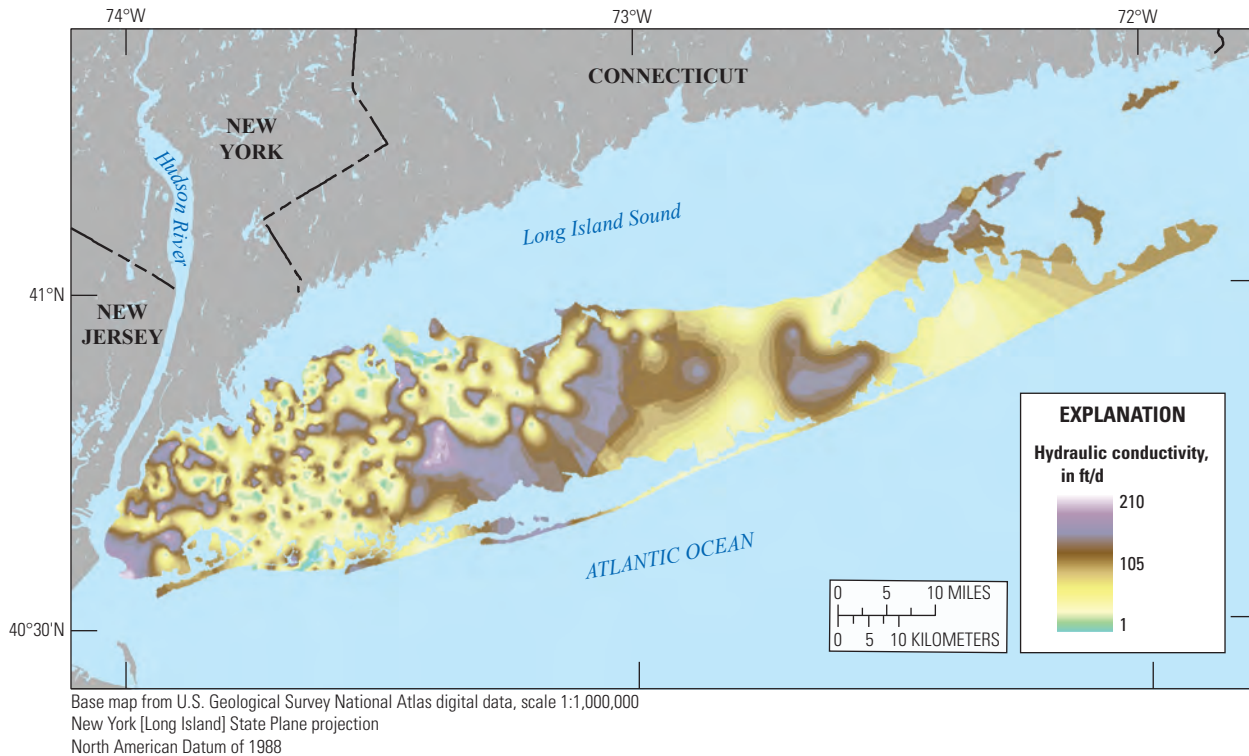
Figure 9.   Maps showing estimated hydraulic conductivity for *A*, the upper glacial (near sea level) and *B*, the lower part of the Magothy aquifer on Long Island, New York. ft/d, foot per day
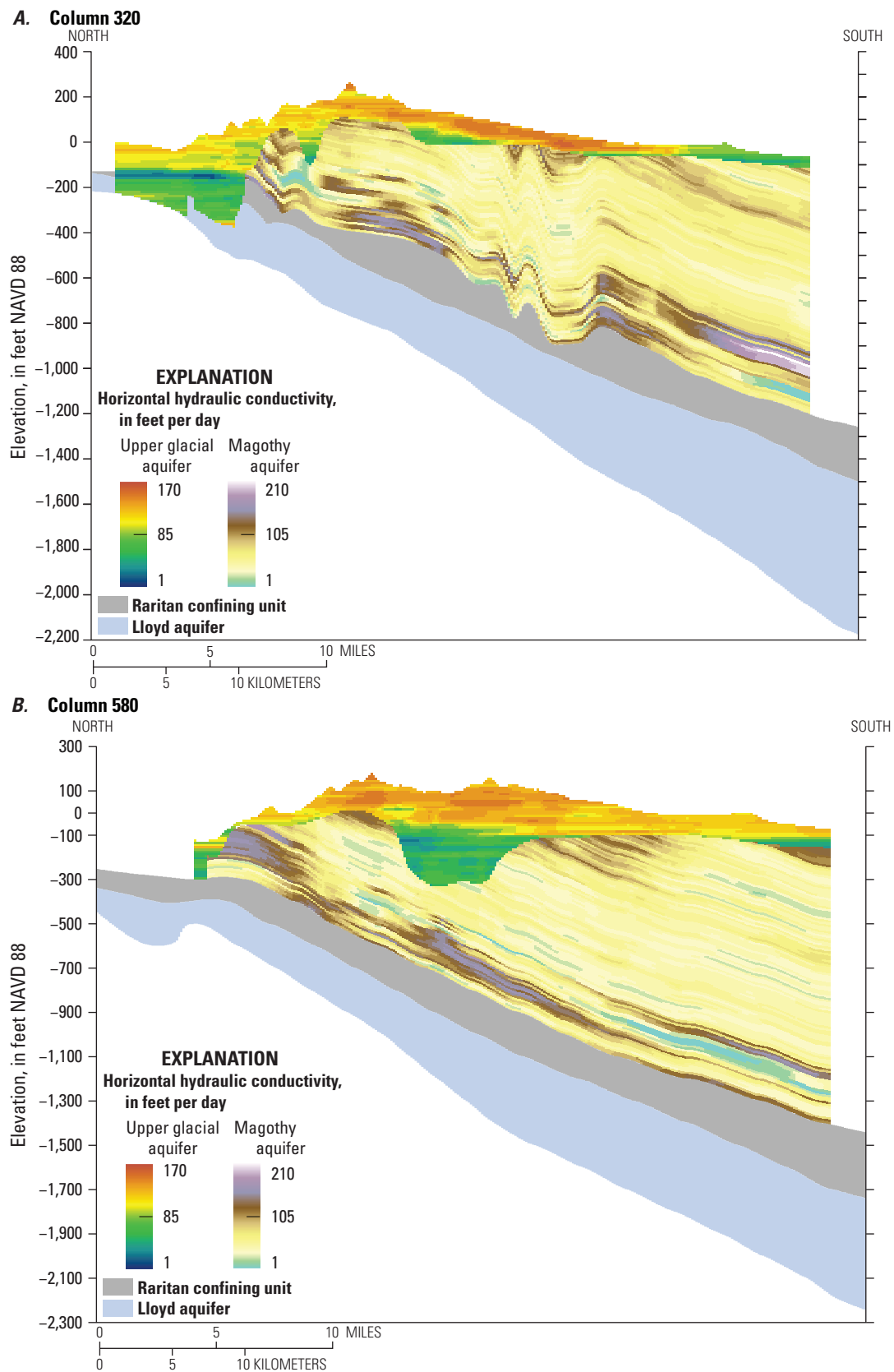
Figure 10.   Section showing the vertical distribution of estimated horizontal hydraulic conductivity along *A* and *B*, two north-south and *C*, an east-west section on Long Island, New York. Section lines shown on figure 1.

EXPLANATION

Horizontal hydraulic conductivity, in feet per day

Upper glacial aquifer

Magothy aquifer

Raritan confining unit

Lloyd aquifer

Figure 10. —Continued
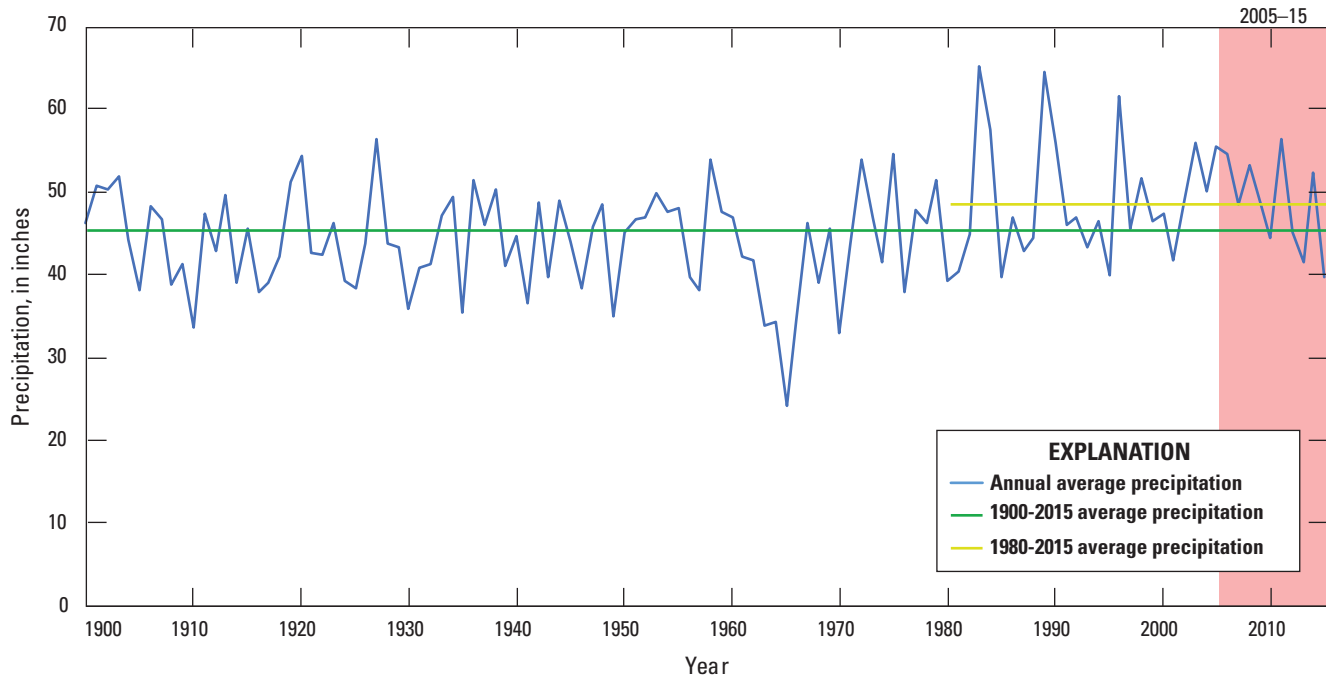
Figure 11.   Graph showing average annual precipitation and estimated recharge from 1900 to 2015 on Long Island, New York.

1957). The method incorporates land slope, soil proper-
ties, and climatic data, and it produces a spatially distributed
recharge grid. The computer code uses commonly available
GIS data layers in combination with tabular climatological
data to produce gridded recharge data that can be imported
into the groundwater model.

The application of the SWB model to Long Island is
described by Misut and others (2020). Average precipitation
for 2005–15 differed from the average for 1900–2015 by
about 3.7 in/yr (or 6 percent) and differed from the average for
1980–2015 by about 0.4 in/yr (or less than 1 percent; fig. 11).
Average estimated recharge, which is a function of land use
and soil characteristics as well as precipitation, for 2005–15
differed by about 0.5 in/yr (or about 2 percent) from the aver-
age for 1980–2015. This indicated that the simulated 2005–15
recharge period generally is representative of long-term aver-
age recharge conditions. Recharge exhibited substantial spatial
variations owing to its dependence on land use, soil type, and
available water capacity (fig. 12A). Recharge from precipita-
tion, as estimated using the SWB model, ranged from less
than 1 to 35.1 in/yr and had an island-wide average of about
19.9 in/yr.

The distribution of recharge rates differs considerably
under the assumption of no impervious surfaces and land use
representative of predevelopment conditions. Predevelopment
recharge, as estimated from the SWB model, ranged from less
than 1 to 31.5 in/yr and averaged about 19.3 in/yr. Impervious
surfaces can intercept precipitation in developed areas,

resulting in lower recharge rates, whereas conversion of unde-
veloped to low-density residential land-use areas can result in
higher recharge rates because of low rates of evapotranspira-
tion for low-density residential land use as compared with
those in forested land (Yang and others, 2015). The difference
in recharge arising from changes from undeveloped land use
to land use in 2005 to 2015 averaged about 0.1 in/yr, ranging
from a gain of about 7.8 in/yr to a deficit of about 10.6 in/yr,
suggesting that land use can substantially affect recharge rates
locally (fig. 12B). The largest deficits from impervious sur-
faces occur in urbanized areas of New York City and southern
Nassau County; however, much of the recharge potentially
lost to impervious surfaces in Nassau County can recharge the
aquifer through sumps, storm drains, and a network of more
than 6,000 recharge basins.

About 85 percent of water pumped for water supply is
returned to the aquifer as wastewater return flow in unsew-
ered areas; the remainder is assumed to be consumptive
loss. Wastewater return flow was estimated using population
density derived from the 2010 census (U.S. Census Bureau,
2018). The distribution of wastewater return flow reflects
patterns of development and associated water use, which is
largest in urbanized areas on western Long Island (fig. 13A).
The distribution of wastewater return flow to the water table
was lowered in areas served by public sewering, where it was
assumed that about 10 percent of wastewater recharged the
aquifer. Most wastewater enters the aquifer as septic-system
return flow in unsewered areas in western Suffolk County;

A. **Recharge from precipitation**
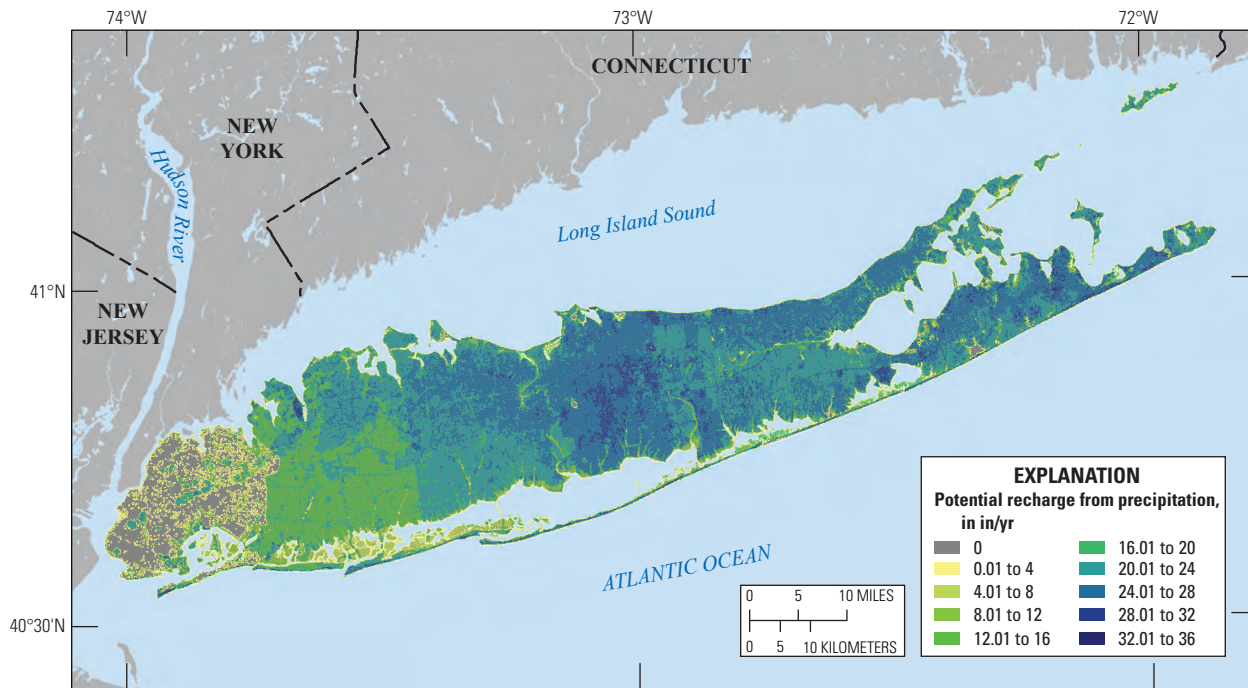
Base map from U.S. Geological Survey National Atlas digital data, scale 1:1,000,000
New York [Long Island] State Plane projection
North American Datum of 1988

B. **Potential recharge lost from impervious surfaces**
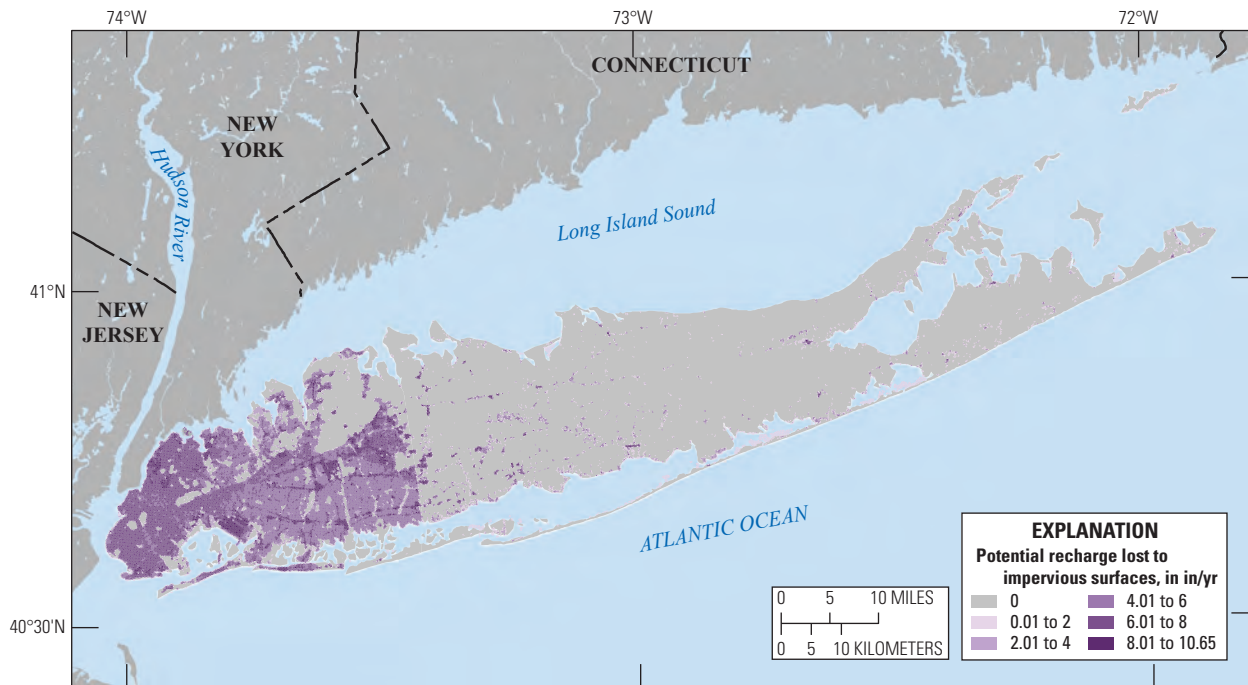
Base map from U.S. Geological Survey National Atlas digital data, scale 1:1,000,000
New York [Long Island] State Plane projection
North American Datum of 1988

Figure 12.   Maps showing distribution of estimated recharge from precipitation on Long Island, New York, for 2005–15 based on *A*, land use and impervious surfaces and *B*, estimated recharge lost to impervious surfaces for the same. in/yr, inch per year.

A. **Population and sewered areas**

Base map from U.S. Geological Survey National Atlas digital data, scale 1:1,000,000
New York [Long Island] State Plane projection
North American Datum of 1988

B. **Road length and areas with private water supply**
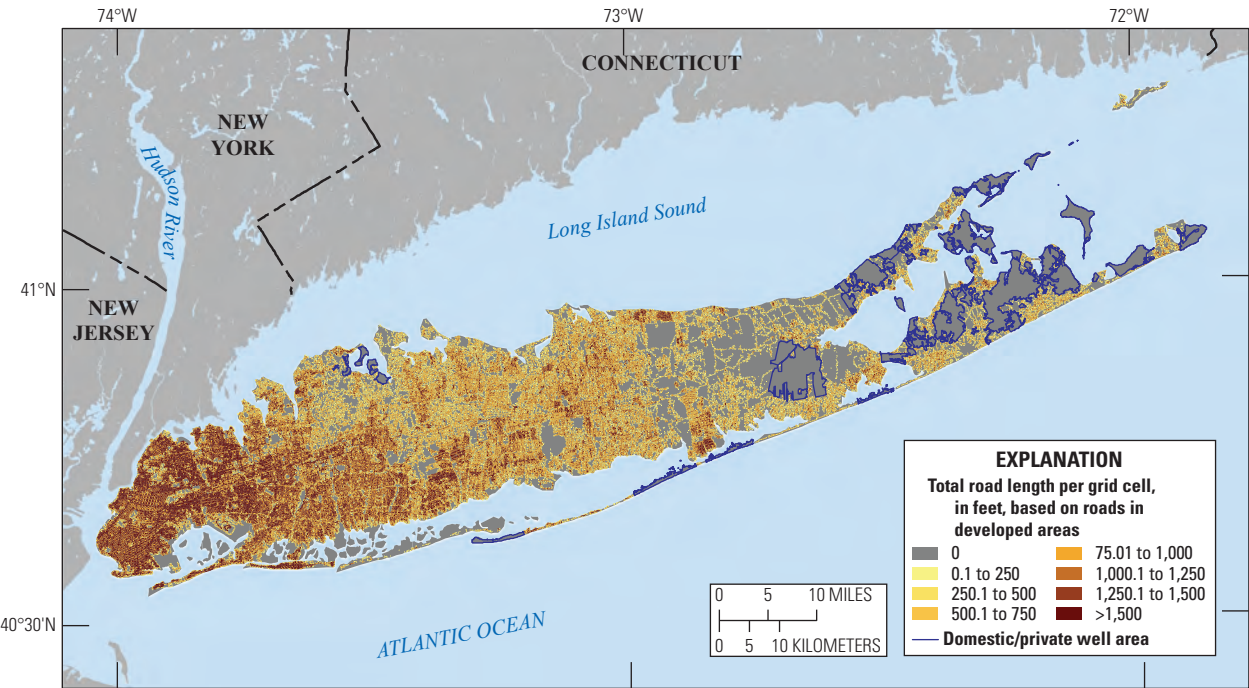
Base map from U.S. Geological Survey National Atlas digital data, scale 1:1,000,000
North American Datum of 1988

Figure 13. Maps showing distribution of *A*, population and sewered areas and *B*, public-supply lines, as indicated from road length, and areas of private water supply on Long Island, New York.

some wastewater also can enter the aquifer from leaky sewer lines in sewered areas, primarily in New York City and Nassau County.

An additional source of artificial recharge to the aquifer system is leakage from public-supply infrastructure. Most of Long Island is served by public supply; private water supplies do exist but are limited to small areas of eastern Suffolk County and the northern shore of Nassau County (fig. 13*B*). The distribution of public-supply lines was estimated from the length of roads in developed areas. The potential for recharge from leaky infrastructure (as indicated by road length) generally reflects patterns of population and development and is largest in New York City and parts of Nassau County. In Kings and Queens Counties, about 700 million gallons per day (Mgal/d) of water is imported from a reservoir system in upstate New York, and assuming a 10 percent loss of water from the water distribution system, may result in about 70 Mgal/d of additional recharge to the water table on western Long Island (Misut and Monti, 1999).

Water Use

Groundwater use has varied temporally and spatially across Long Island since 1900. Prior to 1950, nearly all groundwater pumping occurred in Kings and Queens Counties where it was the primary source of drinking water for the residents in these counties (fig. 14). By 1950, overpumping in these counties had resulted in a large drawdown of the water table and widespread saltwater intrusion throughout the aquifer system in western Long Island, necessitating the importation of water from the upstate reservoir system (Buxton and Shernoff, 1999). Water use generally increased between the late 1940s (when water supplies from surface-water reservoirs began to be implemented) to the early-1990s, after which

water use generally leveled off (fig. 14). Average groundwater withdrawals during the calibration and analysis period [2005–15] were within 4 percent of the average withdrawals since the early 1990s.

From 2005 to 2015, about 424 Mgal/d of groundwater was withdrawn annually from the Long Island aquifer system for multiple uses, including public supply, agricultural, and industrial purposes (fig. 15*A*). The groundwater withdrawn for public supply accounted for nearly all (95 percent) of groundwater withdrawals on Long Island. The public supply of drinking water for 2005–15 was withdrawn from a total of 1,680 pumping wells in Nassau and Suffolk Counties (fig. 16; U.S. Geological Survey, 2018; New York State Department of Environmental Conservation, 2020). Contaminant remediation, agricultural, and industrial uses each accounted for about 2 percent of groundwater withdrawals, respectively; the percentages do not add up because of individual rounding.

About 74 percent of groundwater withdrawals come from the Magothy and Jameco aquifers; about 23 and 3 percent of pumped groundwater is from the upper glacial and Lloyd aquifers, respectively (fig. 15*B*). Agricultural withdrawals for crop irrigation generally are limited to eastern Suffolk County on or near the North and South Forks (fig. 16). Specific well locations and withdrawal rates for irrigation wells are poorly understood. The total amount of potential agricultural pumping was estimated using the SWB model by estimating water demand by crop type and available recharge from precipitation. This deficit was assumed to represent the amount of pumped groundwater required for irrigation. The estimated deficit was about 2 Mgal/d, or less than 0.5 percent of total groundwater withdrawals from other sources, supporting the decision to not explicitly represent individual agricultural pumping wells in the regional-scale model of the Long Island aquifer system.
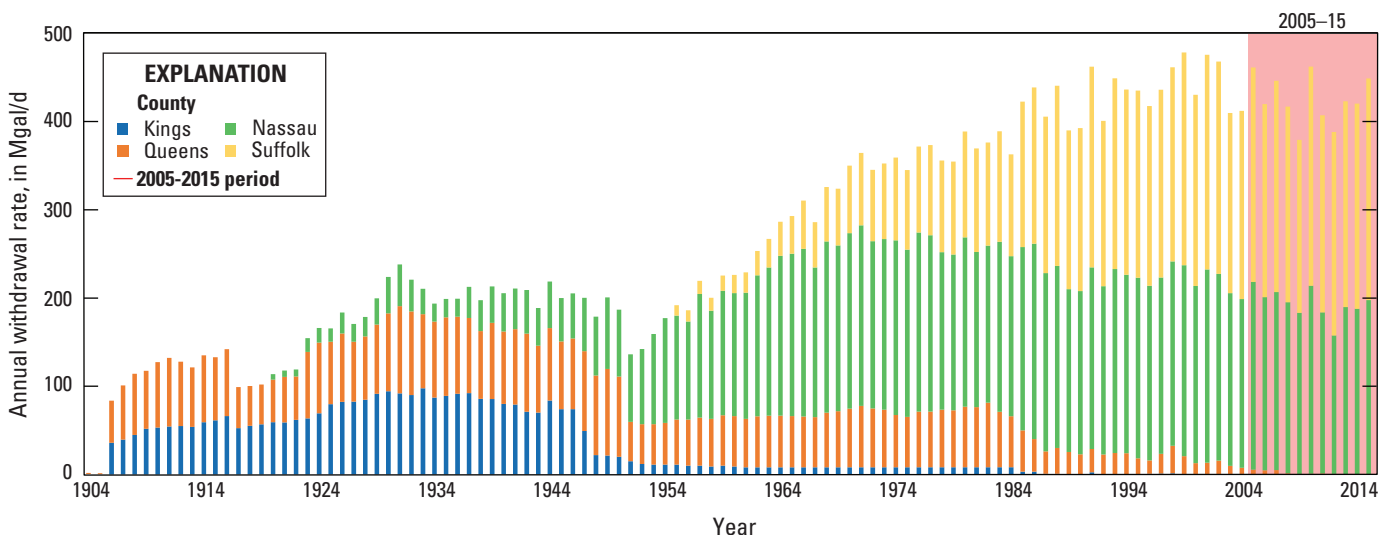
Figure 14. Graph showing total annual groundwater withdrawals on Long Island, New York, by county, for 1900–2015. Mgal/d, million gallons per day.

A. Source of consumption
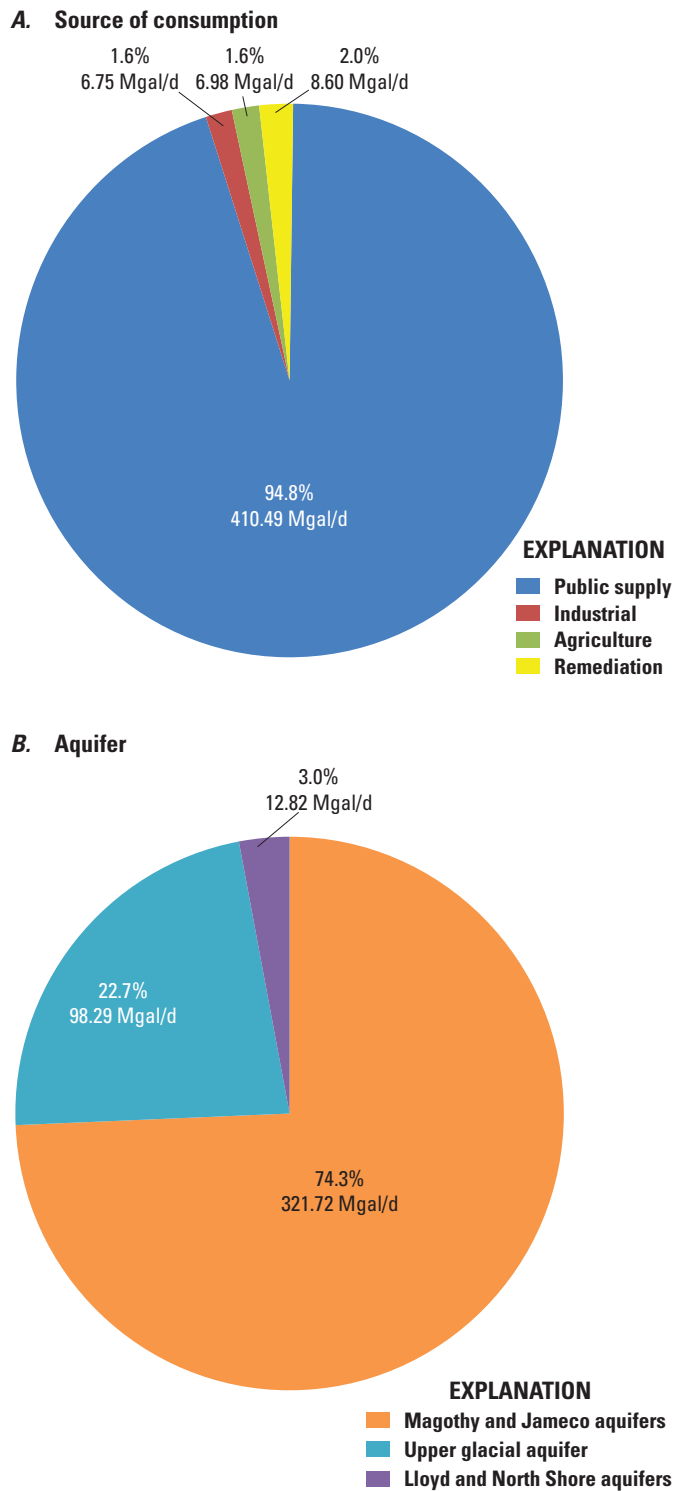
B. Aquifer

Figure 15. Graph showing total annual groundwater withdrawals *A*, by type of water use and *B*, by aquifer for conditions for 2005–15 on Long Island, New York. Mgal/d, million gallons per day; %, percent.

Hydrologic Data

Groundwater levels and streamflows have been measured throughout Long Island, with some measurements dating back to the early 1900s (U.S. Geological Survey, 2018). A total of 24,964 water-level and 65,471 streamflow measurements were obtained from the USGS National Water Information System (NWIS) database (U.S. Geological Survey, 2018) from 290 observation wells and 67 streamflow sites (fig. 17). These data were examined to identify wells and streamflow sites with sufficient data to suitably represent average hydrologic conditions for 2005–15. Data differed among the sites, with different periods of record and total number of individual observations.

The shallow Cretaceous and glacial aquifers generally are unconfined, and hydrologic conditions—water levels and streamflows—change in response to time-varying hydrologic stresses (pumping and recharge). Time-varying changes in water levels are greatest near regional groundwater divides inland of the coast. Water levels in well S5517, which is near a groundwater divide, were measured monthly from 1948 to 2015 and ranged from 32.3 ft in 1967 to 46.5 ft in 2010, mainly in response to changes in recharge (fig. 18). Daily mean streamflow in the Peconic River varied substantially from 1942 to 2015, also mainly in response to changes in recharge from a low of about 8 cubic feet per second (ft^3/s) in 1965 to a high of 81 ft^3/s in 2005. Although there is large variability in observed long-term water levels and streamflow measurements over time, the calibration of the numerical model described in this report is based on steady-state conditions and, therefore, requires observations that generally represent long-term average hydrologic conditions. The calibration period selected for this analysis is 2005–15, which generally represents a period of near-average hydrologic conditions, as indicated by time-varying recharge (fig. 11) and by water levels and streamflows (fig. 18). The average water level in well S5517 for the calibration period [2005–15] was within 0.65 ft of the long-term average for the period of record (1948–2015). Average streamflow in the Peconic River for 2005–15 differed from the mean for the period of record (1942–2015) by about 1.8 ft^3/s, or about 4.6 percent. The data confirm that the 2005–15 calibration period reasonably represents long-term average hydrologic conditions.

Most (205) observation wells are screened in the upper glacial aquifer. A total of 52 and 33 wells are screened within the Magothy and Lloyd aquifers, respectively. Water-level sites included wells measured monthly as part of USGS monitoring networks (200 wells) and partial-record wells where measurements are made sporadically (91 wells). Streamflow sites include real-time or continuous-record sites (17 sites), at which measurements are made regularly, and partial-record sites (50 sites), at which measurements are made sporadically (fig. 17). Mean and median values were computed for each water-level and streamflow site. These values were assumed

CONNECTICUT

72°W

73°W

74°W

NEW YORK

NEW JERSEY

Hudson River

Long Island Sound

ATLANTIC OCEAN

SUFFOLK

NASSAU

QUEENS

KINGS

41°30'N

41°N

40°30'N

0   5   10   15   20 MILES
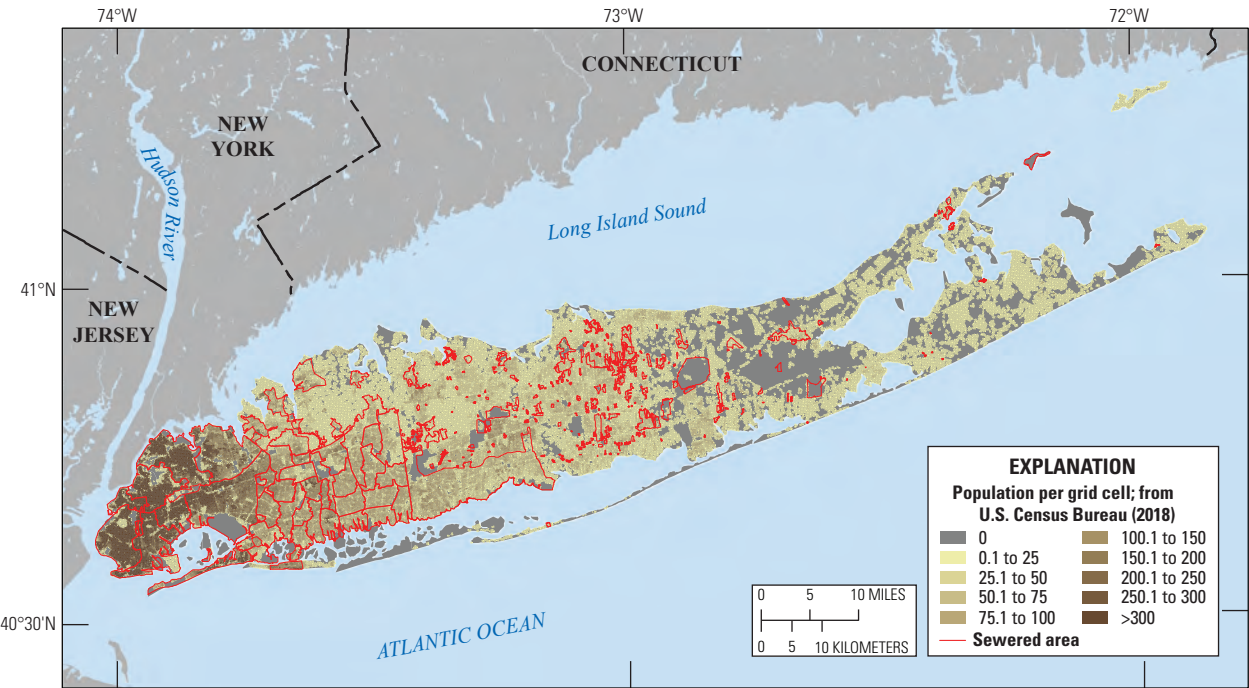
0   5   10   15   20 KILOMETERS

Base map from U.S. Geological Survey National Atlas digital data, scale 1:1,000,000
New York [Long Island] State Plane projection
North American Datum of 1927
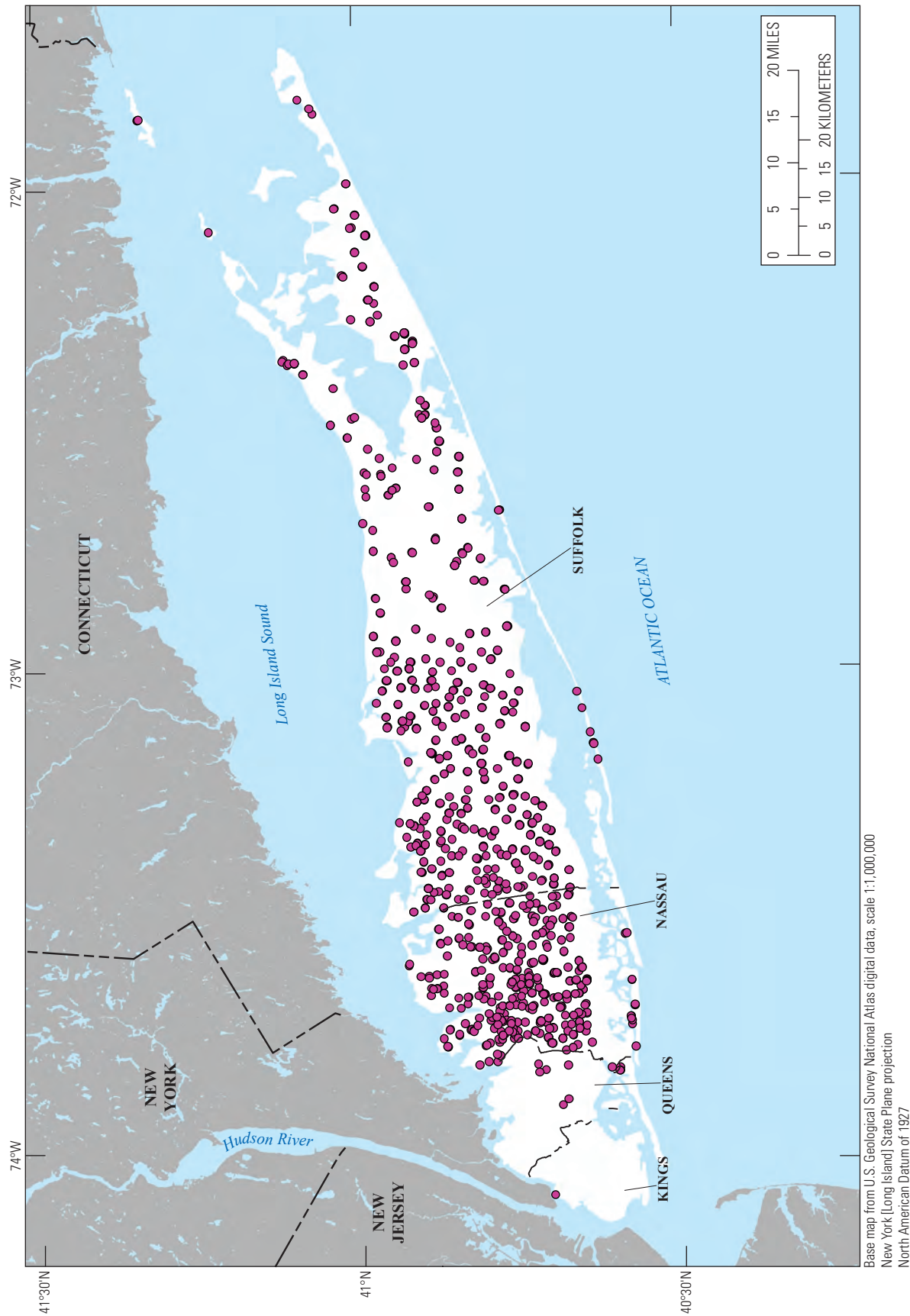
Figure 16.   Map showing location of groundwater withdrawals for 2005–15 on Long Island, New York.
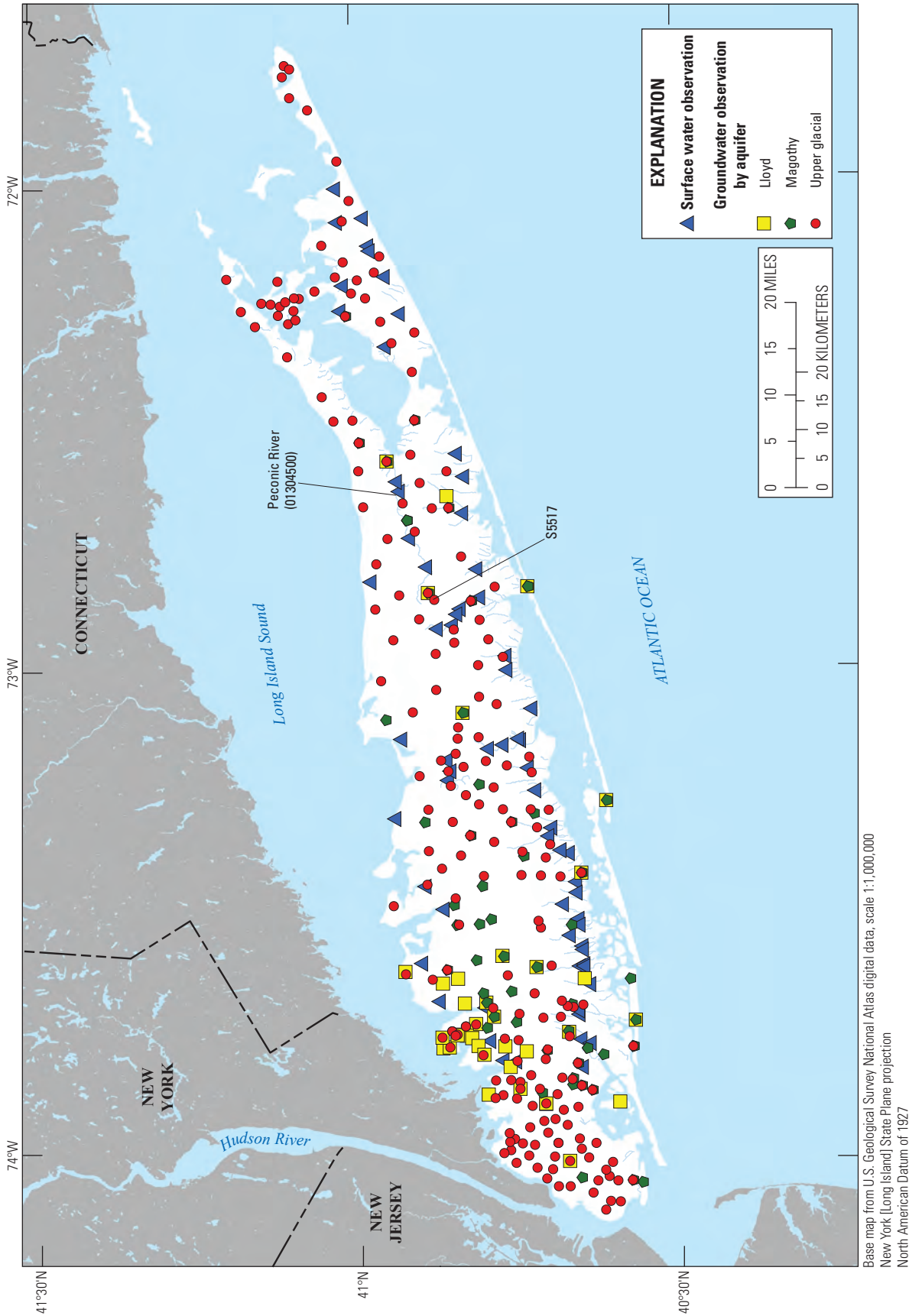
Figure 17. Map showing locations of observation wells and streamflow sites on Long Island, New York, grouped by hydrogeologic unit.
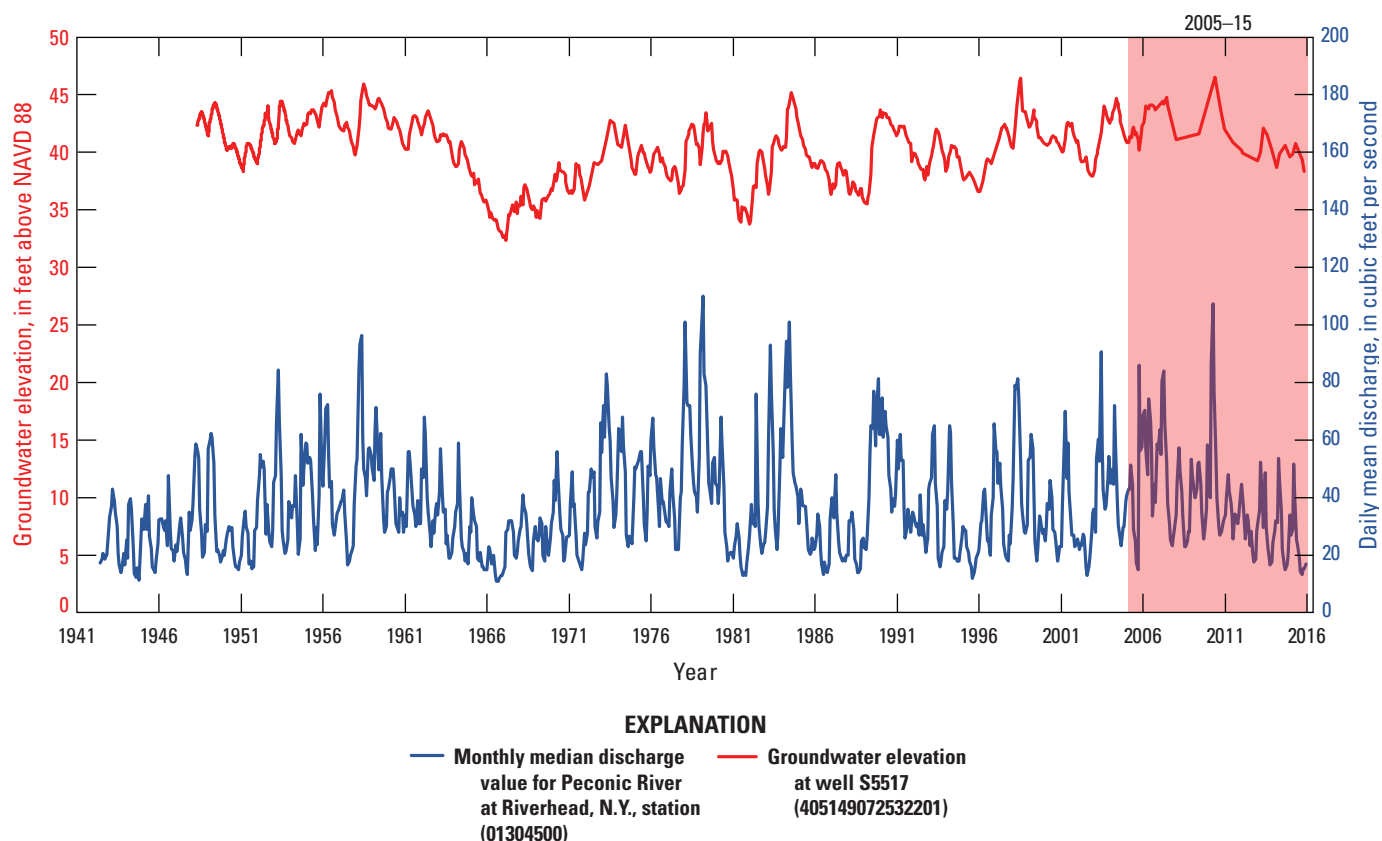
Figure 18.   Graph showing water levels in well S5517 and streamflow in the Peconic River (from U.S. Geological Survey streamgage 01304500; U.S. Geological Survey, 2018) from 1900 to 2015 on Long Island, New York. NAVD 88, North American Vertical Datum of 1988.

to represent steady-state conditions for 2005–15 for use in calibration of the numerical model, which requires observations that generally represent long-term average hydrologic conditions. The number of measurements for each water-level and streamflow site and the type of site—continuous-record or partial-record—were used as criteria for inclusion of mean or median water levels and streamflows in the model calibration.

Development and Calibration of the Numerical Model

Numerical models provide a means to synthesize existing hydrogeologic information into an internally consistent mathematical representation of a real system or process and, thus, are useful tools for testing and improving conceptual models or hypotheses of groundwater flow systems (Konikow and Reilly, 1998). A numerical model calibrated to reasonably match observed hydrologic conditions can be used to predict how a hydrologic system will respond to future changes in hydraulic stresses.

A three-dimensional finite-difference groundwater flow model of the Long Island aquifer system was developed using the USGS finite-difference modeling program MODFLOW–NWT (Niswonger and others, 2011), a modified version of

MODFLOW–2005 (Harbaugh, 2005) used to solve the three-dimensional groundwater flow equation using the Newton method. The USGS particle-tracking program MODPATH version 6 (Pollock, 2012) was used in conjunction with simulated cell-by-cell heads and flows calculated by MODFLOW–NWT to simulate advective transport in the aquifer, delineate the areas at the water table that contribute water to coastal and freshwater bodies and public-supply wells, and estimate total travel times of water from the water table to discharge locations. Parameters—including recharge, boundary leakances, and hydraulic conductivity—for the model were estimated by matching modeled and measured groundwater levels and streamflows using the inverse-modeling parameter estimation (PEST) software suite (Doherty and Hunt, 2010), based on averaged values of observation data from 2005 to 2015. A detailed description of the model parameter estimation process is presented in the "Model Calibration" section of this report.

The model archive for the numerical model (Walter and others, 2020) developed for this investigation contains the input and output files and the executable file needed to run the model. The archive also contains georeferenced files that can be used to display the finite-difference model grid as well as the hydrologic data—water levels and streamflow sites— used in calibration of the three-dimensional groundwater flow model.

Model Discretization

The finite-difference model grid consists of a grid of square model cells in which user-specified hydraulic parameters, model stresses, and boundary conditions are varied spatially. The conceptualization of how and where water enters, moves through, and leaves the aquifer system is critical to the development of an accurate flow model (Reilly, 2001). Boundary conditions are applied at some model cells to simulate hydrologic features, including wells, streams, and coastal waters. A detailed discussion of grid discretization, boundary conditions, and the use of finite-difference equations to simulate groundwater flow is presented in McDonald and Harbaugh (1988).

Spatial Discretization

The lateral extent of the shallow part of the active onshore modeled area of the Long Island aquifer system (fig. 19) is about 1,400 mi^2. The finite-difference grid for the numerical model consists of 348 rows and 1,309 columns of uniformly spaced model cells that are 500 ft on each side. The aquifer system was subdivided vertically from land surface to bedrock into 25 layers of variable thickness (fig. 20) to allow for the detail necessary to represent both vertical changes in the lithology and the screen zone thickness of the large-scale pumping wells throughout the Long Island aquifer system.

Each of the regional aquifers and confining units generally is represented as a separate layer in the model. Additional layers were added within the upper glacial and Magothy aquifers to provide a better representation of pumping well screen zones and to minimize the effects of weak sinks, which result in the overrepresentation of the capture zones to pumping wells as described in Pollock (2012). Where a hydrogeologic unit does not extend across a given layer, a zone with a minimum thickness of 1 ft was created, and the hydraulic properties of the overlying unit were applied in order to make the layer continuous across the entire model domain—a requirement of the finite-difference solution.

The hydrogeologic unit altitudes and extents that were used to represent the tops and bottoms of each layer were derived from a regional synthesis of the altitudes and extents of the surface layer of the hydrogeologic units developed by Smolensky and others (1989). Minor, local-scale revisions to the top surface of the Raritan clay were made near Bethpage using borehole data collected by the U.S. Department of the Navy as part of remedial investigations (Misut and others, 2020; Walter and Finkelstein, 2020). Additional information from subsequent geologic investigations along the northwestern shore of the island (Stumm, 2001) and on the North Fork (Schubert and others, 2004) also were used to develop model layering that better represents the hydrogeologic framework.

The upper glacial aquifer generally is represented by three model layers (fig. 20) and is simulated as unconfined. The top of the model (layer 1), which represents the shallow part of the upper glacial aquifer, is land surface derived from

light detection and ranging (lidar) data in onshore areas and the seabed derived from bathymetry in offshore areas (fig. 4). The top of layer 2, which explicitly represents previously mapped intraglacial clays (where present) is derived from the surface altitudes of those units (figs. 5 and 7B). The top of the underlying layer, representing deep parts of the upper glacial aquifer (fig. 20), is derived from the estimated bottom of the mapped intraglacial clays. Cells in layer 1 with thicknesses of less than 1 ft seaward by the freshwater/saltwater interface were specified to be inactive to remove laterally isolated offshore cells.

The top of layer 4, which explicitly represents the Gardiners clay, where present, is based on the mapped surface altitude of that unit (figs. 5B and 7A and B). Glacial sediments also are represented in deep layers of the model in areas where Cretaceous sediments are absent along the northern shore of the island and in deep erosional channels within the uppermost Cretaceous units. The top of layer 5 is the mapped surface altitude of the Jameco aquifer and, elsewhere, the contiguous Cretaceous aquifers—the Monmouth greensand and Magothy aquifer (figs. 6A and 7A and B). The bottom of layer 23 is the modified surface of the Raritan clay (fig. 6B). The bottoms of layer 5 and the intervening layers (6 through 22) were calculated as equal divisions of those two surfaces such that the Jameco aquifer and contiguous Cretaceous aquifers and the Jameco aquifer are represented by 19 model layers of equal thickness (fig. 20). The mapped extents and thicknesses of the Monmouth greensand and the Jameco aquifer were used to differentiate those units within the corresponding model layers. The Cretaceous sediments are separated from the overlying glacial sediments by an unconformity, and numerous erosional channels are incised into the surface of the Cretaceous sediments. Glacial sediments are represented within these channels and where the Cretaceous aquifers are absent. Shallow parts of the Pleistocene North Shore confining unit along the northern shore of Nassau County are contiguous with the Magothy aquifer and are represented in the corresponding model layers where the unit is present.

Layer 24 of the model explicitly represents the Raritan confining unit. The bottom of the layer is the mapped surface altitude of the underlying Lloyd aquifer (fig. 6C). Layer 25 represents the Lloyd aquifer. The bottom of the layer is the mapped surface altitude of the underlying crystalline bedrock (fig. 3). Layers 24 and 25 (fig. 20) represent Pleistocene sediments where both the Raritan confining units and Lloyd aquifers are absent (figs. 6B and C and 7A and B). The layer represents the deepest overlying unit present at a given location where one or both of the units are absent. The aquifer sediments become thin and are absent in a limited area along the northeastern shore of Queens County, where outcrops of bedrock occur. The model layers are thin but remain active in these areas to minimize potential model instability (fig. 20). This assumes that the shallow part of the bedrock is part of the unconsolidated aquifer system and the corresponding layers are simulated as having a very low transmissivity in this area.

A. **Upper glacial aquifer**
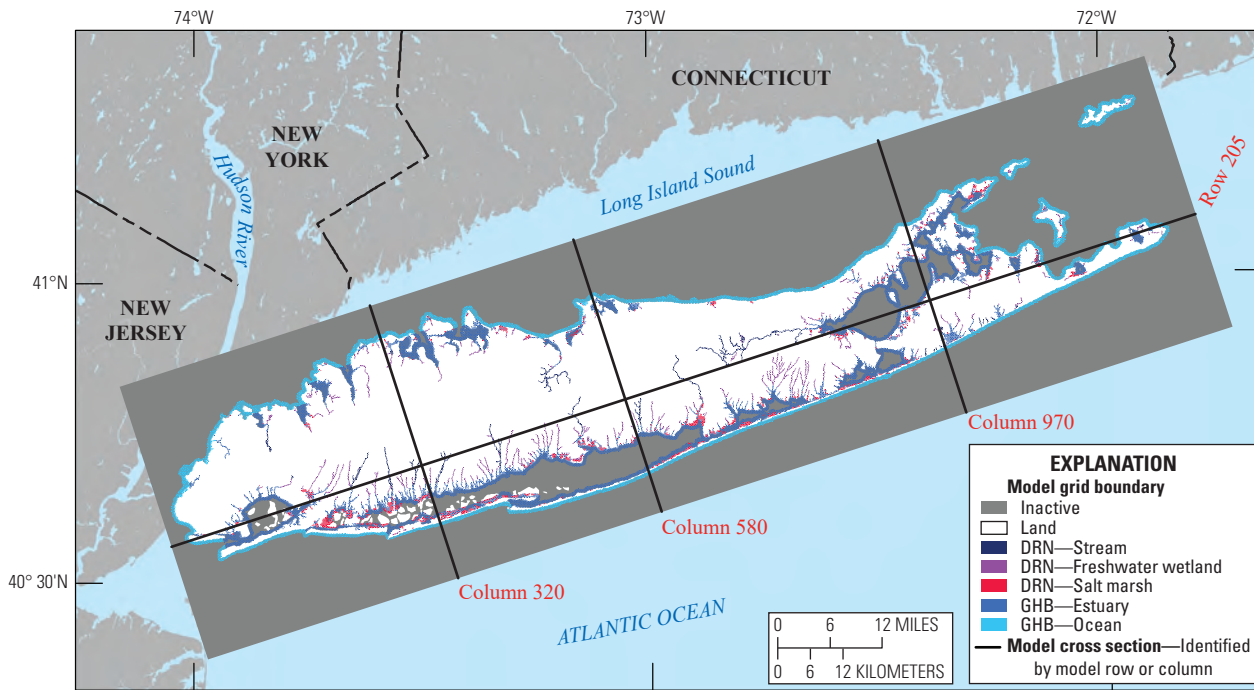
Base map from U.S. Geological Survey National Atlas digital data, scale 1:1,000,000
New York [Long Island] State Plane projection
North American Datum of 1988

B. **Magothy aquifer**
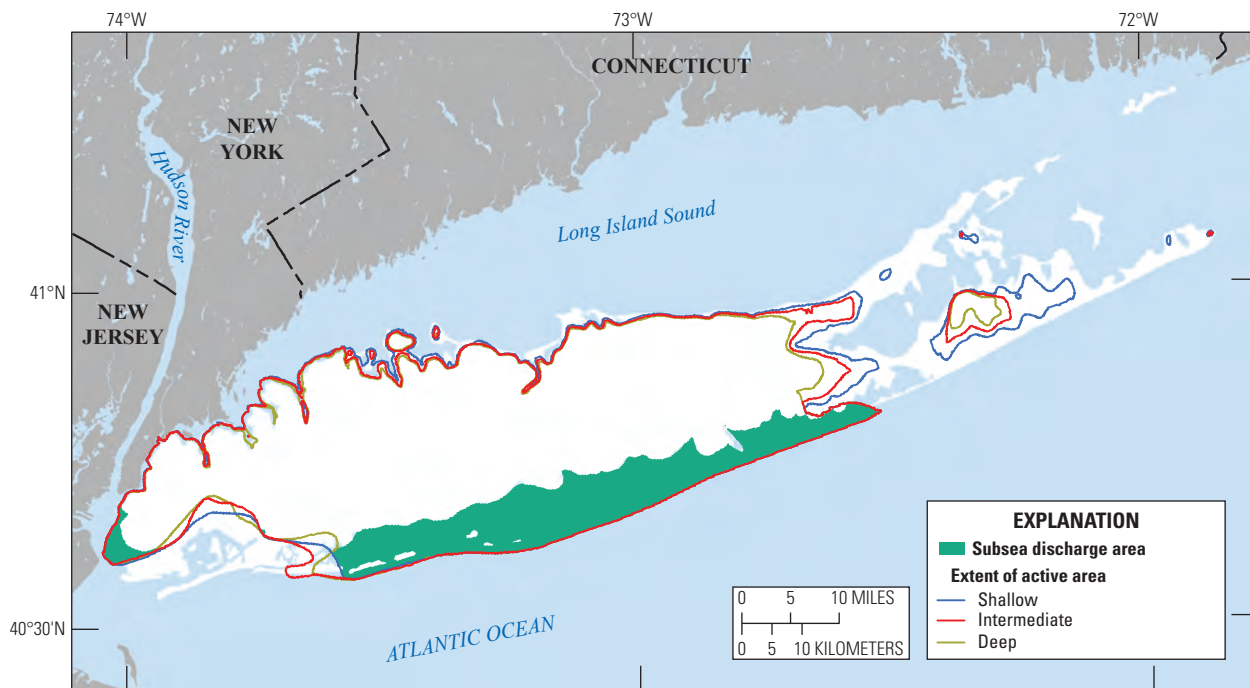
Base map from U.S. Geological Survey National Atlas digital data, scale 1:1,000,000
New York [Long Island] State Plane projection
North American Datum of 1988

Figure 19.   Maps showing extents of *A*, model grid, active area, and hydrologic boundaries in the upper glacial aquifer, and of active area and locations of subsea discharge boundaries in *B*, the Magothy aquifer and *C*, the Lloyd aquifer on Long Island, New York. DRN, Drain package of the U.S. Geological Survey finite-difference modeling program MODFLOW (McDonald and Harbaugh, 1988); GHB, General Head Boundary package of MODFLOW (McDonald and Harbaugh, 1988).

C. **Lloyd aquifer**

Base map from U.S. Geological Survey National Atlas digital data, scale 1:1,000,000
New York [Long Island] State Plane projection
North American Datum of 1927
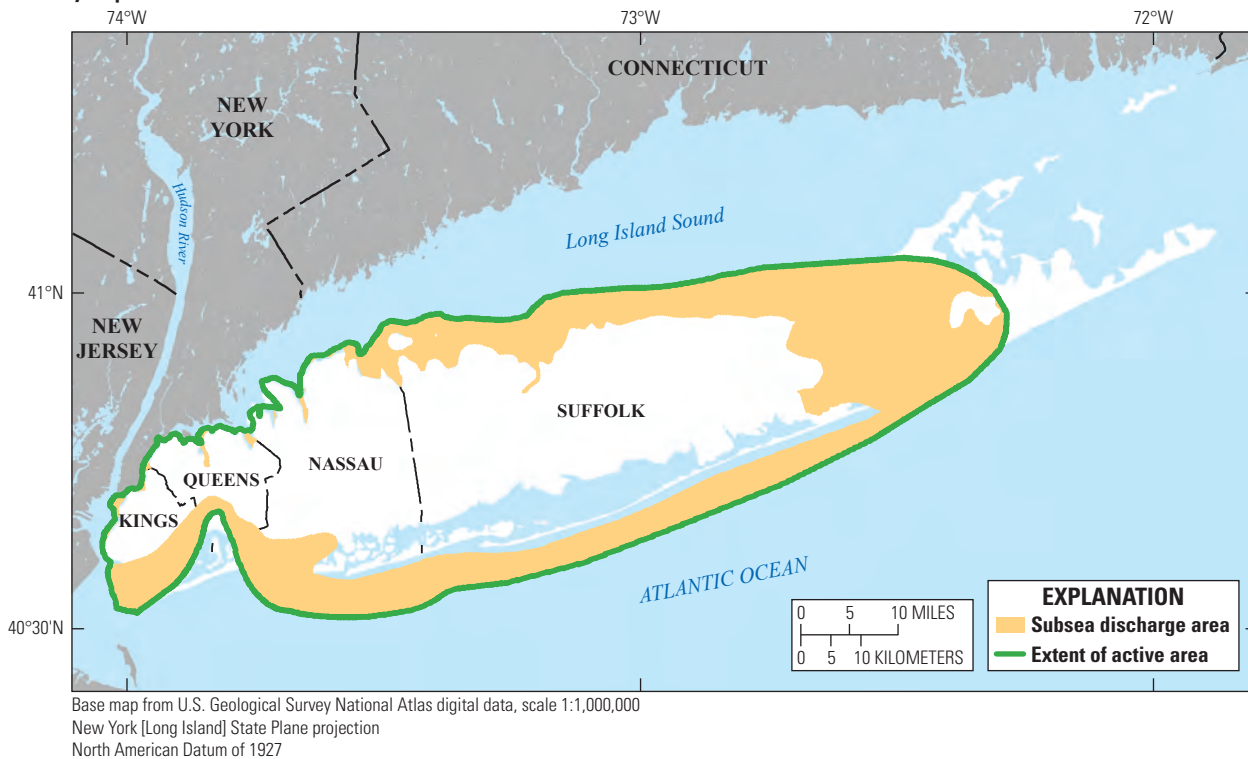
Figure 19.   —Continued

Temporal Discretization

Hydrologic stresses—groundwater withdrawals and aquifer recharge—were simulated for current, average conditions for 2005–15. Pumping stresses in the Long Island aquifer system have varied considerably in time and space since the beginning of large-scale pumping in 1900. However, total withdrawal amounts have leveled off since the mid-1980s and, thus, the 2005–15 period appears to be representative of long-term average pumping for the past 30 years (fig. 14). A comparison of the average aquifer recharge for 2005–15 with the long-term average for 1900–2015 also indicated that 2005–15 is representative of long-term average conditions (fig. 18).

Hydrologic Boundaries

The hydrologic boundaries in the groundwater flow model are defined as the areas from which and the method by which all the waters entering and leaving the numerical model are specified. The Long Island aquifer system is bounded below by bedrock and laterally by the interface between fresh and saline groundwater (the freshwater/saltwater interface). The upper boundary of the active modeled area is the water table, which is a free-surface boundary that receives spatially variable recharge. The Recharge (RCH) package of the USGS three-dimensional finite-difference groundwater model

MODFLOW (McDonald and Harbaugh, 1988) was used to spatially model how recharge is distributed across the water table.

Surface-water features are represented as head-dependent flux boundaries (fig. 19A). Coastal waterbodies, including tidal rivers, estuaries, and open coastal waters, are represented using the General Head Boundary (GHB) package for MODFLOW (McDonald and Harbaugh, 1988); salt marshes and fresh surface waters, which include streams, wetlands connected to streams, and pond outlets, are represented (fig. 19A) using the Drain (DRN) package for MODFLOW (McDonald and Harbaugh, 1988). Coastal boundaries were determined using the coastal geometry as determined from 1:24,000-scale digitized linework. The boundaries were modified by visual inspection of aerial photographs to address anomalies and ensure consistency between simulated boundaries and actual conditions. Seabed altitudes in saltwater boundaries were specified freshwater-equivalent heads relative to the mean seabed altitudes within each model cell representing a boundary, as determined from bathymetric data (Danielson and Haines, 2017). The height of the saltwater column used to estimate freshwater-equivalent heads was the difference between the estimated seabed altitude and 0 ft MSL (NAVD 88). Streams and wetland boundaries were determined by 1:24,000-scale hydrography followed by visual inspection of aerial photographs. Boundary altitudes in streams were specified to be the minimum lidar value within each 500-ft boundary cell that represents a stream; boundary altitudes in
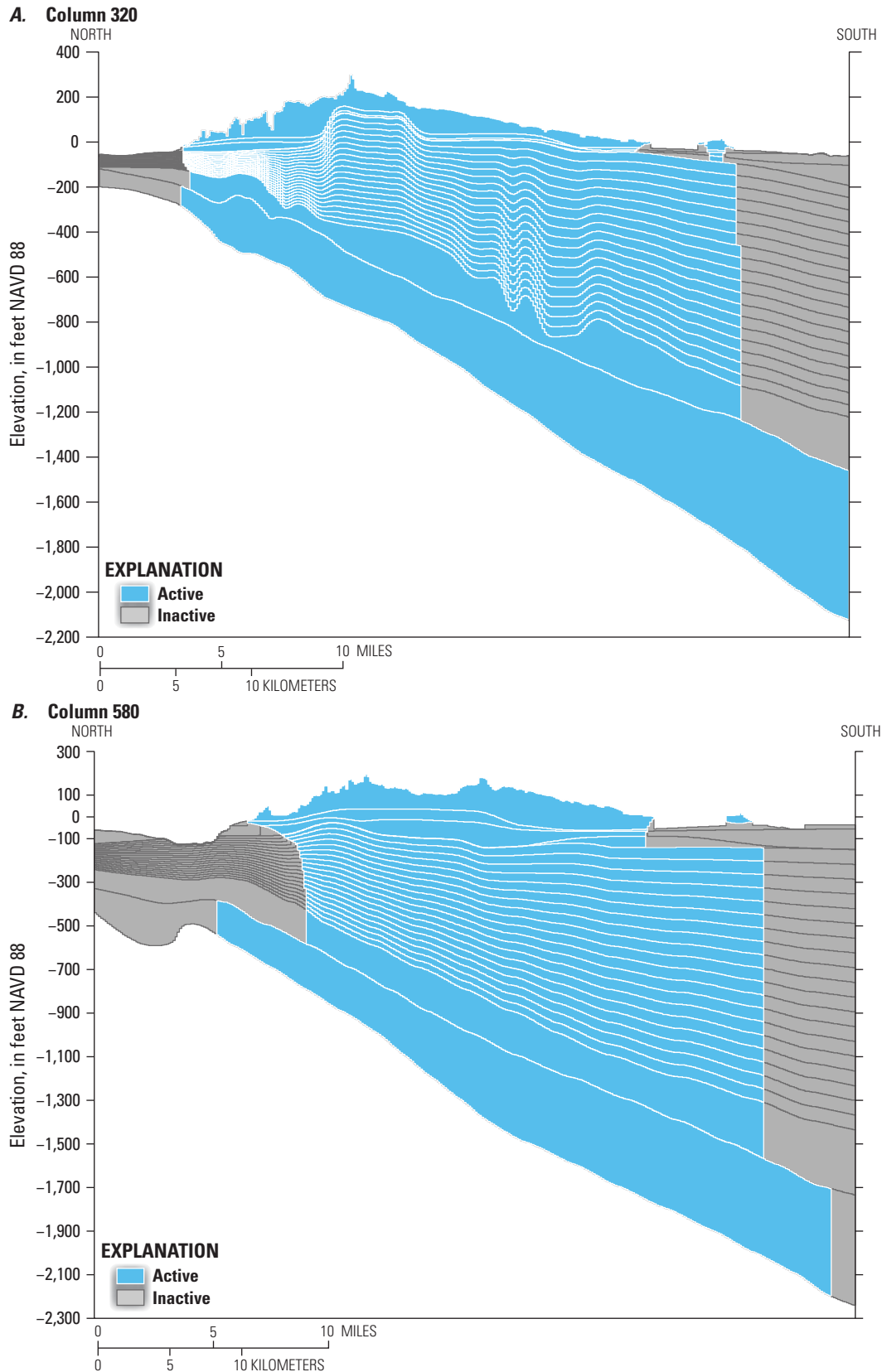
Figure 20. Sections showing vertical layering along *A*, column 320, *B*, column 580, *C*, column 970, and *D*, row 205 of the three-dimensional numerical model of the Long Island aquifer system. Locations of sections shown in figure 19*A*.
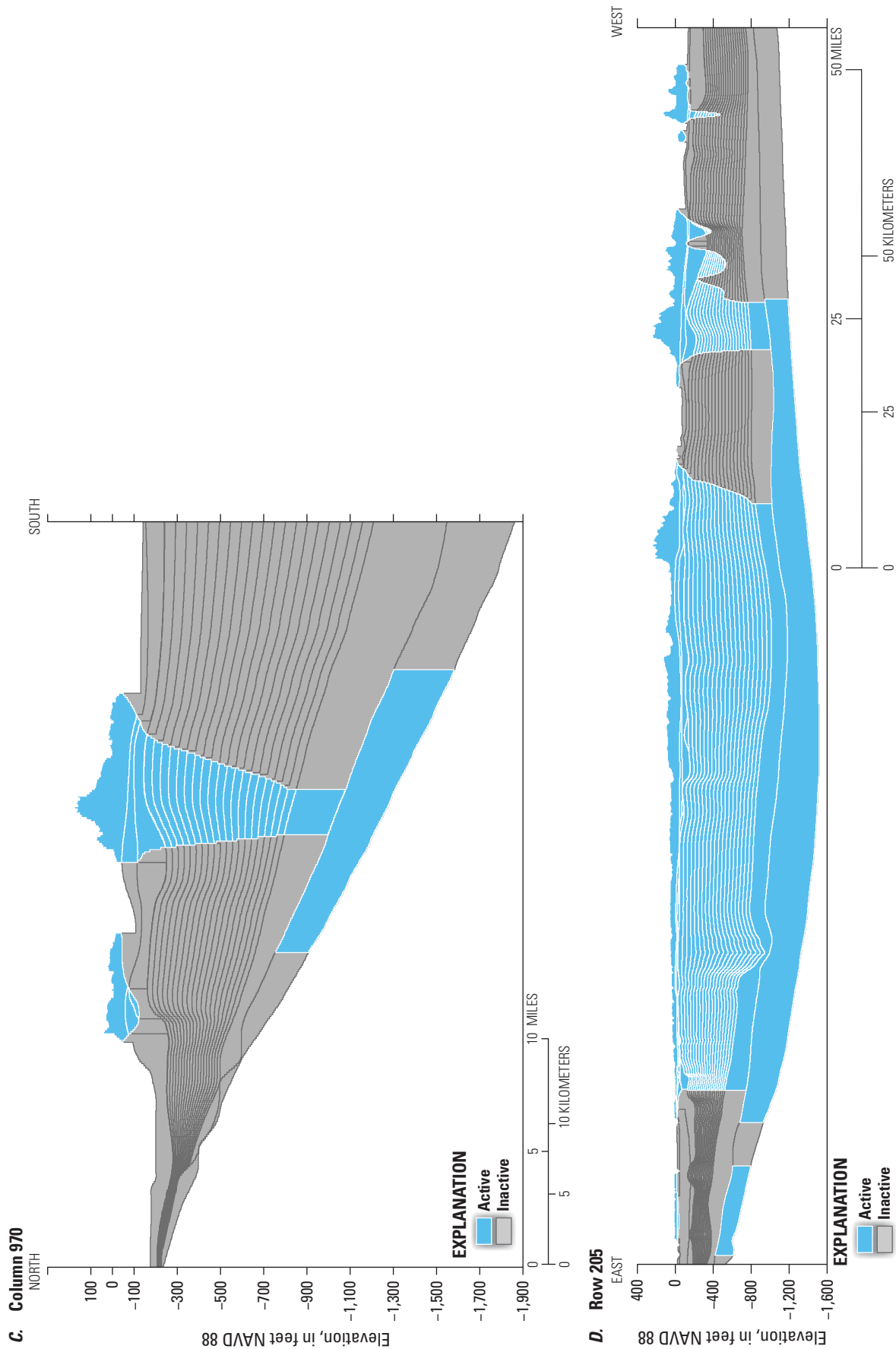
Figure 20.   —Continued

freshwater wetlands and salt marshes were specified to be the mean lidar value in cells representing those features. Freshwater and saltwater discharge boundaries were assigned to the top layer of the model (layer 1); the top of layer 1 was specified to be the seabed and streambed altitudes in these locations. Unlike the GHB package, the DRN package does not allow streams influenced by pumping to serve as an infinite source of water to the underlying aquifer; instead, streams represented with the DRN package can only receive groundwater discharge; once the water level in the aquifer falls below the specified streambed altitude in the DRN cells, groundwater no longer discharges to the surface waters.

The lateral boundaries in layers 4 through 25 are defined by the inferred position of the freshwater/saltwater interface. Taken together, these layers represent pre-Wisconsin sediments, except where Cretaceous and pre-Wisconsin Pleistocene sediments are absent, and the layers represent glacial sediments. The seaward extents of fresh groundwater (fig. 8) are represented as no-flow boundaries generally based on isochlor delineations estimated for each hydrogeologic unit in the Long Island aquifer system (Charles, 2016; Stumm and others, 2020).

The modeled extent of freshwater in the Magothy aquifer was determined using mapped isochlors, the estimated altitude of the freshwater/saltwater interface, and such ancillary information as the location of water-supply wells in the unit. The extent of freshwater within the Magothy aquifer generally is based on mapped 10,000-mg/L isochlors (fig. 8A; Charles, 2016) and 5,000 mg/L isochlors (fig. 8A; Stumm and others, 2020). The active modeled areas within those model layers representing the Magothy aquifer varies with depth. The lateral extent of the Magothy aquifer in areas where it is unconfined is determined by the altitude of the freshwater/saltwater interface as computed from the 2010 water table (Monti and others, 2013). Model cells in which the computed interface altitude is above the top of the model cell are specified to be inactive, and therefore, the seaward extent of the active modeled area decreases monotonically with depth (fig. 19B).

The eastern extent of freshwater as initially estimated from mapped 5,000-mg/L isochlors was extended by including areas where the mapped isochlors suggested salty groundwater but where the computed interface altitude is below the top of the Raritan Formation. The eastern extent of freshwater also was extended by including areas developed for water supply that were mapped as salty (fig. 8A). The modeled extent of the Magothy aquifer along the southern shore of central and eastern Long Island, where it is confined by the Gardiners clay, is defined by a 10,000-mg/L isochlor (Charles, 2016) and is assumed to be vertical and coincident across all the model layers representing the unit. The modeled extent of the Magothy aquifer in southern Kings and Queens Counties is determined by separate isochlors for the shallow, middle, and deep parts of the Magothy aquifer (Stumm and others, 2020). The seaward extent of freshwater in areas where the Magothy aquifer is unconfined is determined by the altitude of the interface as computed from water-table altitudes (fig. 8A) and the altitude of the seabed.

The active modeled area of the Lloyd aquifer (fig. 19C) generally is based on mapped 5,000- and 10,000-mg/L isochlors (fig. 8B; Charles, 2016; Stumm and others, 2020). The Lloyd aquifer is represented as a single model layer, so the interface is vertical. The Lloyd aquifer is confined throughout its extent and freshwater generally is assumed to extend further offshore than in the overlying Magothy aquifer (figs. 3 and 19B and C).

The freshwater/saltwater interface is assumed to be displaced seaward under confined conditions, as in parts of the Magothy aquifer, along the southern shore, and in the underlying Lloyd aquifer. The overlying confining units are assumed to be freshwater but are, in turn, overlain by salty groundwater seaward of the shore in most areas. Discharge from confined aquifers where they are overlain by salty groundwater is referred to as subsea discharge. Areas of subsea discharge in the Magothy aquifer generally are limited to the southern shore where the unit is confined by the Gardiners clay and that confining unit in turn is overlain by salty groundwater in the upper glacial aquifer (fig. 19B). The freshwater/saltwater interface in the Lloyd aquifer is displaced further seaward in most areas and the extent of subsea discharge is broader than in the overlying Magothy aquifer, particularly on eastern Long Island (fig. 19C). Discharge from confined aquifers is at the seabed where all the overlying units have fresh groundwater.

The GHB package was used as a means for allowing freshwater to discharge at depth through subsea discharge. This head-dependent flux boundary condition was applied to the top of the underlying aquifers where there is seaward displacement of freshwater beneath the Gardiners clay confining unit (model layer 5) and beneath the Raritan and North Shore confining units (layer 25; fig. 19). The boundary altitudes specified in these areas were the freshwater equivalent heads as estimated from the top of the overlying confining unit. The overlying confining units are specified to be inactive in these areas and, therefore, are represented implicitly by the subsea discharge boundaries.

In highly urbanized areas of New York City, groundwater potentially infiltrates into leaky or failing infrastructure (Misut and Monti, 1999). Groundwater is most likely to be intercepted by infrastructure in areas with a shallow depth to water and a densely urbanized land use. This process was accounted for in the model by using the DRN package to implicitly represent these features in areas where the water table as defined in 2010 was within 10 ft of land surface and the overlying land surface was predominantly impervious, suggesting the potential for the interception of groundwater by subterranean infrastructure, such as stormwater and wastewater conveyances. The exact location of these features, referred to as urban drains, is unknown, but the specification of urban drains in the model provides a mechanism for the potential removal of water below the specified depth to subterranean infrastructure. Water only discharges to these features where the simulated water table is less than 10 ft from land surface.

Ponds are surface-water features represented by infinite horizontal and vertical hydraulic conductivity values of 50,000 and 5,000 ft/d, respectively. This modeling

method allows simulated ponds to respond to changes in hydraulic stresses and reasonably creates the hydraulic gradients observed upgradient and downgradient from flow-through ponds.

Initial estimates of boundary leakances differed by boundary type and were equivalent to values obtained from vertical leakances (which are analogous to vertical hydraulic conductivity) that are generally typical of the bottom sediments likely present in each type of boundary: 0.1 ft/d for estuaries, 0.2 ft/d for open coastal waters, and 1 ft/d for streams. The resistance to flow across the boundaries was a function of seabed or streambed sediment thickness and leakance, both of which are largely unknown. The initial values were adjusted during model calibration to achieve an optimal fit to observed heads and streamflows. The hydraulic conductance of subsea discharge boundaries was based on the 0.001-ft/d previous estimate of the vertical hydraulic conductivity of the overlying confining units (Buxton and Smolensky, 1999). Leakances in urban drains are unknown but were specified to be comparatively high (10 ft/d) to allow for the ready discharge of water into these potential receptors.

Hydraulic Properties

The initial values of horizontal and vertical hydraulic conductivity were derived from the lithologic texture model (Walter and Finkelstein, 2020) for the upper glacial and Magothy aquifers. The numerical model uses the same grid dimensions and discretization as the texture model so that no spatial averaging was required to map the estimated hydraulic conductivity for each texture-model layer to the two-dimensional model grid for each layer. The texture model has a vertical resolution of 10 ft, whereas numerical model layers can exceed 100 ft in the upper glacial aquifer and are as thick as 60 ft in the Magothy aquifer (fig. 20). Hydraulic conductivities—horizontal and vertical—from the lithologic texture model were vertically mapped to the numerical model layers in each cell by computing the thickness-weighted mean of values from the texture model for each coincident model layer. An arithmetic mean was computed for horizontal hydraulic conductivity, and a geometric mean, for vertical hydraulic conductivity.

Spatial patterns in initial hydraulic conductivity are like those in the texture model (fig. 9). Generally lower initial hydraulic conductivities are present in northern and central parts of the island, associated with moraines and ice-contact deposits, and generally higher hydraulic conductivity values are present in southern parts of the island, associated with outwash deposits (fig. 21A). There are few broad spatial patterns in the hydraulic conductivity of the Magothy aquifer, which has a complex depositional history. Vertical patterns in hydraulic conductivity generally reflect observed geologic trends in the upper glacial and Magothy aquifers (fig. 22A and B). The largest hydraulic conductivity values within the upper glacial aquifer are within outwash deposits, and the lowest hydraulic

conductivity values generally are within glacial moraines. The largest values of hydraulic conductivity in the Magothy aquifer are in the basal part of the unit, which was deposited in higher-energy environments; the lowest values of hydraulic conductivity generally are in the middle part of the Magothy aquifer, which is a zone with large amounts of lignite, suggesting deposition in low-energy environments.

Simulated hydraulic heads and cell-by-cell flow rates can facilitate particle-tracking analyses to delineate recharge areas and travel times in an aquifer. The porosity of aquifer sediments does not affect simulated heads and flows but is an important control on groundwater velocity and travel times. Specified porosities of the aquifer sediments range from 0.25 to 0.5 and vary by hydrogeologic unit. Sediments in the upper glacial aquifer were assumed to have a porosity of 0.35, consistent with porosity values observed in glacial outwash sediments in nearby Cape Cod, Massachusetts (Garabedian and others, 1988). Intraglacial clays were assigned a porosity of 0.4. Cretaceous aquifer sediments generally have a lower hydraulic conductivity and, presumably, porosity than do glacial sediments and were assigned a porosity value of 0.25. Cretaceous and Pleistocene confining units have much lower hydraulic conductivity but were assumed to have a higher porosity of 0.5. Ponds and surface-water impoundments were assigned a porosity of 1.0.

Hydraulic Stresses

The hydrologic stresses simulated in this model are recharge (from both precipitation and anthropogenic return flow) and groundwater withdrawals. Anthropogenic return flow includes wastewater return flow from onsite domestic septic systems in unsewered areas, rejected recharge from the rerouting of overland flow on impervious surfaces to retention or recharge basins, and water from leaky infrastructure in the more developed areas of Long Island. Groundwater withdrawals include those for commercial, domestic, industrial, and public supply uses. Both recharge and groundwater withdrawal stresses represent average conditions for 2005–15.

Recharge

Recharge into the model was simulated by use of the Recharge (RCH) package (McDonald and Harbaugh, 1988). The spatial variability of natural recharge arising from vegetation, soil type, and water capacity as computed using the SWB model is represented as multipliers within the modeled area. Recharge into the model was determined by applying these multipliers to a single scaling parameter that can facilitate a change in total recharge into the model while preserving the spatial variability determined from the SWB model; this scaling parameter was adjusted during model calibration. Additional spatial adjustment of recharge was facilitated by use of recharge parameters, represented as pilot points (fig. 23).

A. **Model layer 1**
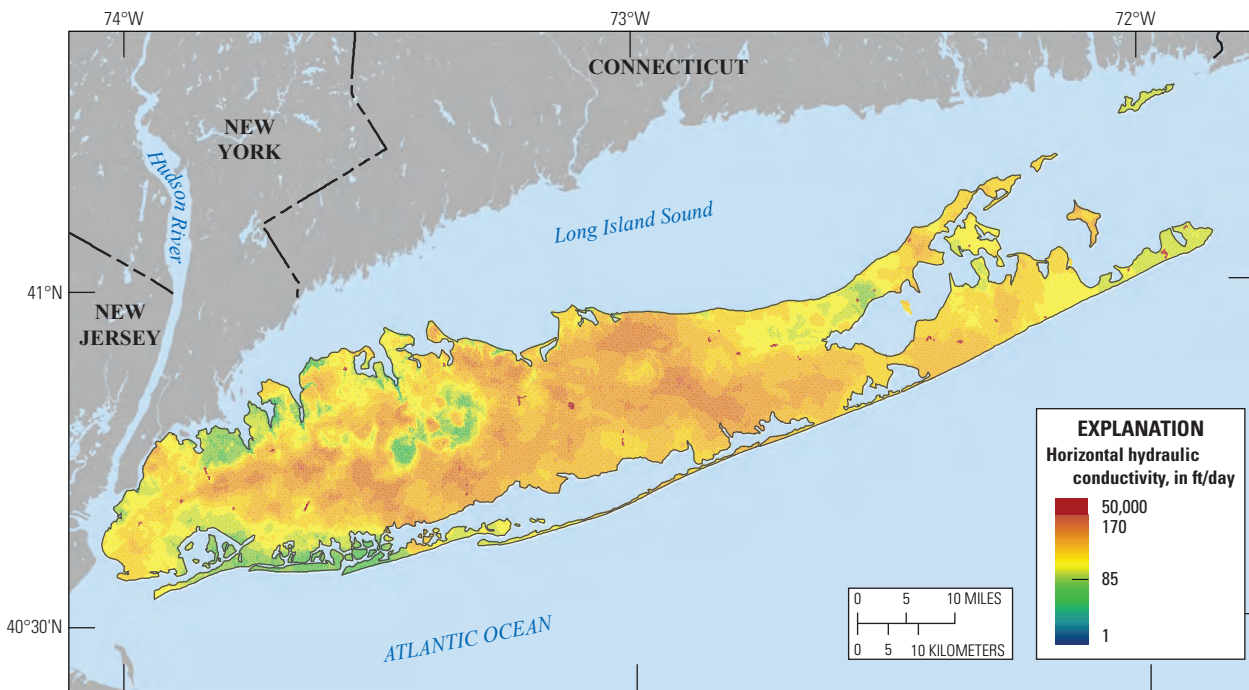
Base map from U.S. Geological Survey National Atlas digital data, scale 1:1,000,000
New York [Long Island] State Plane projection
North American Datum of 1988

B. **Model layer 23**
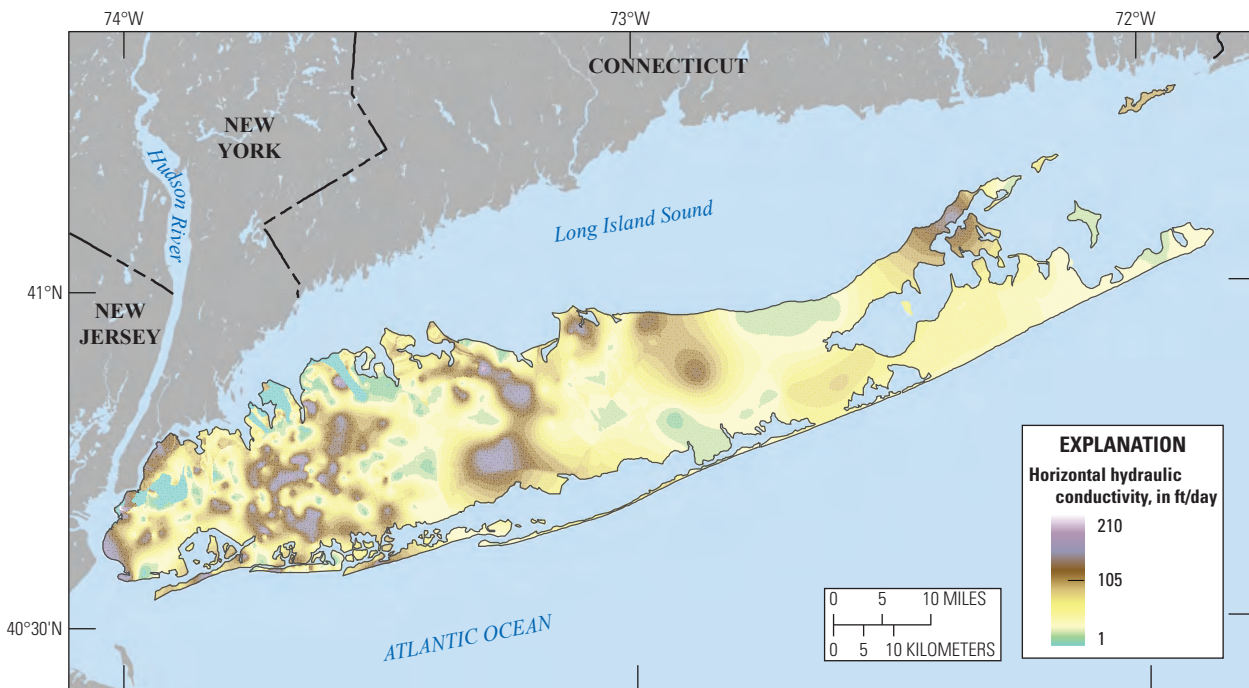
Base map from U.S. Geological Survey National Atlas digital data, scale 1:1,000,000
New York [Long Island] State Plane projection
North American Datum of 1988

Figure 21. Maps showing initial hydraulic conductivity for *A,* the upper glacial aquifer (near sea level; model layer 1) and *B*, the lower part of the Magothy aquifer (model layer 23), as mapped to the numerical model grid representing Long Island, New York. ft/day, foot per day.

Figure 22.   Sections showing the vertical distribution of estimated hydraulic conductivity *A*, along a north-south section and *B*, along an east-west section, as mapped to the numerical model grid representing Long Island, New York. Locations of sections shown in figure 19*A*.

Base map from U.S. Geological Survey National Atlas digital data, scale 1:1,000,000
New York [Long Island] State Plane projection
North American Datum of 1927

Figure 23.   Map showing locations of pilot-point parameters for recharge in the regional model of Long Island, New York.

All sources of anthropogenic return flow were included as additional sources of recharge represented in the RCH package. As with natural recharge, these spatially variable recharge values were represented as arrays of multipliers to which single-scaling parameters were applied; this allows for adjustment of these anthropogenic recharge rates during the model calibration process while preserving the desired spatial variability.

Groundwater Withdrawals

During the simulation period, there were 1,680 wells withdrawing water from the Long Island aquifer system for a variety of uses, including public supply, contaminant remediation, and industrial uses. These pumping wells, which are represented by a specified-flux boundary condition, were simulated by the Well (WEL) package (McDonald and Harbaugh, 1988). The pumping well locations, screened intervals, and pumping rates were obtained from the NWIS database (U.S. Geological Survey, 2018) and supplemented by additional water-use data provided by the New York State Department of Environmental Conservation (written commun., 2017). The pumping rates for all wells simulated in the model were averaged for the 2005–15 period.

Model Calibration

The regional model of Long Island was calibrated by adjusting model input parameters—hydraulic conductivity, boundary leakances, and recharge—to yield simulated equivalents of hydraulic heads and streamflows that reasonably match observed long-term water levels and streamflows. The inverse calibration modeling software package PEST version 9 (Doherty, 2010) was used to calibrate the model. More traditional trial-and-error methods can be used to produce calibrated models that reasonably match observed hydrologic conditions; however, the resulting parameters are highly nonunique, and the match to observed conditions does not represent a statistical best fit.

Inverse Calibration

Inverse calibration methods can estimate a set of parameters that represent a statistical best fit to observed hydrologic conditions by use of nonlinear regression. It should be noted that while inversely calibrated models produce a s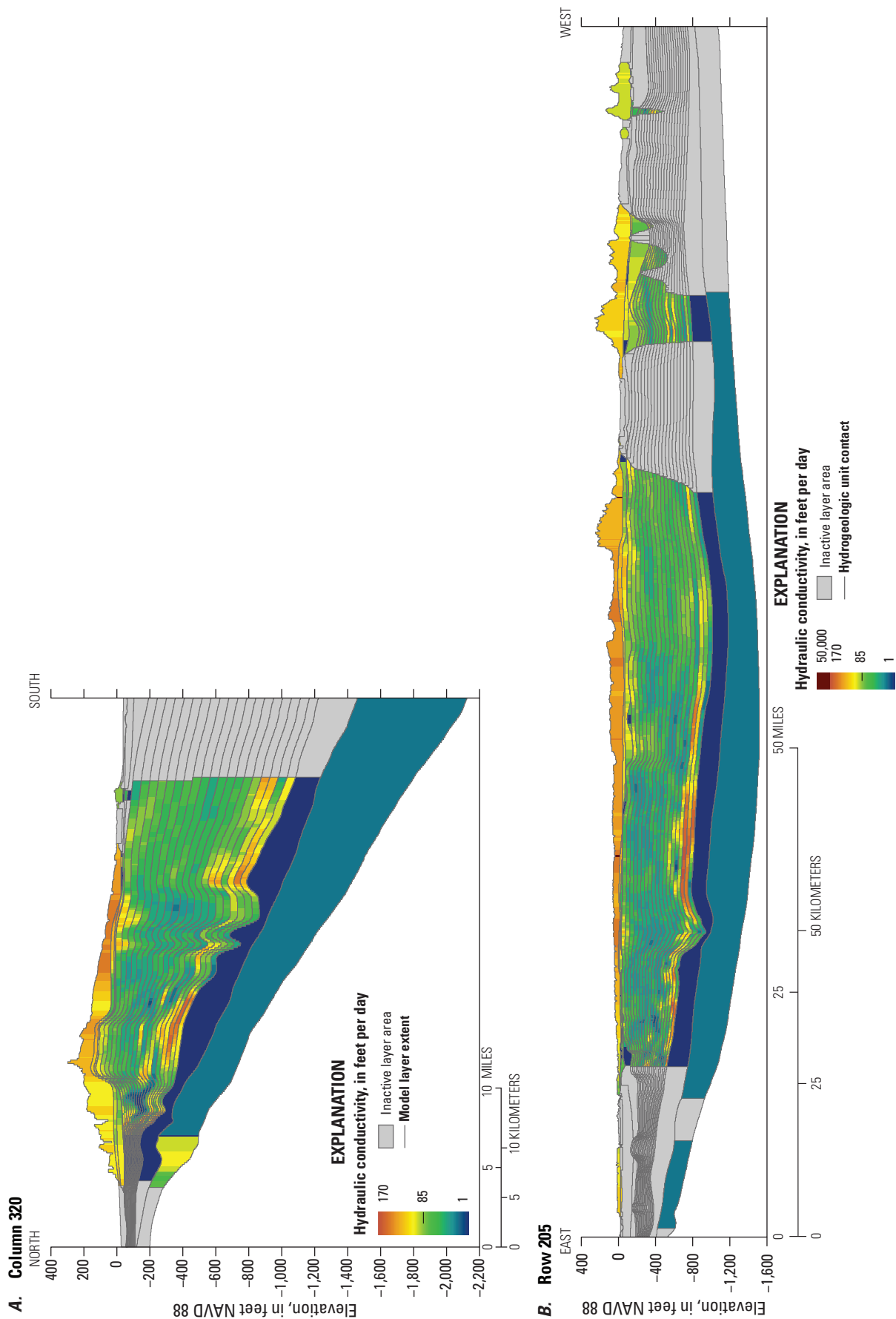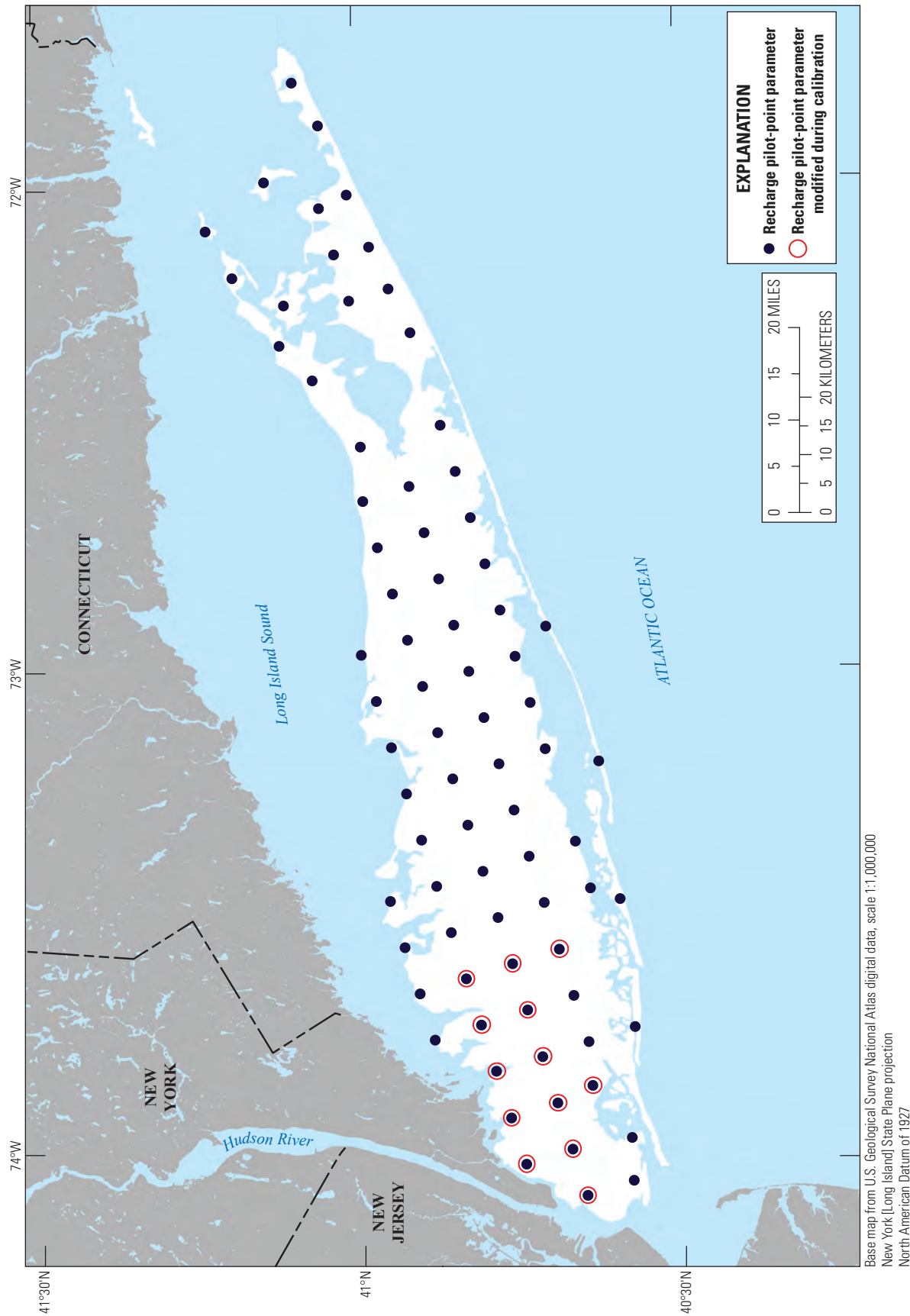tatistical best fit to observations, the estimated parameters are a function of the location and types of observations, weights applied to those observations, and prior information on aquifer properties used in the regression. Calibration of the Long Island regional model involved a two-step process: (1) inverse calibration to estimate the subset of parameters that yield the optimal model fit to observations of hydraulic heads and flows that is in balance with adherence to prior geologic knowledge and (2) additional adjustment of model parameters to either improve

model fit in selected areas or to adjust any model inputs that are outside a range of values considered reasonable. Step 1 produces the inversely calibrated model and step 2 modifies that model to ensure reasonable model inputs and produces the final, calibrated model.

Inverse calibration methods determine the model parameters that best fit a given set of observations using an iterative form of Gauss-Levenberg-Marquardt nonlinear regression to minimize an objective function (Levenberg, 1944; Marquardt, 1963). The objective function formulates the weighted fit between observations and simulated equivalents and can include prior information on aquifer characteristics. Two sets of tasks are required to utilize inverse calibration methods in model calibration: definition of model parameters that can be adjusted between regression iterations and conversion of observations to a form for which simulated equivalents can be computed from the model. In this analysis, PEST (Doherty, 2010) was used to calibrate the regional model of Long Island. The software package allows for the use of highly parameterized model inputs, can incorporate prior geologic knowledge, and has a large degree of flexibility in defining observations and associated weights.

A Levenberg-Marquardt nonlinear regression is a gradient-based modified Gauss-Newton technique that minimizes the weighted misfit between observations and model-calculated equivalents. The nonlinearity typical of a groundwater system requires an iterative approach to minimization. Observation sensitivities with respect to each parameter are computed by perturbing (by 1 percent) individual parameters and evaluating the change in simulated equivalents for each observation; this process requires a model run for each parameter and results in a matrix of sensitivities, referred to as a Jacobian matrix. The Jacobian matrix is computed initially and updated between successive iterations to guide the nonlinear regression. Exploratory runs between each iteration are performed to determine the local objective function gradient, update parameter values, and lower the value of the objective function. This process is repeated until updated parameters change by less than the specified closure criterion (typically 1 percent) and the regression is complete.

Singular-value decomposition (SVD) is used to improve stability in regressions by including large numbers of parameters to suppress variability of insensitive parameters based on a user-defined range of eigenvalues (analogous to sensitivities) from SVD performed on the weighted Jacobian matrix (Doherty and Hunt, 2010). In addition, the SVD-based parameter estimation methodology SVD–Assist of PEST (Tonkin and Doherty, 2005) is used to more efficiently manage model run times by reducing the number of parameters to fewer linear combinations of parameters, referred to as superparameters. Application of SVD–Assist assumes that the model generally is linear and that a full Jacobian matrix does not need to be computed for each successive iteration of the regression.

Model Parameterization

Model inputs were expressed as parameters to facilitate an inverse calibration of model characteristics to observed steady-state hydrologic conditions. Three types of model parameters were included in the inverse calibration: recharge, boundary leakances, and hydraulic conductivity (horizontal and vertical). The parameters were assigned upper and lower constraints that reflected a range of values that would be considered reasonable based on prior understanding of the hydrologic system.

Recharge

Natural recharge to aquifer sediments is represented in the model as a specified stress that is the product of the array of recharge values estimated with the SWB model (fig. 13A) and a single scaling parameter; a recharge scaling value of 1.0 results in a specified recharge rate that is equal to that estimated from the SWB model. A change in the parameter changes the simulated recharge rates in the model but preserves the spatial variability of the recharge. Recharge generally is about half or more of precipitation, which averages about 48 in/yr on Long Island. Recharge estimated from the SWB model averaged 19.9 in/yr, lower than what would generally be expected in coastal aquifers of the northeastern United States (Walter and others, 2018). Inverse calibration generally performs better when initial parameter values are close to those expected. An initial value of the recharge-scaling parameter was specified to be 1.3, which results in a mean specified recharge of rate of 25.8 in/yr, closer to values expected in the Long Island aquifer system. An upper and lower constraint of 0.8 and 1.5, which represent the range that a parameter can vary to an inverse calibration, were respectively specified. Recharge onto surface waters was specified to be 16 in/yr representing the difference between precipitation and pan evaporation for the northeastern United States and was not varied during calibration (Farnsworth and others, 1982).

Spatial variability in recharge was calibrated using an additional set of scaling parameters that were represented by a network of 78 pilot points (fig. 23). Each pilot point was an individual parameter that was used in conjunction with the remaining pilot points to develop an array of continuous values by use of ordinary kriging (Oliver and Webster, 1990). The pilot points are scaling parameters, and the resulting array is a set of multipliers. The final simulated recharge is the product of (1) recharge values derived from those estimated by use of the SWB model and the global scaling parameter and (2) the array of multipliers estimated from the pilot-point scaling parameters. A value of 1.0 for all pilot points results in a uniform array of 1, and the resulting recharge is the same as that derived from the SWB model and the global scaling parameter.

Recharge in urbanized areas with extensive impervious surfaces, as computed by the SWB model, is lower than in other areas (fig. 12A). The difference between recharge computed in urbanized areas with impervious surfaces and recharge computed assuming predevelopment land uses is assumed to represent the recharge potentially unavailable to the aquifer as direct recharge to the water table (fig. 12B); this component of recharge is referred to as rejected recharge. Some portion of this recharge component is known to enter the aquifer through sumps and recharge basins, particularly in urbanized areas of Nassau County. Therefore, this component of recharge is considered as potential recharge, in addition to that calculated through use of the SWB model. This potential recharge is represented in a similar way as direct recharge to the aquifer. The differences between recharge rates computed by use of the SWB model for current [2019] and predevelopment land uses were used as multipliers.

The simulated recharge is represented as the product of these multipliers and a scaling parameter. Separate scaling parameters were used for rejected recharge in New York City (Brooklyn and Queens Counties), where there are few recharge basins, and rejected recharge in Nassau and Suffolk Counties, where recharge is more likely to be enhanced by extensive networks of recharge basins. The scaling parameter applied to rejected recharge rates in New York City was assigned an initial value of 0.01, which allows 1 percent of this recharge component to enter the aquifer system. The upper and lower constraint was specified to be 0.1 and 0.01, respectively. The scaling parameter applied to Nassau and Suffolk Counties, was assigned an initial value of 1.0, which allows all of this component of recharge to enter the aquifer. The upper and lower constraint was specified to be 1.0 and 0.1, respectively. Scaling parameters for New York City and for Nassau and Suffolk Counties were adjusted during model calibration. The upper and lower constraints were specified to be 1.0 and 0.1, respectively.

Water also recharges the aquifer from wastewater return flow from septic systems and leaky sewer lines. These components of recharge are similarly represented as a combination of arrays of multipliers. Potential total wastewater return flow was estimated in each model cell using the estimated population (fig. 13A; U.S. Census Bureau, 2018; National Historical Geographic Information System, undated b) and a per capita water use of 75 gallons per day (National Historical Geographic Information System, undated a). The estimated water use in each cell was applied as an array of multipliers. The simulated wastewater return flow represents the product of the potential wastewater return flow (fig. 24A) and global scaling parameters for sewered and unsewered areas.

Two separate scaling parameters were applied to sewered and unsewered areas. Wastewater recharge in unsewered areas represents septic-system return flow and was assigned an initial parameter value of 0.85, representing a consumptive loss of 15 percent. The upper and lower constraints were specified to be 0.8 and 0.9, respectively, and the scaling parameter was adjusted during calibration. Wastewater recharge in sewered

A. **Wastewater return flow**

Base map from U.S. Geological Survey National Atlas digital data, scale 1:1,000,000
New York [Long Island] State Plane projection
North American Datum of 1988

B. **Recharge from leaky infrastructure**

Base map from U.S. Geological Survey National Atlas digital data, scale 1:1,000,000
New York [Long Island] State Plane projection
North American Datum of 1988
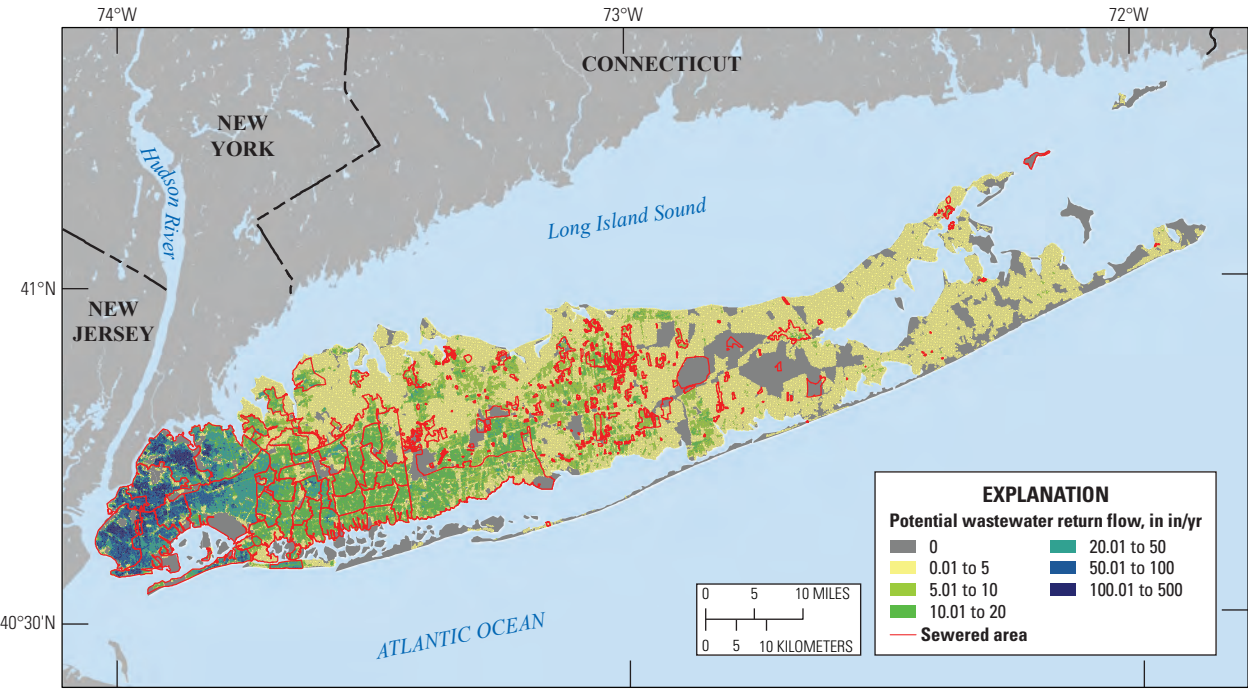
Figure 24. Maps showing spatially distributed values of *A*, wastewater return flow and *B*, recharge from leaky infrastructure on Long Island, New York. in/yr, inch per year.

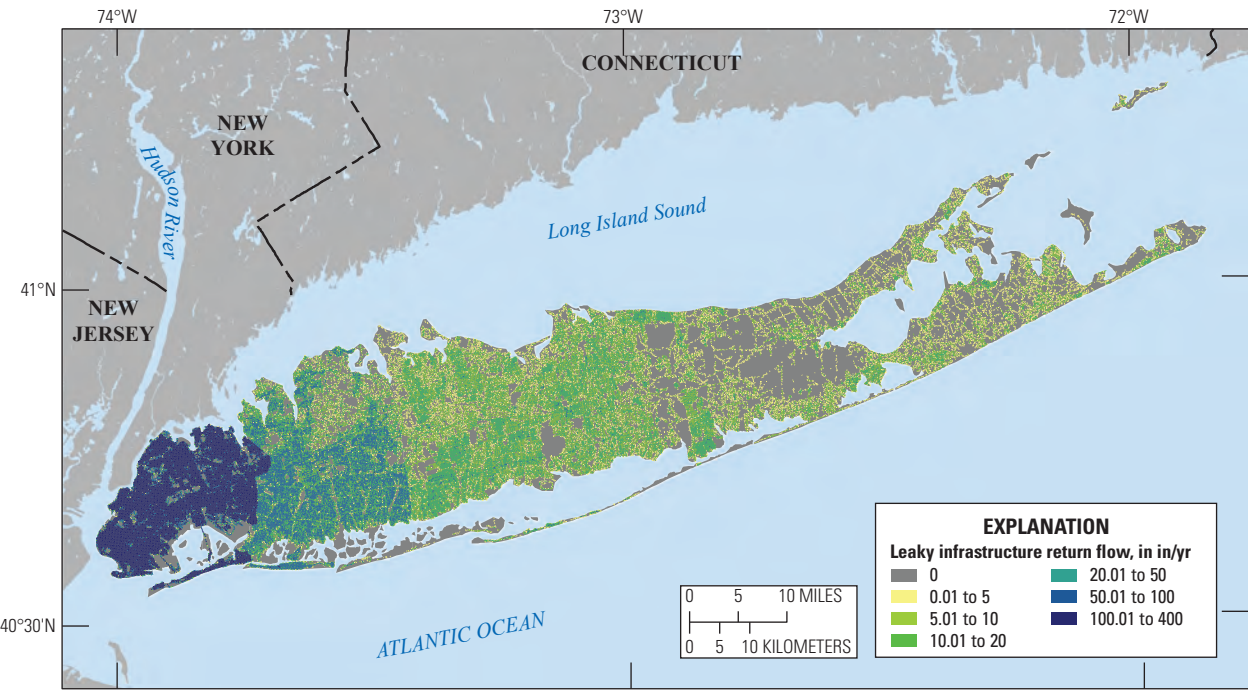areas represents leakage from sewer lines and was assigned an initial parameter value of 0.1, representing a consumptive loss of 10 percent. The parameter was adjusted during calibration between the upper and lower constraints of 0.15 and 0.01, respectively.

An additional component of anthropogenic recharge is leakage from water-supply infrastructure. The distribution of leaky infrastructure was estimated using the road length, which was assumed to approximate the length of leaky infrastructure, in each model cell. The relative proportion of road length in each cell within areas of public-supply service areas to the total of road lengths for the county in which the cell occurs was calculated; the total amount of groundwater withdrawals was assigned to each cell based on the estimated proportionality. These volumetric rates were represented as an array of multipliers (fig. 24B), and the simulated recharge representing leaky-infrastructure recharge is the product of these multipliers and a scaling parameter. Recharge from leaky infrastructure in areas serviced by public supply was assigned an initial parameter value of 0.1, representing a loss of 10 percent from infrastructure. The parameter was adjusted during calibration between the upper and lower constraints of 0.15 and 0.01, respectively. It was assumed that there was no recharge from leaky infrastructure in areas without public-supply service, where water is supplied from private wells (fig. 13B).

Boundary Leakance

Leakance at boundaries refers to the vertical resistance to flow within the sediments of the bottom of the surface water-bodies and is a function of vertical hydraulic conductivity and the thickness of the bottom sediments; leakance at boundaries is therefore a lumped parameter. The vertical hydraulic conductivity of these bottom sediments—for both freshwater and saltwater surface waters—was represented as parameters that varied during calibration. The initial vertical hydraulic conductivity of streams and salt marshes, represented as drains by use of the DRN package, were specified to be 1 ft/d, which is consistent with silty sand deposits. These parameters varied during calibration. The lower and upper constraints of vertical hydraulic conductivity of streambed sediments were 0.2 and 20 ft/d, respectively; those for salt marshes were lower at 0.1 and 10 ft/d, respectively, to allow for the potential for fine-grained sediments.

The vertical hydraulic conductivities of the seabed sediments of open coastal waters and semienclosed estuaries were coupled during calibration to ensure reasonable hydraulic gradients in coastal areas, such as barrier islands. It was assumed that the vertical hydraulic conductivity of offshore coastal seabed sediments is twice that of those in semienclosed estuaries, where sediments likely are finer grained than sandy sediments likely present in high energy, coastal environments. The initial value of vertical hydraulic conductivity in offshore seabed sediments was 2 ft/d (corresponding with 1 ft/d in semienclosed estuaries). The parameter varied during calibration between the upper and lower constraints of 0.2 and 20 ft/d, respectively, in coastal waters (0.1 and 10 ft/d, respectively, in estuaries).

Hydraulic Conductivity

Horizontal and vertical hydraulic conductivity parameters were defined using a combination of zones, pilot-point parameters, and values derived from the lithologic texture model. Using only zones of piecewise constancy to define parameter complexity, in combination with Gauss-Levenberg-Marquardt nonlinear regression, generally is limited by the need for a given problem to be invertible for a solution to be achieved. Conversely, overly complex parameterization schemes can result in highly correlated or insensitive parameters that can limit the ability to achieve a reasonable solution or an acceptable fit to observations. The use of pilot points addresses both limitations by allowing parameters to be represented at discrete points and allowing regions between each pilot-point parameter to be defined by kriging (Oliver and Webster, 1990), using the estimated values at the pilot points (Doherty, 2003). This approach, when combined with SVD (Doherty and Hunt, 2010), may allow for complex and gradational hydraulic conductivity fields and, often, an improved fit to observations. The method also allows for regularization to balance prior information on hydraulic conductivity with fit to observations. Regularization allows for the preservation of prior geologic knowledge and can minimize overfitting to observations that can arise in highly parameterized models.

The network of pilot-point parameters represents a set of dimensionless multipliers that, when combined with two-dimensional ordinary kriging, are used to produce a quasi-three-dimensional array of multipliers. The three-dimensional array of hydraulic conductivity simulated in the numerical model is the product of this array of multipliers and the three-dimensional array of hydraulic conductivity derived from the lithologic texture model (Walter and Finkelstein, 2020). A value of 1 for all the pilot-points results in a three-dimensional array of multipliers with a uniform value of 1 and an array of simulated hydraulic conductivity that is the same as the values derived from the texture model (figs. 21 and 22). This approach allows hydraulic conductivity to be estimated during calibration while preserving, to a degree, the underlying structure of the initial hydraulic conductivity field, as represented by the texture model. The texture model is based on field data and, therefore, represents independent prior geologic knowledge; the balance between fit to observations and adherence to this prior knowledge provides for a more informed model calibration.

The simulated aquifer system was zoned for calibration using the existing mapped hydrogeology of the Cretaceous and Pleistocene aquifer system (Doriski and Wilde-Katz, 1982; Krulikas and Koszalka, 1982; Cadwell and Muller, 1986; Cadwell, 1989; Smolensky and others, 1989; Stumm, 2001; Schubert and others, 2004). This zonation represents a reasonable limit of prior geologic knowledge regarding the extent of major hydrogeologic units at a regional scale; thus, no

arbitrary zones were defined within these mapped hydrogeo-logic zones. However, the Magothy aquifer was represented as three separate vertical zones, each with a separate set of pilot-point parameters, to better represent observed heterogeneity within that unit; these vertical zones represent the vertical extents to which multiplier values are interpolated, by use of ordinary kriging within the aquifer.

The pilot-point network consists of a total of 3,333 verti-cal zones of horizontal and vertical hydraulic conductivity parameters within the 14 aquifer zones (figs. 25 and 26). Pilot points generally are defined at regular intervals—where possible—with additional, randomly placed pilot points placed in some areas to ensure reasonable definition of the interpolated hydraulic conductivity field, particularly in small irregular zones. Most (3,131) pilot-point parameters are speci-fied within major aquifers (fig. 25). Pilot points in the upper glacial aquifer were spaced at a regular interval of 7,000 ft; separate pilot-point networks totaling 946 pilot points were defined for glacial outwash, moraines, and ice-contact depos-its (fig. 25A). A total of 175 pilot points within the Jameco aquifer and Monmouth greensand also were placed at regular intervals of 7,000 ft (fig. 25B). The Magothy aquifer, which is more than 1,000 ft thick in some areas, contains a total of 1,915 pilot-point parameters across three vertical zones. There are 667 points in the shallow Magothy aquifer (fig. 25B), 638 points in the intermediate part of the Magothy aquifer, and 610 points in the deep part of the Magothy aquifer (fig. 25C); pilot points in the Magothy aquifer also have a regular spacing of 7,000 ft. The Lloyd aquifer contains 85 pilot points that are spaced at a regular interval of 25,000 ft, and the contiguous North Shore aquifer had 10 pilot-point parameters spaced at random locations to ensure a reasonably interpolated hydraulic conductivity field (fig. 25D).

There are 202 pilot-point parameters defined within con-fining units (fig. 26). There are 52 points within the Smithtown clay, the 20-foot clay, and the North Fork clay (fig. 26A). Pilot points within the Smithtown clay were placed at a regular interval of 12,500 ft. Pilot points were placed at irregular intervals within the 20-foot clay and the North Fork clay. The Gardiners clay contains 89 pilot points spaced at regular inter-vals of 7,500 ft (fig. 26B). There are 11 pilot-point parameters within the North Shore confining unit placed at random loca-tions to ensure adequate definition of the interpolated hydrau-lic conductivity field (fig. 26A). The Raritan confining units contains 50 pilot points that are spaced at regular intervals of 25,000 ft (fig. 26B).

Ordinary kriging was used to interpolate a two-dimensional array of values within each geologic zone from the individual values at pilot points within that zone and model layer. Pilot points are specified in only 9 of the 25 layers in the numerical model (fig. 27), and therefore, the kriging process results in a partially complete three-dimensional array of mul-tipliers. Regions with no specified multipliers occur in areas where a geologic unit is represented by more than one model layer. Multipliers in these remaining regions of the model are populated by copying values in the appropriate zone from model layers above or below the layer of interest.

The upper glacial aquifer generally is represented by three model layers, the active extents of which decrease monotonically with depth. Glacial sediments are represented by as many as 18 model layers in erosional channels within the underlying Cretaceous sediments. Pilot-points are defined in only the top layer of the unit (fig. 27). The two-dimensional array of multipliers produced by kriging in that layer are cop-ied to the underlying two layers of the upper glacial aquifer. Intraglacial clays are represented in a single layer (model layer 2) requiring no additional copying.

The combination of multipliers in the glacial aquifers and clays results in a three-dimensional array of multipliers in all model cells representing glacial sediments (fig. 27). The same approach was used to populate regions of undefined multipliers in the Jameco aquifer and Monmouth greensand. Pilot points were defined in the top layer of each unit and used to populate those regions by use of ordinary kriging. The associated multipliers were copied into regions of the underly-ing layers representing the corresponding geologic units. The North Shore confining unit underlies glacial sediments along the northern shore. The unit extends to bedrock in some areas, decreases in extent monotonically with depth, and is repre-sented by as many as 22 layers. Pilot points are defined in the top layer (layer 4) and estimated multipliers are copied into the corresponding regions representing the unit in underlying lay-ers. The Gardiners clay underlies glacial sediments along the southern shore and is also represented in a single model layer (layer 4); pilot points are defined, and multipliers are estimated in that part of the model layer representing this unit.

Cretaceous and Pleistocene sediments are separated by an unconformity. This erosional surface reflects how Pleistocene sediments are deeply incised into the uppermost Cretaceous Magothy aquifer in some areas and that the spatial extent of the Magothy aquifer increases monotonically with depth, in contrast to the overlying Pleistocene sediments. The thick-ness of the Magothy aquifer exceeds 1,000 ft in some areas (fig. 6), and the unit is vertically heterogenous and has variable hydraulic conductivity with depth (fig. 10). This variability reflects the presence of mostly coarse sediments in the lower part of the aquifer and extensive areas of silt and clay in the intermediate part of the aquifer.

The Magothy aquifer (and contiguous units) is rep-resented by 19 model layers (layers 5–23); the maximum thickness of any model layer does not exceed 60 ft, which is the typical screen length for public-supply wells in the aquifer. The aquifer was subdivided into three separate groups to bet-ter represent the vertical heterogeneity within the aquifer; the top group is represented by layers 5 to 11, and the lower two groups subdivide layers 12 to 23 into two equal groups of six layers each (fig. 27). Pilot points were defined in the bottom layer of each vertical group: model layers 11, 17, and 23. Multipliers were estimated by ordinary kriging within those regions representing the Magothy aquifer in those layers and duplicated for the corresponding regions in the overlying lay-ers within each group.

A. **Upper glacial aquifer**
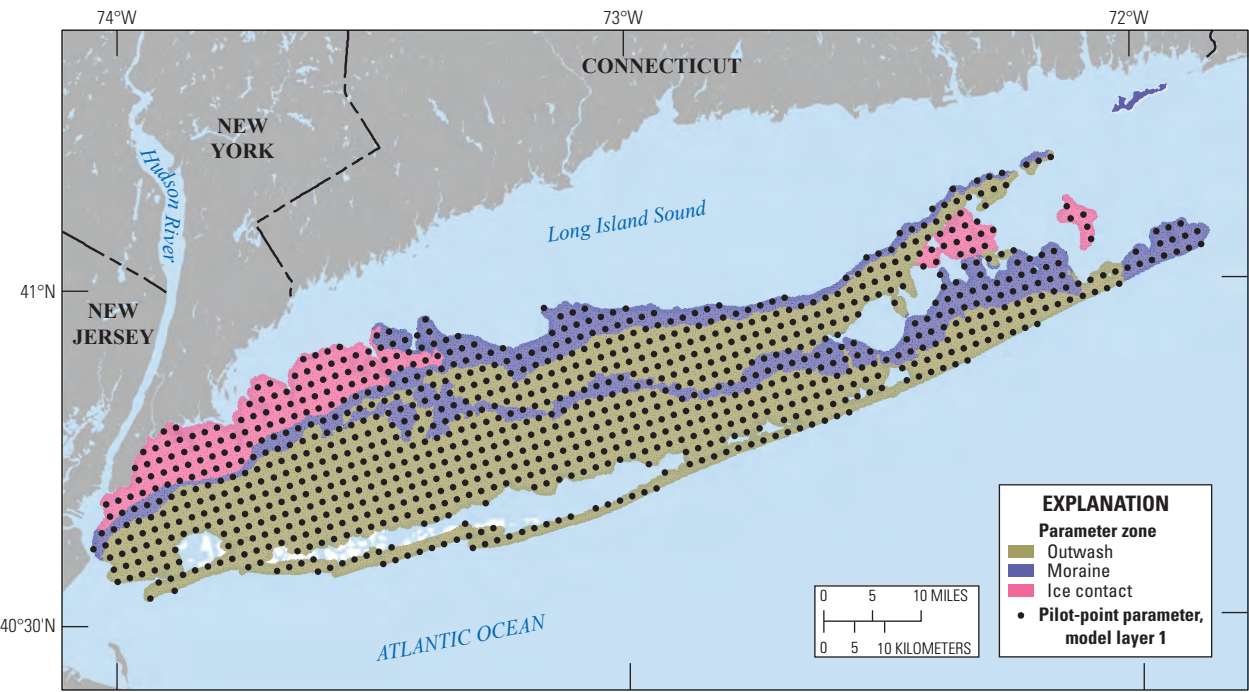
B. **Shallow Magothy aquifer**
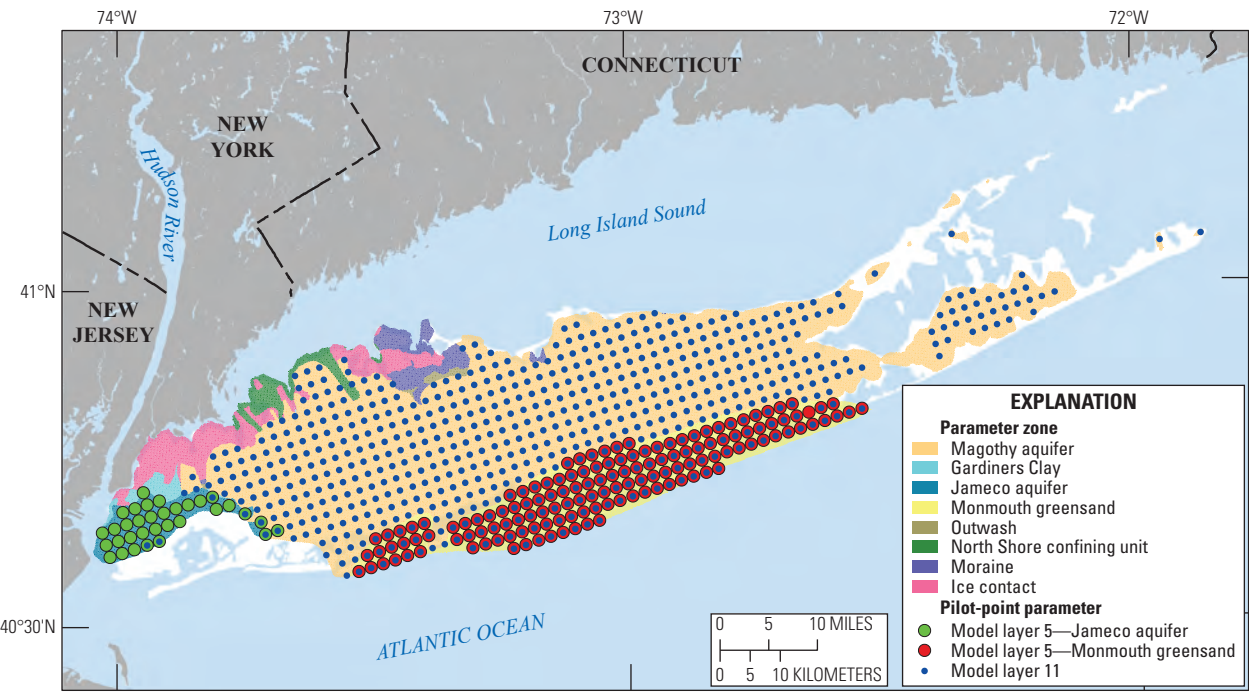
Figure 25. Map showing hydraulic conductivity parameter zones and locations of pilot-point parameters for hydraulic conductivity for the *A*, upper glacial aquifer, *B*, shallow Magothy aquifer and contiguous units, *C*, intermediate and deep Magothy aquifer, and *D*, Lloyd aquifer and contiguous units on Long Island, New York.

C. **Intermediate and deep Magothy aquifer**

Base map from U.S. Geological Survey National Atlas digital data, scale 1:1,000,000
New York [Long Island] State Plane projection
North American Datum of 1988

D. **Lloyd aquifer**

Base map from U.S. Geological Survey National Atlas digital data, scale 1:1,000,000
New York [Long Island] State Plane projection
North American Datum of 1988

Figure 25.   —Continued

A. **Pleistocene confining units**
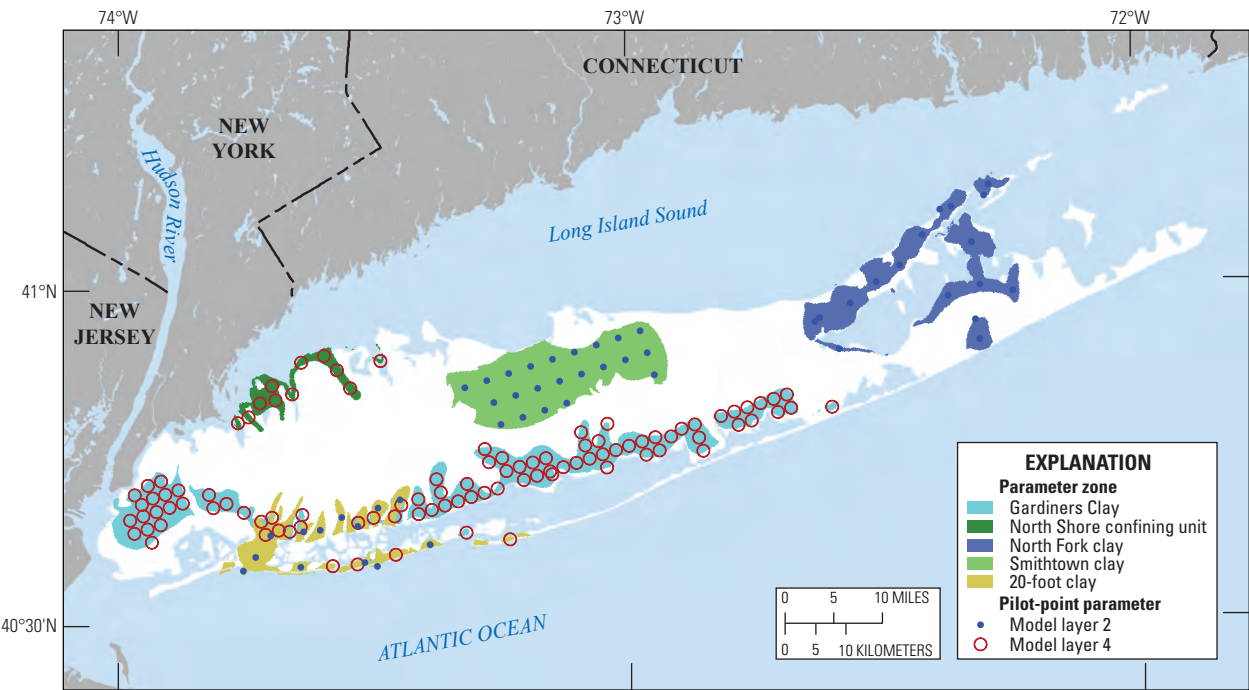
B. **Cretaceous confining units**
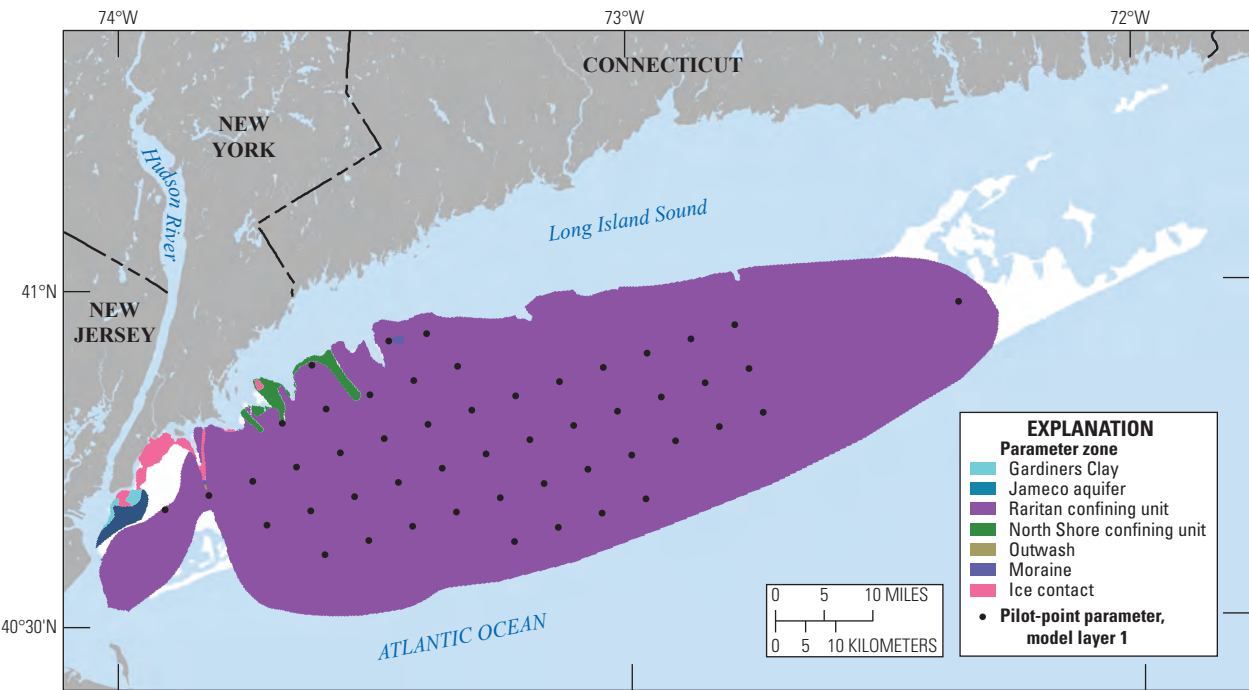
Figure 26. Map showing hydraulic conductivity parameter zones and locations of hydraulic conductivity pilot-point parameters in the *A*, Pleistocene and *B*, Cretaceous confining units on Long Island, New York.
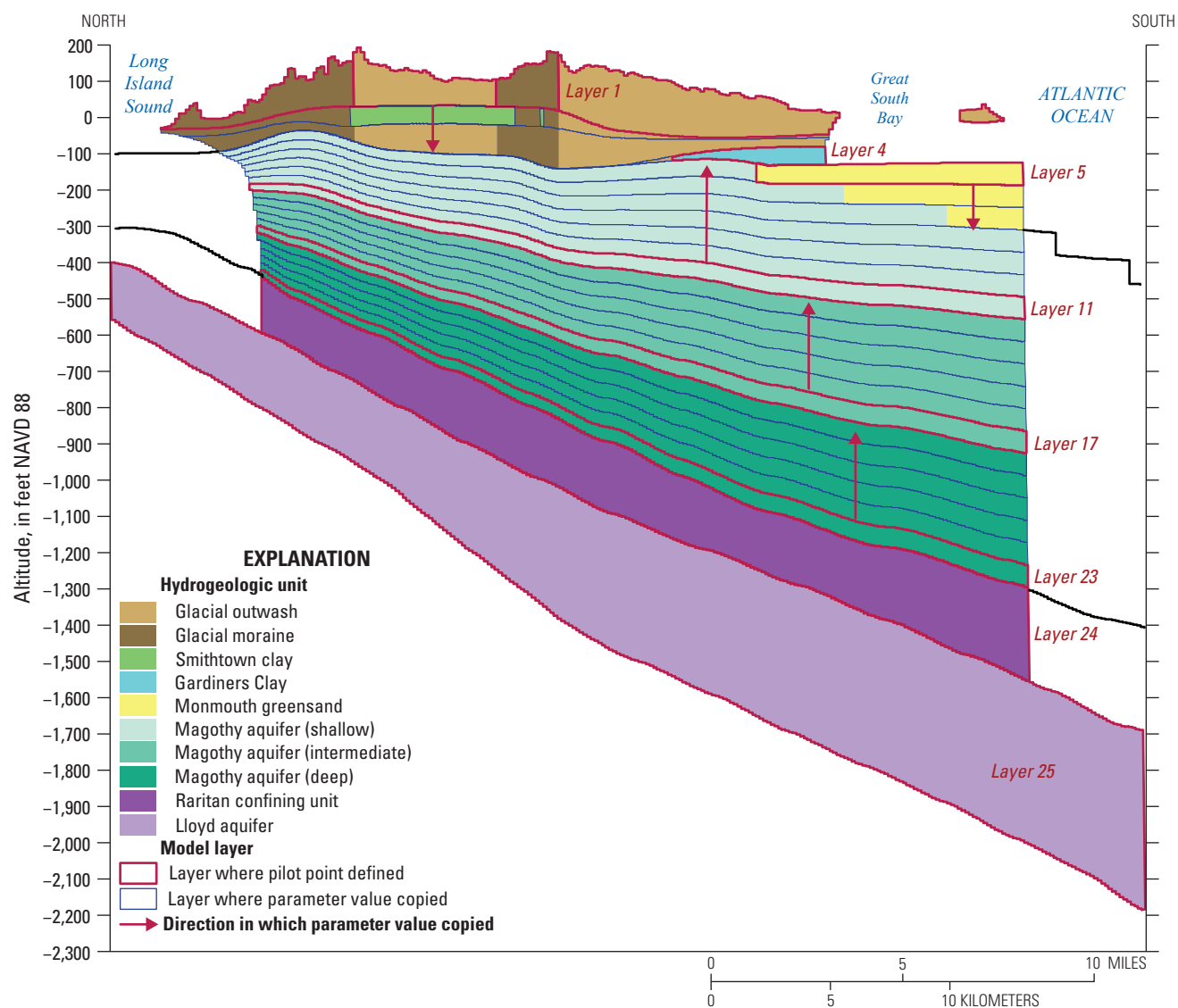
Figure 27.   Vertical sections showing parameter zones along a north-south section for model column 580 in a three-dimensional groundwater-flow model for Long Island, New York.

The Raritan confining unit (and contiguous units) is represented in most areas by a single layer, in which pilot points are defined and multipliers are estimated (fig. 27). The unit is represented by a second layer (layer 25) in areas where the underlying Lloyd aquifer is absent. Multipliers in these regions are copied from the overlying layer. The Lloyd aquifer and the contiguous North Shore aquifer are both represented only in the bottom layer of the model (layer 25). Pilot points are defined, and multipliers estimated in that layer and requires no additional copying.

The initial values of pilot-point parameters for horizontal and vertical hydraulic conductivity were specified to be 1, which results in three-dimensional array of multipliers with a uniform value of 1 and an initial hydraulic conductivity field that is the same as that mapped from the texture model (figs. 21 and 22). Each individual pilot-point parameter was adjusted, and a new three-dimensional hydraulic conductivity field was produced during model calibration. The upper and lower constraints for pilot-point parameters were 1.5 and 0.5, respectively. A set of 16 scaling parameters were also used to estimate horizontal and vertical hydraulic conductivity, 8 parameters each for horizontal and vertical hydraulic conductivity. These parameters were global multipliers applied to groups of one or more model layers. The eight groups were layers 1 and 3 (glacial aquifer sediments), layer 2 (intraglacial clays), layer 4 (Gardiners clay), layers 4 to 11 (shallow Magothy aquifer), layers 12 to 17 (intermediate Magothy aquifer), layers 18 to 23 (deep Magothy aquifer), layer 24 (Raritan confining unit), and layer 25 (Lloyd and North Shore aquifers). The hydraulic conductivity fields simulated in the model represent the product of these global multipliers and the hydraulic conductivity fields estimated as the product of the three-dimensional multiplier arrays (derived from the pilot points) and the initial hydraulic conductivity fields (derived from the texture model). The upper and lower constraints for the global parameters were 1.5 and 0.5, respectively.

Observations and Weighting

Observations of long-term average (steady-state) heads and streamflows were used to formulate the objective function used in the inverse calibration of the groundwater-flow model. The objective function includes individual terms for each observation that are equal to the square of the difference between the observed quantity and the simulated equivalent multiplied by the weight of the observation; the weight is the inverse of the estimate of error for each observation associated with the observation. Weighting reflects the confidence in the observation and, to a degree, the importance of the observation. Weighting can represent physically based errors associated with the measurement; however, such estimates are often difficult to quantify, and the use of a diverse set of observations with differing units can complicate weighting schemes based strictly on estimates of error. This is further exacerbated by differing numbers of observations of different groups because a large number of observations—even with relatively small values of misfit—can dominate the objective function such that groups with more observations or larger units can have disproportionate influence on the regression than groups with fewer or smaller observations. It is also difficult to quantify the error incurred by modeling assumptions and structure (Doherty and Welter, 2010).

An alternative methodology is the application of a relative weighting scheme whereby a more qualitative measure of the importance of a set of observations, as indicated by the fraction of the objective function a given group of observations contributes to its total value, can be used to order weights to reflect the user's confidence in individual groups. Initial weights are set based strictly on assumption of error, but they can be adjusted to trade off the desired influence of specific groups based on other factors. This level of subjectivity can improve the calibration results, provided there is disclosure of the assumptions made (Fienen, 2013). The use of relative weighting requires that observations be grouped in a way that reflects similar units and confidence in the value of the observation. The inverse calibration in this study used a relative-weighting scheme owing to the diverse set of observation types, the difficulty in assigning physically based measures of error to inferred observations, and the difficulty in quantifying the degree to which steady-state observations match true average conditions. The development of a reasonable weighting scheme is a subjective, knowledge-based process that often involves evaluation of several alternatives.

Water-level (hydraulic-head) observations were obtained from the NWIS database (U.S. Geological Survey, 2018) and used to estimate long-term averages for the steady-state calibration period [2005–15] at 290 observation wells (fig. 28). These observations of hydraulic head were grouped by the suitability of the computed averages for representing long-term average conditions. The suitability of an observation to represent long-term average conditions is based primarily on the number of observations during the calibration period [2005–15] and the continuity of those observations during that period. Average water levels in 146 of the 290 wells were assumed to be representative of long-term average conditions, thus the wells where these levels were observed were assigned a higher weight than other wells during calibration. These highly weighted wells generally had more than 100 water-level observations and an adequate temporal distribution across the calibration period. Additional wells with fewer than 100 observations were included in this highly weighted group if they were in areas with a paucity of observation wells. An additional set of 70 wells that represented an adequate spatial distribution within highly urbanized Kings and Queens Counties in New York City were assigned a nonzero but lower weight in the calibration. The remaining 74 wells were included in the calibration, but were assigned a zero weight and, therefore, had no influence on the inverse calibration results. These observations were included to assess residuals, which are the differences between observations and their simulated equivalents, where a difference of greater than zero indicates model underprediction and a difference less than zero indicates model overprediction.

Base map from U.S. Geological Survey National Atlas digital data, scale 1:1,000,000
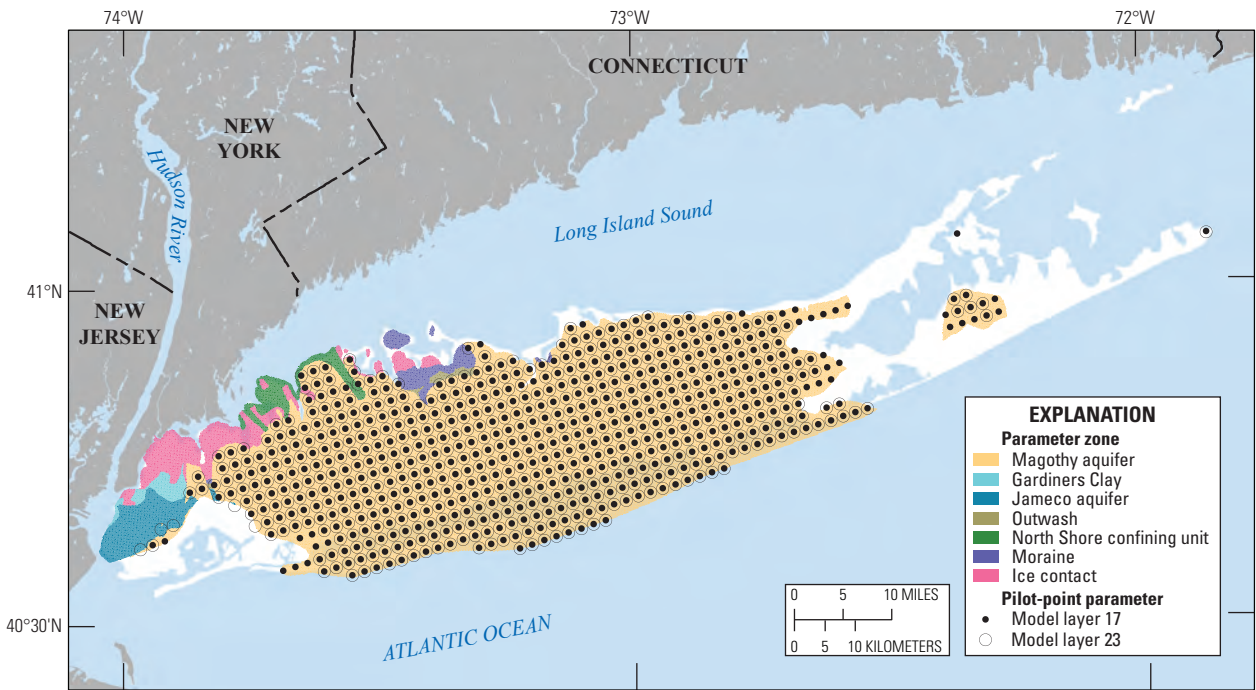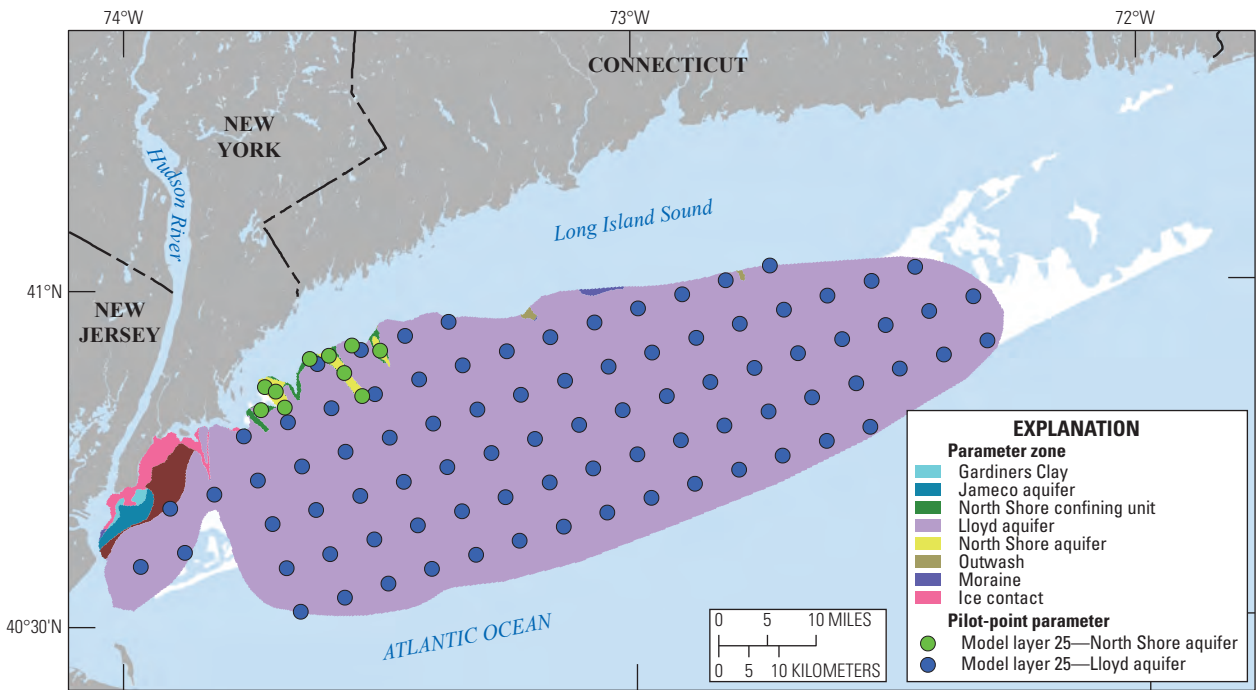New York [Long Island] State Plane projection
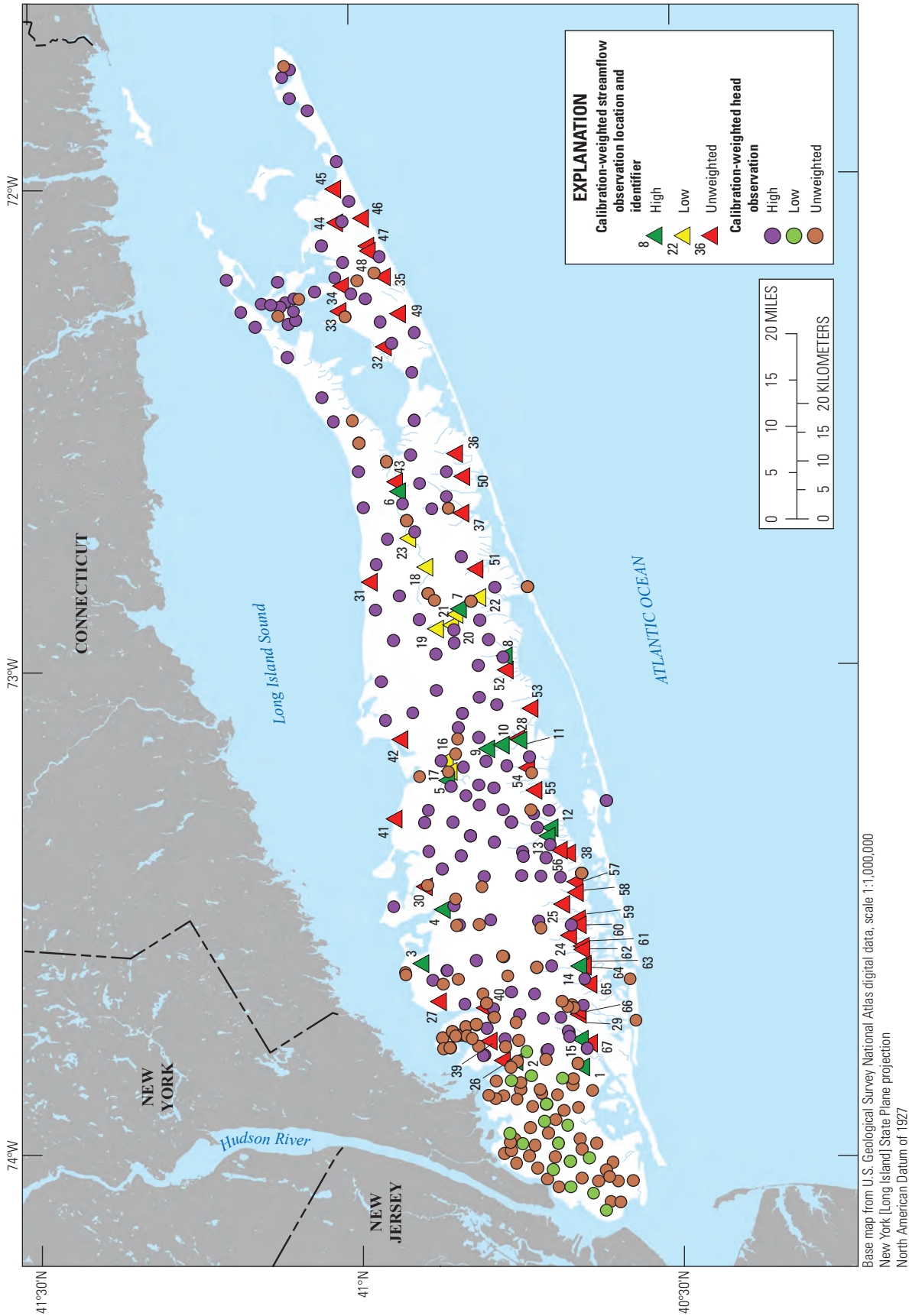North American Datum of 1927

Figure 28.   Map showing location of hydraulic head and streamflow observations and associated weighting on Long Island, New York.

Streamflow observations were used to estimate long-term average flows for the steady-state calibration period [2005–15] at 67 streamflow measurements sites (fig. 28). Similar to water-level observations, these flow observations were grouped by the suitability of these computed averages for representing long-term average conditions. The suitability of an observation to represent long-term average conditions during the calibration period [2005–15] was evaluated by assessing the number and distribution of observations during the calibration period. A total of 14 of the 67 sites were either continuous or real-time measurement sites that were assigned a higher weight than partial-record sites. These continuous-record sites had more than 50 measurements that were well distributed during the calibration period. A total of 8 of the remaining 52 partial-record sites were included as an additional weight group. These sites were along upstream reaches of major streams that were considered important hydrologic features for model calibration. The remaining 44 partial-record sites were included in the calibration but were assigned zero weights.

A relative-weighting scheme was used in the inverse calibration whereby the assigned weights reflected the confidence and identified importance of individual observation groups for estimating parameters as part of the calibration process. The weights were expressed as the fraction of the initial objective function (φ) contributed by residuals for that group of observations. The weights for each observation within a group are the same and are calculated from the desired fraction. The two weighted water-level observation groups—wells with large numbers of observations (group 1) and selected wells in New York City (group 2)—were assigned weights that contributed 42 and 8 percent, respectively, of the objective function. Observations in a third head-observation group had weights of zero. Similarly, two weighted streamflow observation groups—sites with continuous measurements (group 1) and partial-record sites located along major streams (group 2)—were assigned weights that contributed 45 and 5 percent, respectively, of the initial objective function. Observations in a third stream observation group, remaining partial-record sites with fewer than 50 measurements, had weights of zero.

Model Fit to Observations

The model calibration was a three-step process:

1. an inverse calibration to estimate parameters that result in an optimal fit to observed hydrologic conditions for the set of observations and associated weights,

2. adjustments of those parameters to address local misfit between observed and simulated equivalents that result in spatial bias in residuals and

3. adjustments to ensure all values are within ranges considered to be acceptable.

The inverse-calibration results were evaluated to determine the set of estimated parameters that best balanced model fit and adherence to prior geologic knowledge. Postregression adjustments included local and global conditioning of recharge and hydraulic conductivity parameters.

Inverse Calibration

Calibration of a numerical model by nonlinear regression, as implemented in PEST, is an iterative technique that estimates a set of optimal parameter values that minimizes the weighted sum of squares objective function. A Jacobean matrix of parameter sensitivities is produced by piecewise perturbation of the parameters. Parameter estimates are updated after each iteration and ideally result in lower values of the objective function with successive iterations. In a well-posed regression, the process continues until the value of the objective function has reached a minimum value and is stable, as indicated by a change of less than 1 percent between successive iterations. The set of parameters from the iteration that produces the lowest value of the objective function is the optimal set of parameters; these parameters generally are considered the calibrated values and are often produced in the final iteration. The application of SVD, as implemented in PEST, uses the SVD–Assist methodology. This approach is computationally efficient because it requires the Jacobian matrix to be calculated only once. SVD–Assist uses the calculated sensitivities to produce a set of linear combinations of superparameters (as described in the "Inverse Calibration" section of this report). This relatively small number of superparameters represents the optimal set that effectively can be used to minimize the objective function (Doherty and Hunt, 2010).

The two considerations for evaluating how well a model represents a system are (1) the degree of fit between observations and simulated equivalents and (2) the degree to which the calibrated parameters adhere to prior information about the system. The initial (precalibration) absolute mean residuals for highly weighted hydraulic heads and streamflows were 5.32 ft and 4.41 ft^3/s, respectively. The inverse calibration documented in this report consisted of seven parameter-estimation iterations. The lowest value of the objective function is after the last iteration (iteration 7); the value is about 37 percent of the initial value, indicating a substantial improvement in model fit (fig. 29*A and B*). The absolute mean residuals for highly weighted heads and flows following iteration 7 were 3.5 ft and 1.9 ft^3/s, respectively.

Initial hydraulic conductivities were derived from an independently developed texture model that incorporates lithologic data from 1,780 boreholes and historic aquifer-test results and are considered to represent prior hydrogeologic knowledge with a high degree of confidence (Walter and Finkelstein, 2020). Regularization, as implemented in PEST, was used to balance model fit to observations with adherence to preferred parameter values. Adherence of calibrated hydraulic conductivity values to these initial values was considered along with the improvement in model fit, as indicated by the

A. **Absolute mean residuals**
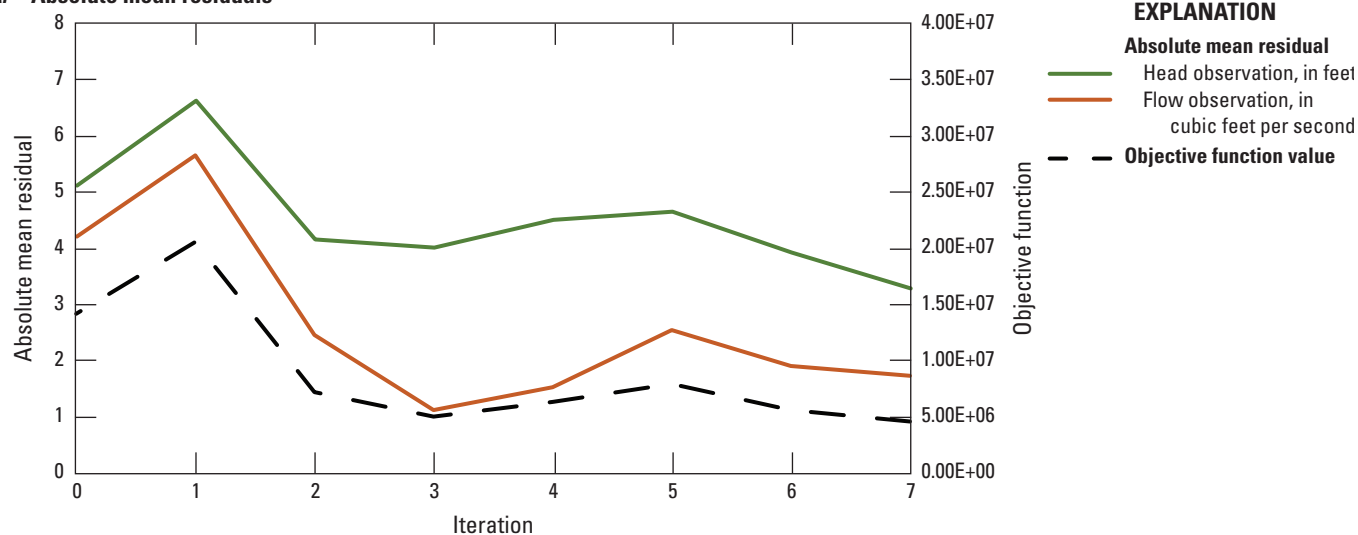
B. **Upper and lower parameter bounds**
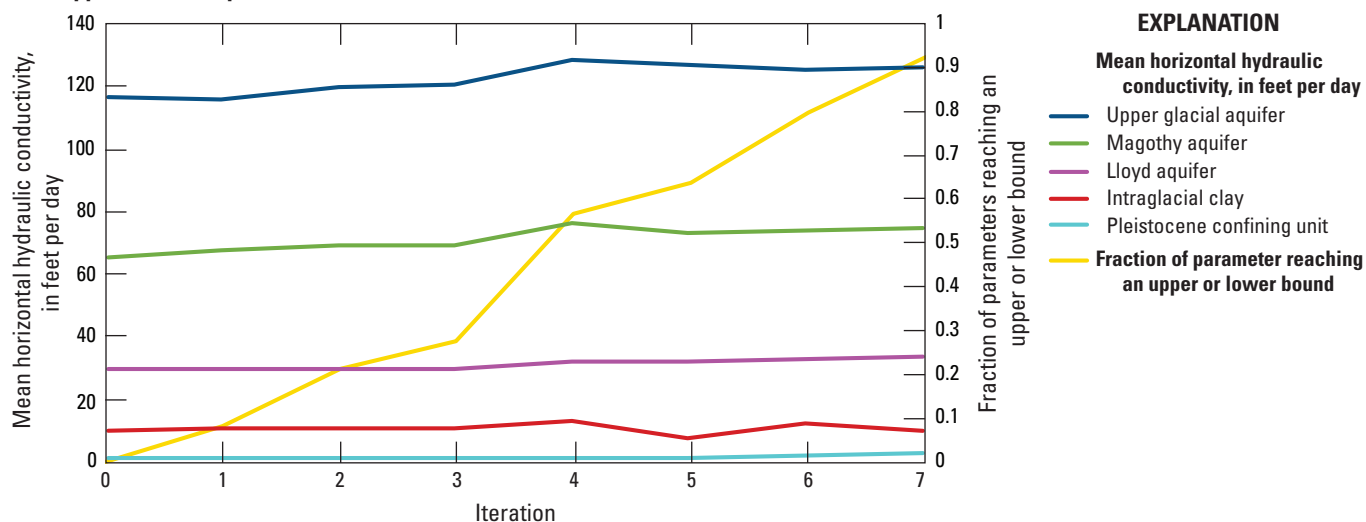
Figure 29.   Graph showing *A*, absolute mean residuals for hydraulic head and streamflow observations and value of the objective function and *B*, number of parameters reaching upper and lower bounds and mean differences in initial and estimated hydraulic conductivities for successive inverse-calibration iterations for a groundwater flow model for Long Island, New York.

value of the objective function. Hydraulic conductivity values from the texture model were represented as multiplier arrays so that the structure of the hydraulic conductivity fields was preserved to a degree. The final hydraulic conductivity values are the product of these arrays and a three-dimensional array of multipliers determined from the pilot-point parameters.

These pilot-point parameters had initial values of 1, resulting in a modeled hydraulic conductivity field that is equivalent to that derived from the texture model; these pilot-point parameters varied during calibration between upper and lower bounds of 1.5 and 0.5. The departure of modeled hydraulic conductivity values from the initial values is indicated by the number of pilot-point parameters that reach an upper or lower bound. The number of parameters that reach an upper or lower bound increased with each successive parameter-estimation iteration (fig. 30A and B). A total of 6,150 (or 92 percent of the total) pilot-point parameters had reached a bound following iteration 7, which also had the lowest value of the objective function.

Although iteration 7 had the lowest objective function and the statistical best fit between observations and simulated equivalents, the parameters produced from iteration 3 were chosen to be the calibrated values. Inspection of model fit and the number of parameters reaching an upper or lower bound indicated that model parameters produced after iteration 3 were considered acceptable. The absolute mean residuals for highly weighted hydraulic heads and streamflows after iteration 3 were 4.2 ft and 1.3 ft3/s, respectively. The absolute mean residual for observations of head was about 5 percent of the total range in head (about 90 ft) and, therefore, considered reasonable. The absolute mean residual for highly weighed streamflows, which were considered the best indicators of long-term average conditions, was the lowest of any iteration. A total of 1,850 parameters (about 27 percent of the total) reached an upper or lower bound, indicating that not only was the model fit to observations reasonable, but far fewer parameters reached a bound in iteration 3 than in iteration 7 (fig. 30B). It was therefore determined that parameters produced in iteration 3 represented the preferred balance between model fit and adherence to prior geologic knowledge.

Adjustments to Model Parameters

The recharge multipliers estimated using the SWB model are based on national-scale spatial data. These datasets were considered imperfect for a local-scale application though preferable to alternative approaches because this approach represents a data-driven analysis that incorporates spatially distributed precipitation, temperature, soil, and land use data that are known to affect recharge. Potential recharge rates calculated using the SWB model often are lower than actual rates (Westenbroek and others, 2010) but were considered to generally represent spatial variations in recharge and useful as a starting point for model calibration.

The network of recharge pilot-point parameters allows for local, spatially gradational adjustments to the SWB multipliers (fig. 23); they were assigned a fixed value of 1.0 during the inverse calibration. The pilot points can be used to locally adjust recharge in areas with higher or lower than expected recharge rates or areas with a lesser model fit to water-level observations. The global fit to water-level observations of 4.2 ft was considered reasonable for the system; however, there were large head residuals in some areas, including central and northern parts of Nassau County where observed heads generally were higher than the simulated equivalents (fig. 30A). Recharge rates in those areas and in New York City, as estimated using the SWB model, were lower than expected, and the values of the westernmost 13 recharge pilot points (fig. 23) were increased by 50 percent to account for possible undercalculated recharge for impervious surfaces by the SWB model in more urbanized areas. The array of multipliers derived from the new pilot-point parameters values were applied to the calculated recharge rates as input into the model.

Adjustments also were made to hydraulic conductivity pilot-point parameters, after the inverse calibration, to improve model fit in three specific areas within the upper glacial aquifer: (1) coastal areas of Kings and Queens Counties in New York City, (2) the Smithtown clay in north-central Suffolk County, and (3) Shelter Island (figs. 25 and 26). The aquifer system near the northern coasts of Kings and Queens Counties thins to a point where bedrock crops out in northern Queens. The simulated altitude of the bedrock surface in this area was lowered by as much as 100 ft in the model to create enough saturated thickness to ensure model stability in these areas. The conceptual model underlying this structural change was that the shallow, weathered bedrock is considered a part of the aquifer system and represents additional saturated thickness in this area. Observed water levels in this area generally were higher than their simulated equivalents, suggesting that the inclusion of shallow bedrock with the same hydraulic conductivity as the aquifer sediments may overestimate total transmissivity in this part of the model. The calibrated values of the westernmost 23 hydraulic conductivity pilot points (fig. 25A) subsequently were decreased by 50 percent to decrease the total transmissivity of the aquifer in this area.

The Smithtown clay is a shallow, extensive clay unit within the upper glacial aquifer in north-central Suffolk County (fig. 5; Krulikas and Koszalka, 1982). The unit has a surface altitude between 75 ft above and 50 ft below MSL and likely is an important control on water levels in the area. The unit ranges in thickness between 50 and 100 ft. Observed water levels near the clay generally were lower than their simulated equivalents. Residuals near the clay generally are reasonable, but the simulated water table generally was higher than observed (Monti and others, 2013). The simulated water table was particularly high in the northwest part of the unit where the top of the clay is highest, about 75 ft above MSL. There was a simulated water table mound in that area, where
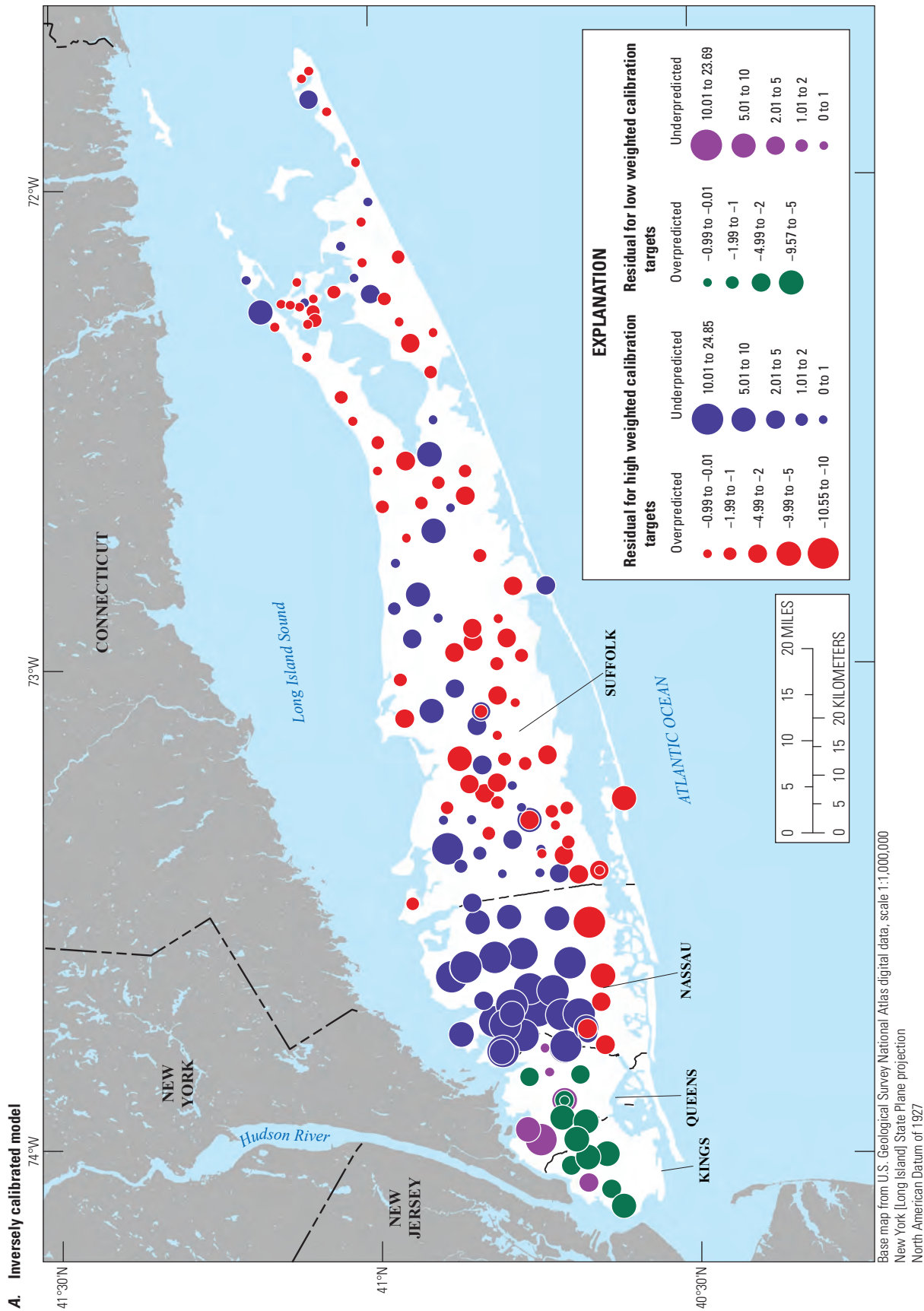
Figure 30. Map showing distribution of hydraulic head (in feet) residuals for highly and low-weighted observations for *A*, the inversely calibrated model and *B*, the adjusted calibrated model for groundwater flow on Long Island, New York.
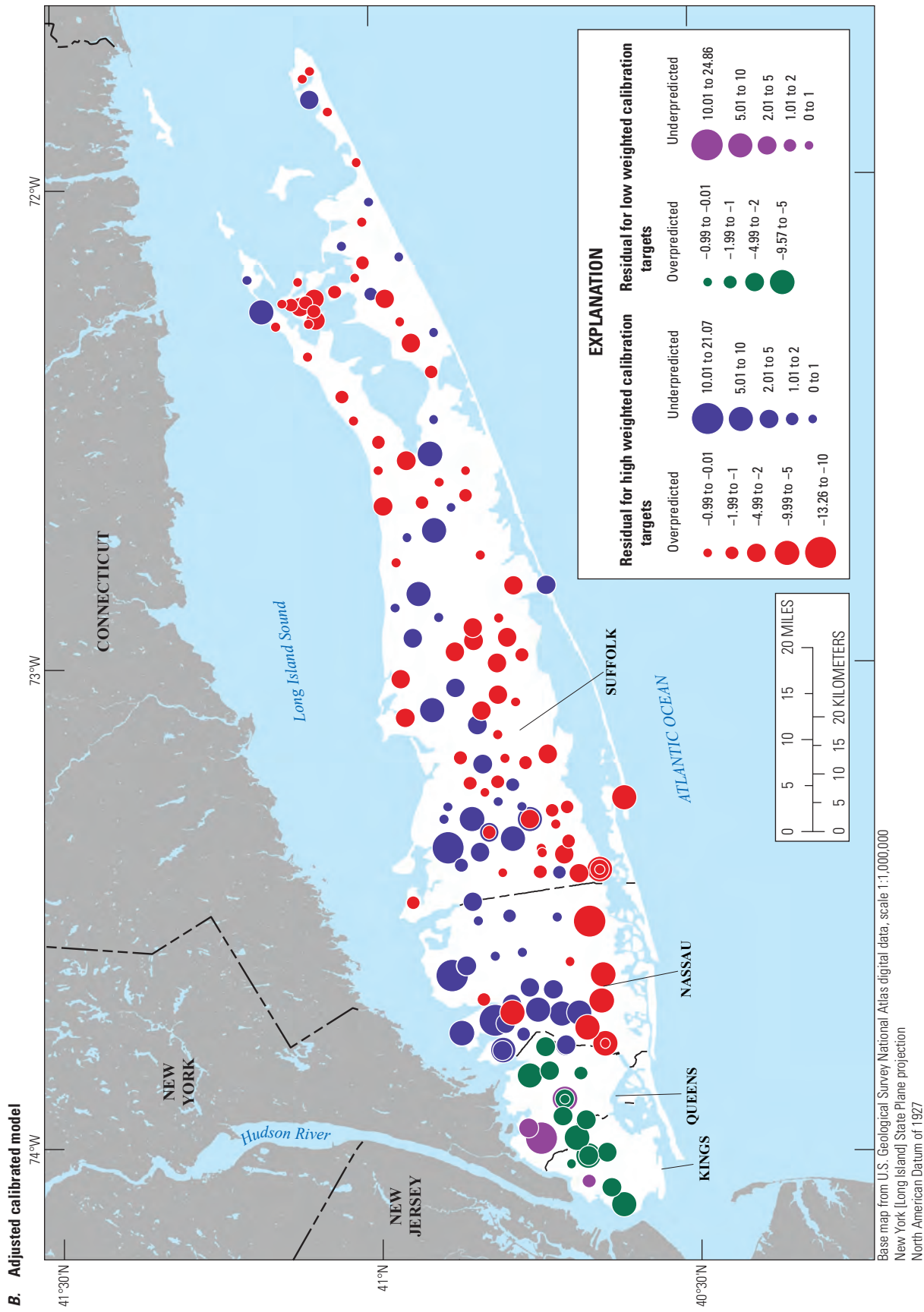
B. Adjusted calibrated model

Figure 30.   —Continued

the water table was more than 90 ft above MSL—the highest simulated water-table altitude in the modeled aquifer system—that was considered to be an anomaly.

The clay unit was assigned an initial horizontal hydraulic conductivity of 10 ft/d, representative of a silt and clay; the calibrated values of pilot points within the clay unit (fig. 26) averaged 1.2 ft/d, indicating that calibrated hydraulic conductivity values were similar to but lower than the initial value of 10 ft/d. Inspection of lithologic logs used to define the geometry of the unit (Krulikas and Koszalka, 1982) showed that the unit, as mapped, contained a large amount of sandy sediments, particularly in the northwestern parts of the unit where borehole data suggest that the top of the unit is lower than was initially mapped. Thus, the hydrogeologic data and hydraulic head residuals suggest that the unit as represented in the model underestimates the transmissivity of the upper glacial aquifer in that area. Pilot points within in the unit were increased by a factor of between 3 and 6 to produce hydraulic conductivity values more consistent with a hydrogeologic unit of mixed silty and sandy sediments.

Shelter Island is in the Peconic estuary system between the North and South Forks (fig. 1) and is generally underlain by ice-contact sediments. Residuals in individual wells were considered reasonable (fig. 30A), but the simulated water table generally was thought to be lower than observed (Monti and others, 2013). There was a paucity of hydrogeologic data available for Shelter Island; therefore, the texture model used to estimate initial hydraulic conductivity values likely is not well-informed in this area. The calibrated values of the 12 pilot points representing hydraulic conductivity on Shelter Island (fig. 25) were reduced by 50 percent to lower the simulated transmissivity of the underlying aquifer to provide a better fit to observed water levels.

The adjusted pilot-point parameters were incorporated into the inversely calibrated model, and new model inputs were generated. The use of pilot points to populate input arrays by use of kriging can result in input values—hydraulic conductivity and recharge—that are above or below values considered reasonable, even if pilot-point parameters themselves are assigned upper and lower bounds that are considered to be reasonable. The upper and lower limits for recharge were assumed to be 1 and 32 in/yr, respectively. Any model cell with a recharge rate less than 1 in/yr was assigned that value, and 32 in/yr was specified in any cell with a recharge rate that exceeded that value.

The upper and lower limits for hydraulic conductivity varied by aquifer. Coarse-grained sediments were assumed to be present in parts of all aquifers; therefore, the upper limit for aquifers was assumed to be 350 ft/d, generally representative of coarse sand and gravel (Walter and Finkelstein, 2020). The lower limit of hydraulic conductivity varied by aquifer. The Cretaceous Monmouth greensand and Magothy and Lloyd

aquifers were assigned a lower limit of horizontal hydraulic conductivity of 10 ft/d, consistent with silty sediments. The Pleistocene Jameco and North Shore aquifers were assigned a lower limit of 30 ft/d. Wisconsin glacial outwash, ice-contact, and morainal deposits were assigned lower limits of 70, 30, and 10 ft/d, respectively.

The lower limit of vertical hydraulic conductivity for the Cretaceous aquifers was 1 ft/d. The lower limit of the Jameco aquifer was specified to be 3 ft/d. Outwash, ice-contact, and morainal deposits were assigned values of 7, 3, and 1 ft/d, respectively. The lower limit of vertical hydraulic conductivity in a confining unit was specified to be 0.001 ft/d. Values of horizontal and vertical hydraulic conductivity in individual model cells that were below the lower limit or above the upper limit for the unit represented by that cell were assigned the value of the corresponding lower or upper limit.

The adjustments applied to the selected recharge and hydraulic-conductivity pilot points resulted in lower (improved) hydraulic head residuals, particularly in Nassau County and New York City (fig. 30B). Observed water levels and simulated equivalents for highly weighted heads generally were in good agreement (fig. 31A), with an absolute mean residual of 2.68 ft, which was about 3.2 percent of the total hydraulic gradient across the aquifer system. The mean residual was 0.36 ft, indicating head observations on average were slightly higher than simulated equivalents and generally were evenly distributed around the mean (fig. 31B). The absolute mean residual for low-weighted heads was 4.7 ft, and the mean for low-weighted heads was −0.75 ft, indicating that simulated heads in New York City were, on average, higher than observed heads (fig. 31C). The large residuals (exceeding 20 ft) are near the coast in northwestern Queens County and in an area with high water-table altitudes overlying a very thin aquifer system, possibly on bedrock (fig. 30B).

The adjusted parameters improved fit between highly weighted observed streamflows and simulated equivalents from about 1.4 to 1.3 ft³/s, respectively. Observed and simulated streamflow are in close agreement at highly weighted observations (fig. 32A). Total measured and simulated streamflow at these observations were about 258 and 257 ft³/s, respectively, which is a difference of about 0.6 percent. The absolute mean and mean residual streamflow were 1.33 and 0.1 ft³/s, respectively. The absolute mean residual was 3.34 ft³/s for low-weighted streamflow observations, which were partial-record sites on major streams. Observed and simulated streamflows at these sites generally were in close agreement (fig. 32B). The mean residual at low-weighted sites was −2.24 ft³/s, indicating that simulated equivalents generally were higher than observed streamflow. Total measured and observed streamflow at these sites differed by about 18 percent.

A.   **Observations and simulated equivalents, highly weighted observations**
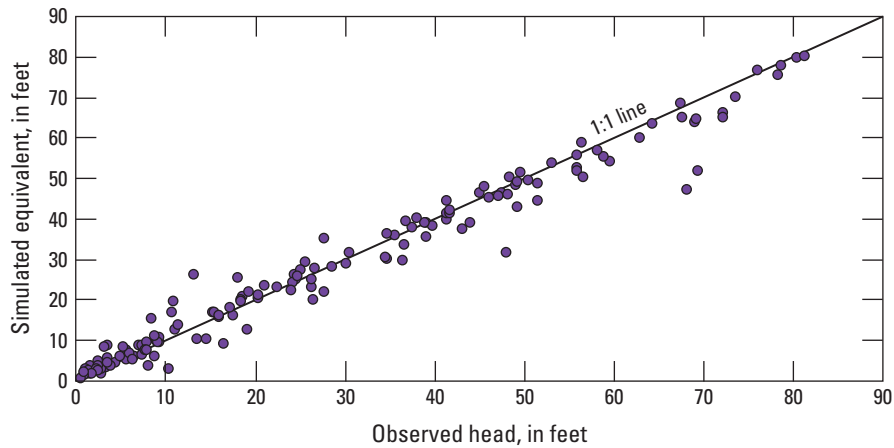
B.   **Head residuals and observed heads, highly weighted observations**
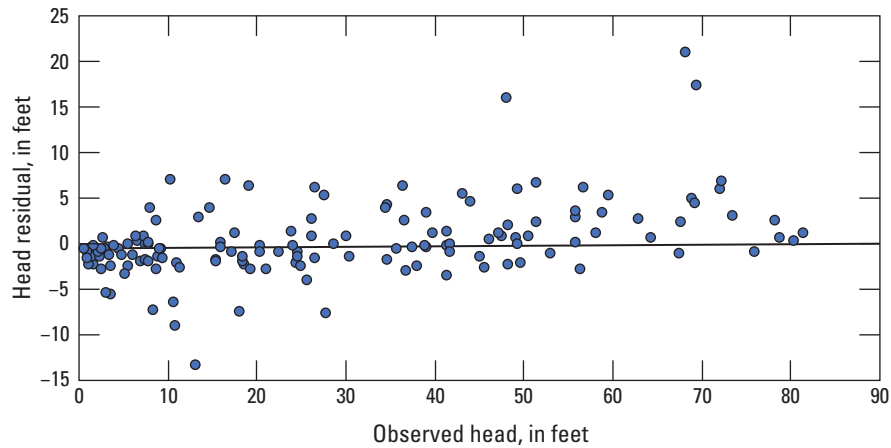
C.   **Observations and simulated equivalents, low-weighted observations**
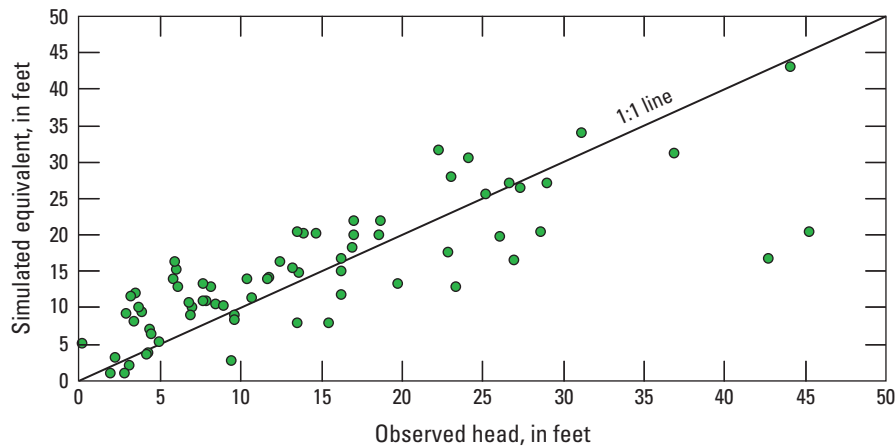
Figure 31.   Graphs showing *A*, highly weighted hydraulic-head observations and simulated equivalents, *B*, hydraulic head observations and residuals for the adjusted calibrated numerical model, and *C*, low-weighted hydraulic head observations and simulated equivalents on Long Island, New York.

A. **Highly weighted observations**
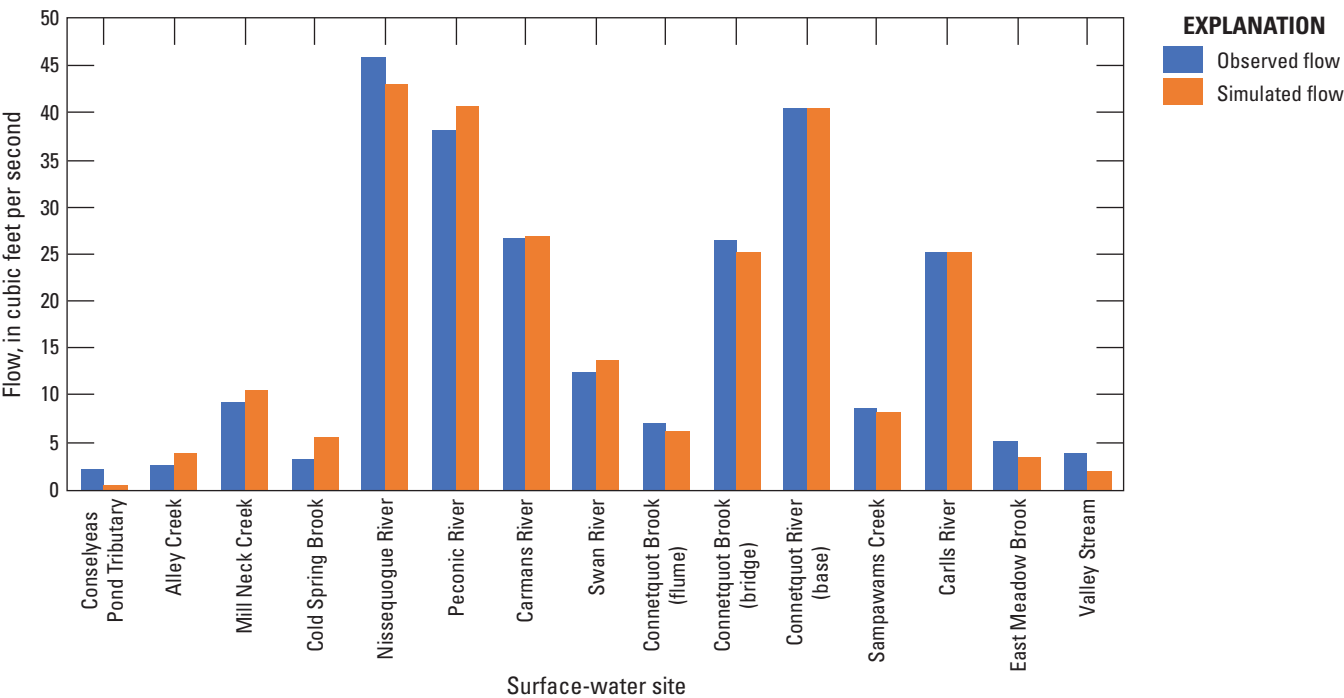
B. **Low-weighted observations**
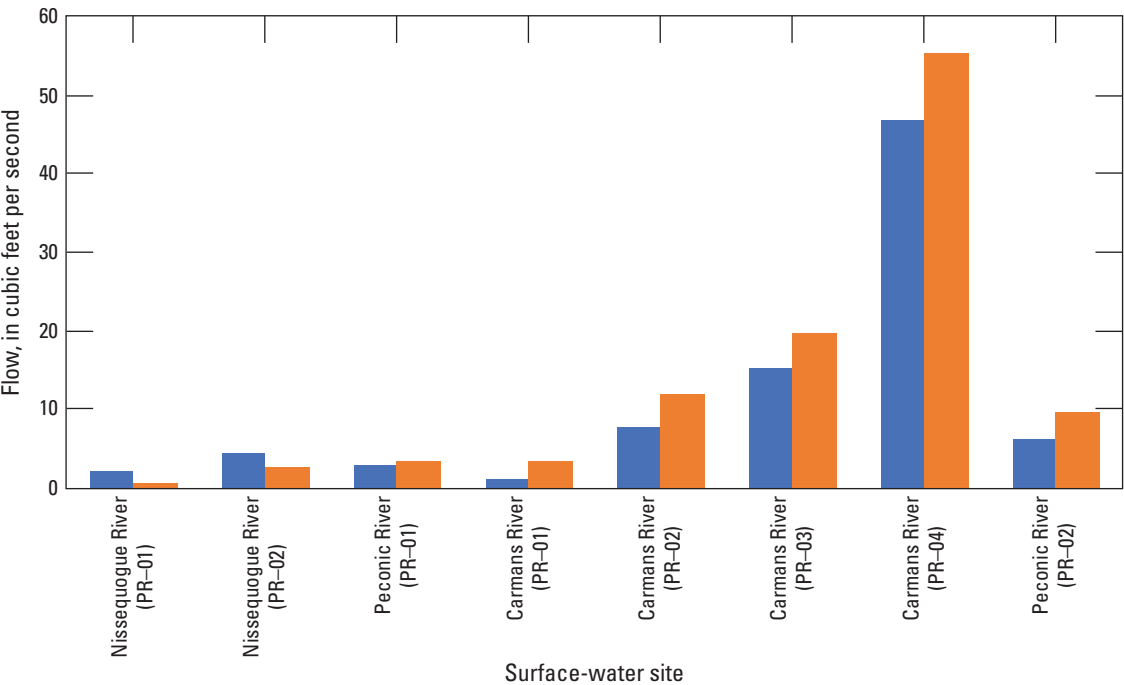
Figure 32.   Graphs showing observed streamflows and simulated equivalents for *A*, highly weighted and *B*, low-weighted observations for groundwater flow on Long Island, New York.

Simulation of Groundwater Flow

The calibrated regional model of Long Island was used to evaluate current hydrologic conditions, including a general hydrologic budget, water-table altitudes, recharge areas to major receptor types, and groundwater travel times calculated from the water table to those receptors. A version of this model for the period before urban development (predevelopment) was constructed using the same natural recharge rates, hydraulic properties, and boundary leakances as the adjusted, calibrated model. Spatially variable recharge in the predevelopment model was estimated using the SWB model and land use representing undeveloped conditions, in which impervious surfaces were removed. Groundwater pumping was not represented in the predevelopment model. The two versions of the model were subsequently used to evaluate the effects of conditions on the hydrologic system for 2005–15.

Hydrologic Budget

About 2,590 ft³/s of water enters the aquifer system from natural recharge under predevelopment conditions from natural recharge (table 2). More than half—about 60 percent—of the water discharges into saline surface waters or subsea saline groundwater. About 51 and 4 percent of the recharged water discharges directly into coastal waters and salt marshes, respectively; the remainder (about 5 percent) discharges from deep, confined aquifers into salty groundwater. A total of 40 percent of groundwater discharges into freshwater streams and wetlands under natural conditions.

The changes to the aquifer system for 2005–15 included withdrawal of water from pumped wells and changes to the distribution and sources of recharge. From 2005 to 2015, about 46 percent of groundwater discharged into saline surface waters or subsea saline groundwater and about 28 percent discharged into freshwater streams (table 2). Natural recharge calculated for current conditions for 2005–15 was about 2,571 ft³/s, or about 1 percent less than that calculated for predevelopment conditions. Additional sources of recharge for current conditions for 2005–15 included leaky infrastructure (179 ft³/s) and wastewater return flow (170 ft³/s). About 87 ft³/s of potential recharge intercepted by impervious surfaces was redirected as recharge at the water table. Total recharge to the system including these additional sources of recharge was 3,007 ft³/s, or about 16 percent more than under predevelopment conditions.

Table 2. Model-calculated hydrologic budget for the aquifer system on Long Island, New York, under average, predevelopment, and current pumping and recharge conditions for 2005–15.

[ft³/s, cubic foot per second; NA, not available]

Hydraulic budget	Predevelopment		Current [2005–15] stresses		Change, in percent
	Flow, in ft³/s	Percent	Flow, in ft³/s	Percent	
Inflow [recharge]					
Natural	2,527.48	100.00	2,571.06	85.49	1.72
Impervious surfaces	NA	NA	87.26	2.90	NA
Infrastructure	NA	NA	179.01	5.95	NA
Wastewater	NA	NA	170.06	5.65	NA
Total recharge	2,527.48	NA	3,007.39	NA	15.99
Outflow					
Freshwater:					
Streams	1,016.90	40.21	854.75	28.42	−15.95
Urban drains	NA	NA	115.90	3.85	NA
Total freshwater	1,016.90	40.21	970.65	32.28	−4.55
Saltwater:					
Coastal waters	1,328.05	52.52	1,223.50	40.68	−7.87
Salt marshes	108.39	4.29	105.84	3.52	−2.35
Subsea discharge	75.37	2.98	52.89	1.76	−29.82
Total saltwater	1,511.82	59.79	1,382.23	45.96	−8.57
Pumped wells	NA	NA	655.99	21.80	NA
Net					
Total discharge	2,592.93	NA	3,008.87	NA	16.04

Impervious surfaces lower natural recharge rates in some areas, and the conversion of land from undeveloped land cover to residential uses can result in locally higher recharge rates when comparing natural recharge rates from predevelopment and current conditions for 2005–15 (Yang and others, 2015). Natural recharge for current [2005–15] conditions was about 44 ft^3/s higher than predevelopment conditions when the natural recharge captured by impervious surfaces (about 87 ft^3/s) and redirected to the aquifer system via retention basins or "sumps" was considered.

Anthropogenic recharge sources include wastewater return flow and loss of water from leaky infrastructure, and combined, contribute an additional 349 ft^3/s of aquifer recharge. Wastewater return flow totaled about 170 ft^3/s and occurred mostly in densely populated, unsewered areas, particularly in western and central Suffolk County. Recharge from leaky infrastructure was assumed to be about 179 ft^3/s, mostly derived from leaky mains transmitting the 1,080 ft^3/s of water imported into Kings and Queens Counties from upstate surface-water reservoirs.

A total of 656 ft^3/s (or about 425 Mgal/d) of water was withdrawn annually for water supply under current [2005–15] conditions, which reduced groundwater discharge to surface waters. Discharge to coastal waters—estuaries, salt marshes, and open waters—decreased by about 107 ft^3/s (or about 8 percent) compared with predevelopment conditions (table 2). Discharge from confined aquifers into overlying salty groundwater decreased by about 1.22 ft^3/s (or about 30 percent), which is the largest proportional decrease in response to groundwater pumping. Discharge to freshwater streams and wetlands decreased by about 170 ft^3/s (or about 17 percent). Combined, the total reduction in discharge to natural receptors in response to groundwater pumping was about 176 ft^3/s, accounting for about 55 percent of total pumping.

The remaining (415 ft^3/s) offset to groundwater pumping came from increased aquifer recharge for current [2005–15] conditions compared with predevelopment conditions. This increase in recharge, when combined with the reduction in discharge to natural receptors (357 ft^3/s), was about 116 ft^3/s more than the total amount of water removed by pumping (656 ft^3/s). The additional 116 ft^3/s of water was accounted for as groundwater discharge to subterranean infrastructure, primarily in urbanized areas with shallow depths to water. This groundwater ultimately leaves the aquifer system by way of stormwater conveyances or combined stormwater-sanitary sewer systems with coastal outfalls.

Simulated Hydrologic Conditions

The simulated water table under predevelopment conditions is controlled by major coastal boundaries and streams (fig. 33). There are two water-table mounds on the mainland of the island, separated by the Nissequogue and Connetquot Rivers in the central part of the island. The maximum altitudes of the western and eastern water-table mounds exceed 90 and

60 ft, respectively, for simulated predevelopment conditions. In addition to the mainland water-table mounds, local water-table mounds occur on the North and South Forks and exceed 5 and 20 ft, respectively.

A regional groundwater divide, representing an area of near-zero horizontal hydraulic gradients and vertical flow, extends generally west to east across the main part of the island. In areas north of the divide, groundwater flow is northward to Long Island Sound and contiguous waterbodies, whereas south of the divide, flow is southward towards the Atlantic Ocean and contiguous waterbodies. The regional groundwater divide bifurcates into two separate divides extending onto the North and South Forks (fig. 33); groundwater flow in areas between the bifurcated divides converges towards the Peconic estuary system. An area of 374 mi^2 of the water table (or about 27 percent of the total area) contributes water to the Cretaceous (Magothy and Lloyd) aquifers and contiguous units. The area at the water table that contributes recharge to the Lloyd aquifer (the deepest aquifer on the island) is about 16 mi^2 (or about 1 percent of the total land area of Long Island). Recharge to the Lloyd aquifer occurs in narrow swaths along the regional groundwater divide and extends northward in interior parts of Nassau and Queens Counties.

The simulated water table under current [2005–15] pumping and recharge stresses generally is similar in shape to that under predevelopment conditions: western and eastern water-table mounds separated by the Nissequogue and Connetquot Rivers and local water table mounds (fig. 34A) on the North and South Forks. The western and eastern water-table mounds have maximum simulated altitudes of more than 80 and 60 ft, respectively, that are somewhat lower than water-table altitudes under unstressed conditions (fig. 33).

Hydrologic conditions under pumping and recharge stresses for 2005–15 differ from those under predevelopment (unstressed) conditions. Development affects natural recharge by increasing the extent of impervious surfaces and by changing land use and associated recharge regimes. About 22 percent of current recharge (from all sources) is withdrawn for water supply from the aquifer system, which results in local decreases in water-table altitudes. The return of pumped water (wastewater return flow) is about 26 percent of the total (island-wide) groundwater pumping; however, most of this wastewater return flow occurs in unsewered areas of Suffolk County (fig. 24A). Pumped groundwater, as well as reservoir water imported from upstate New York, also can provide recharge to the aquifer system through leaky infrastructure (fig. 24B). The interaction of these point and spatially distributed stresses results in complex hydrologic responses that vary spatially (fig. 34B).

Pumping and recharge for 2005–15 have resulted in changes in water-table altitudes across the island compared with predevelopment conditions, with some areas showing large decreases (drawdown) in water-table altitudes, and other areas showing increases (mounding) in water-table altitudes. Water-table altitudes in the western part of the island have
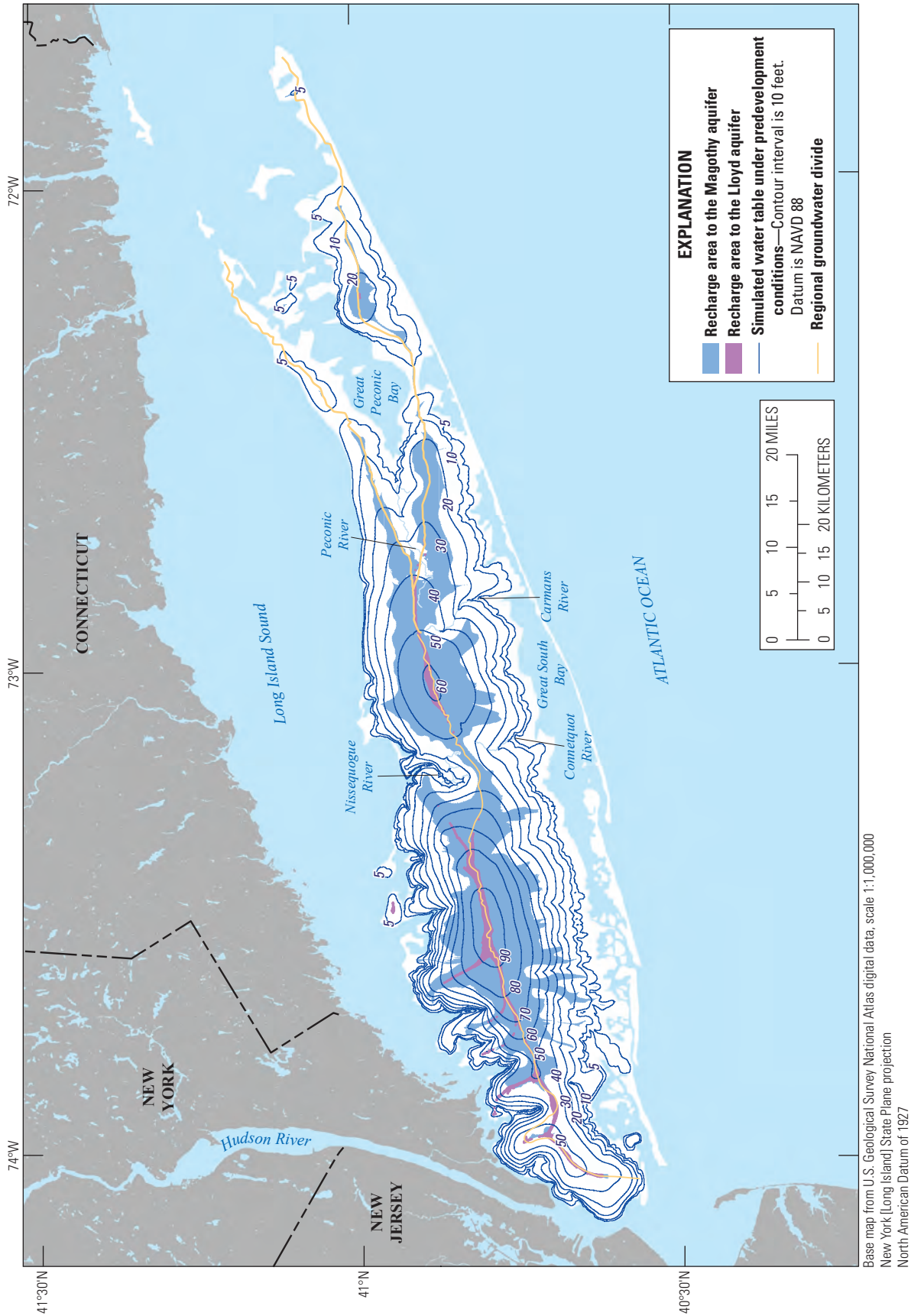
Figure 33. Map showing the simulated water-table altitudes and recharge areas to Cretaceous aquifers for predevelopment conditions on Long Island, New York. NAVD 88, North American Vertical Datum of 1988.

Base map from U.S. Geological Survey National Atlas digital data, scale 1:1,000,000
New York [Long Island] State Plane projection
North American Datum of 1927

EXPLANATION

Recharge area to the Magothy aquifer

Recharge area to the Lloyd aquifer

Simulated water table under predevelopment conditions—Contour interval is 10 feet. Datum is NAVD 88

Regional groundwater divide

A. **Simulated water table**
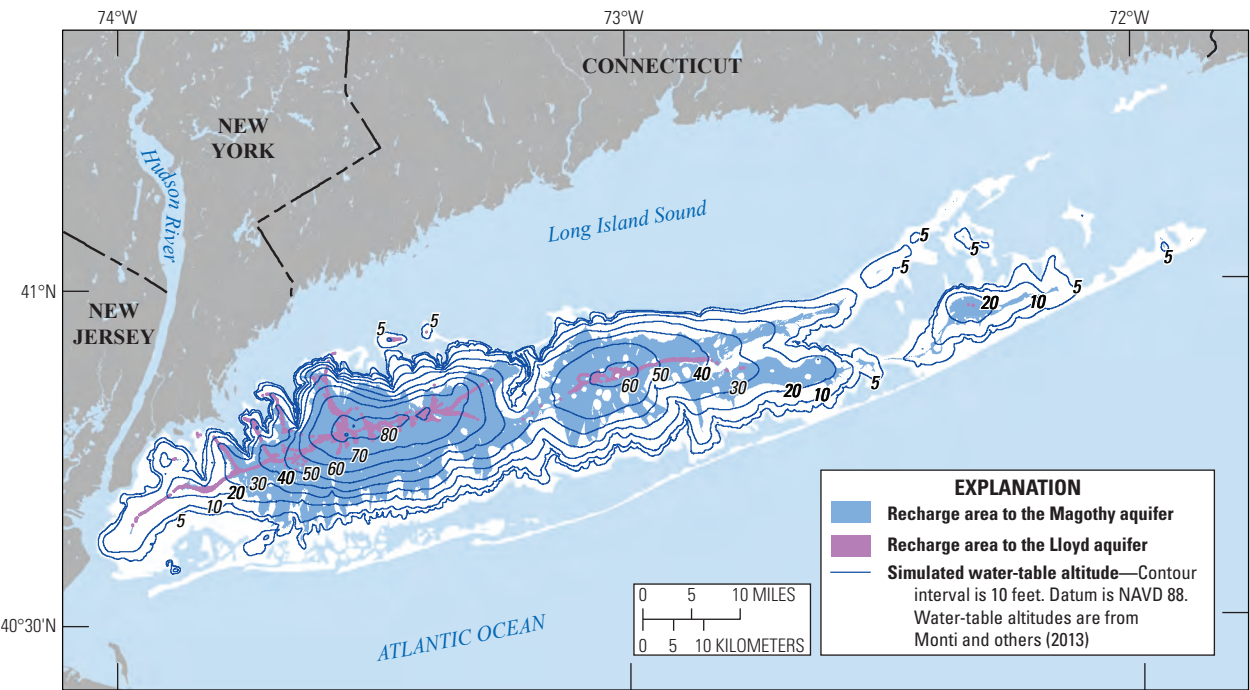
B. **Changes in water-table altitude**
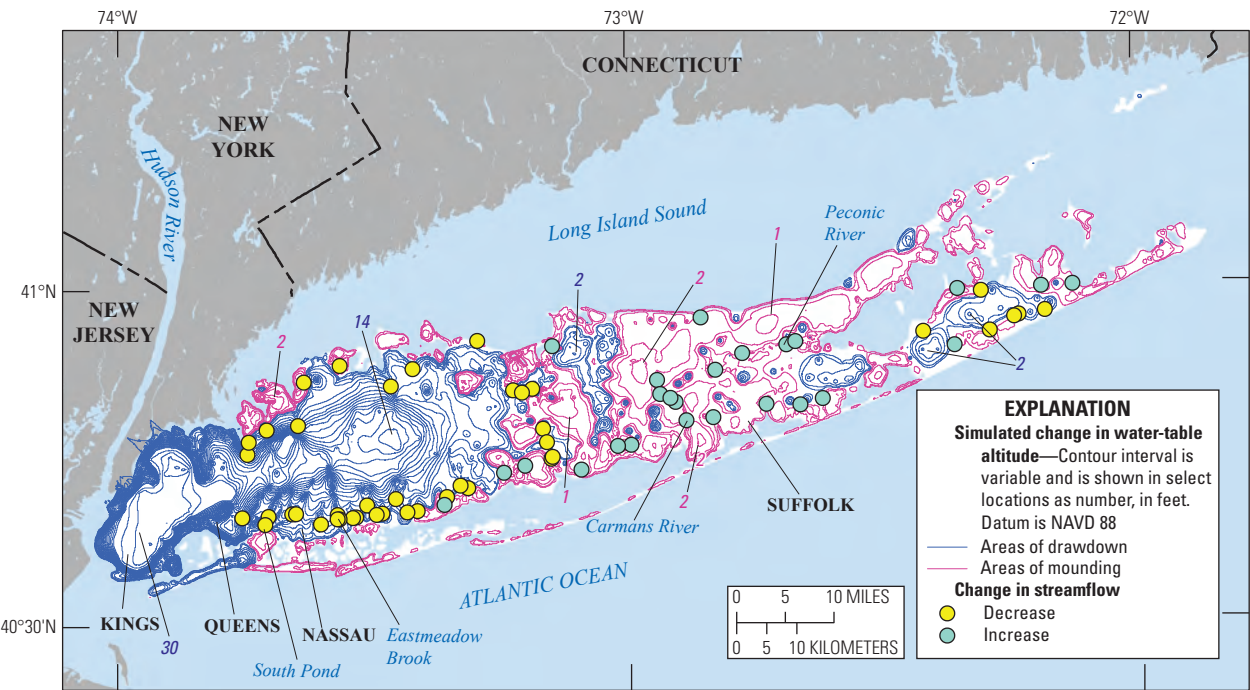
Figure 34. Maps showing *A*, the simulated water table and recharge areas to Cretaceous aquifers for current [2005–15] stresses and *B*, changes in water table altitude resulting from those stresses on Long Island, New York.

generally decreased in response to pumping and recharge stresses (fig. 34B). The largest drawdowns are in New York City (Kings and Queens Counties), where water-table altitudes have decreased by more than 30 ft in response to current stresses. There are few groundwater withdrawals in this area (fig. 18) currently [2019], but the highly urbanized landscape and extensive impervious surfaces have greatly reduced aquifer recharge in Kings and Queens Counties (fig. 12A), resulting in large drawdowns compared with predevelopment conditions.

Large drawdowns also are simulated in Nassau and western Suffolk Counties. Recharge in this area is greater than in Kings and Queens Counties because there are fewer impervious surfaces, and much of the water lost to those surfaces is returned to the aquifer as redirected recharge by sumps and recharge basins. The largest drawdown—about 15 ft—is in eastern Nassau County (fig. 34B). About 297 ft^3/s (or about 57 percent of the total recharge from precipitation) of water currently [2019] is withdrawn from wells for public supply in Nassau County. Most of Nassau and southwestern Suffolk Counties are sewered (fig. 24A); therefore, water pumped from these areas is permanently removed from the aquifer system by way of centralized wastewater treatment facilities with coastal outfalls. This local imbalance between pumping and return flow rates decreases water-table altitudes in these areas.

Water-table altitudes for 2005–15 conditions were higher in northern parts of Nassau County and in central and eastern parts of Suffolk County than they were in areas under predevelopment conditions (fig. 34B). Mounding of greater than 1 ft occurs primarily in central parts of Suffolk County, which generally are characterized by medium- and low-density residential land uses where recharge rates can be larger than rates in undeveloped areas (Yang and others, 2015). In addition, most of this area is unsewered (fig. 24A), and the addition of spatially distributed wastewater return flow may result in elevated water-table altitudes, particularly in unsewered residential areas away from large groundwater withdrawals as is common in central and eastern parts of the island.

The complex interaction between pumping and return flow also affects streamflow (fig. 35), as changes in water-table altitudes alter hydraulic gradients and the amount of groundwater discharge into nearby streams. Total simulated streamflow decreased by about 162 ft^3/s as a result of stresses for 2005–15 (table 2); however, changes in streamflow varied locally throughout the island (fig. 34B). Streamflows generally decreased in western and central parts of the island, corresponding to areas of large groundwater withdrawals and extensive sewering. Simulated decreases in streamflow exceeded 10 ft^3/s for some streams in southwestern Nassau County; the largest simulated decreases were about 15 ft^3/s in South Pond Outlet and East Meadow Brook. Streamflow generally increased in eastern parts of the island where the addition of wastewater return flow and changes in land use increased total recharge rates and resulting water-table altitudes. The largest simulated increases in streamflow were about 4 ft^3/s for the Carmans and Peconic Rivers.

Recharge Areas and Times of Travel to Pumping Wells and Natural Receptors

Recharge to the water table exits the aquifer system as groundwater discharge to streams, wetlands, and coastal waters under natural or predevelopment conditions; under current conditions for 2005–15, additional receptors of groundwater discharge included pumped wells and subterranean infrastructure. The area at the water table that contributed groundwater to these natural and anthropogenic receptors, referred to as the recharge area, is a function of the configuration of the water-table geometry and the hydrologic position of these receptors within the aquifer system (figs. 36A and 37A).
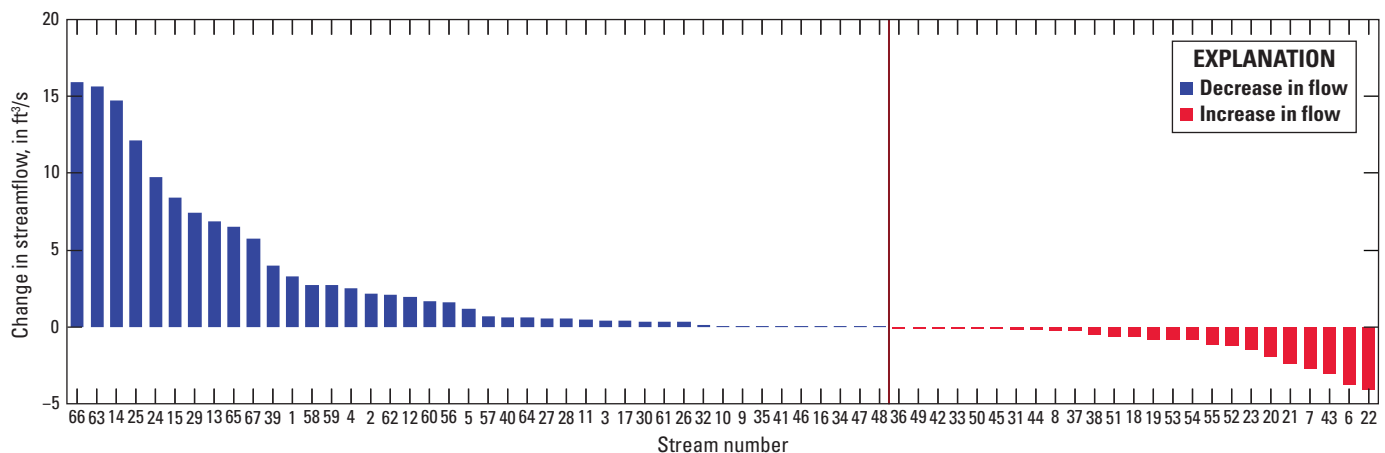
Figure 35. Graph showing change in streamflow resulting from stresses and land use in 2005–15 compared with predevelopment stresses and land use on Long Island, New York. Stream numbers are indicated on figure 28. ft^3/s, cubic foot per second.

A. **Recharge areas**
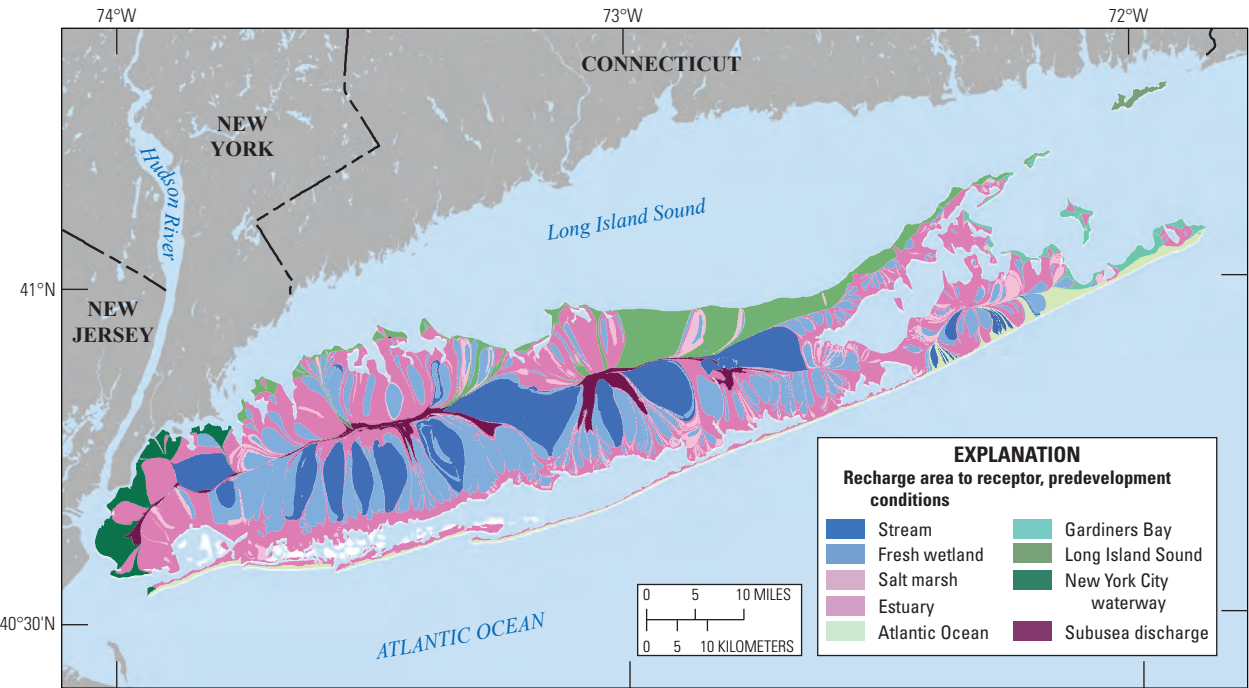
Base map from U.S. Geological Survey National Atlas digital data, scale 1:1,000,000
New York [Long Island] State Plane projection
North American Datum of 1988
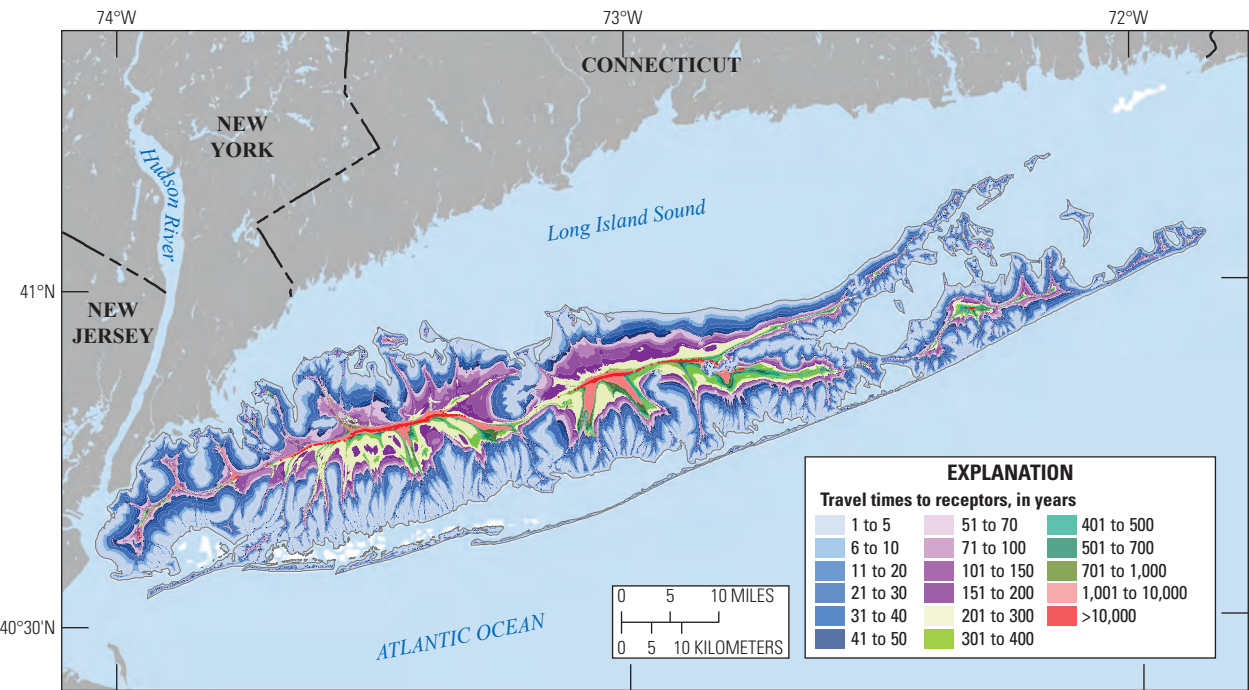
B. **Travel times**

Base map from U.S. Geological Survey National Atlas digital data, scale 1:1,000,000
New York [Long Island] State Plane projection
North American Datum of 1988

Figure 36.   Maps showing *A*, recharge areas and *B*, travel times to hydrologic receptors under predevelopment conditions on Long Island, New York.

A.   **Recharge areas**

Base map from U.S. Geological Survey National Atlas digital data, scale 1:1,000,000
New York [Long Island] State Plane projection
North American Datum of 1988

B.   **Travel times**

Base map from U.S. Geological Survey National Atlas digital data, scale 1:1,000,000
New York [Long Island] State Plane projection
North American Datum of 1988
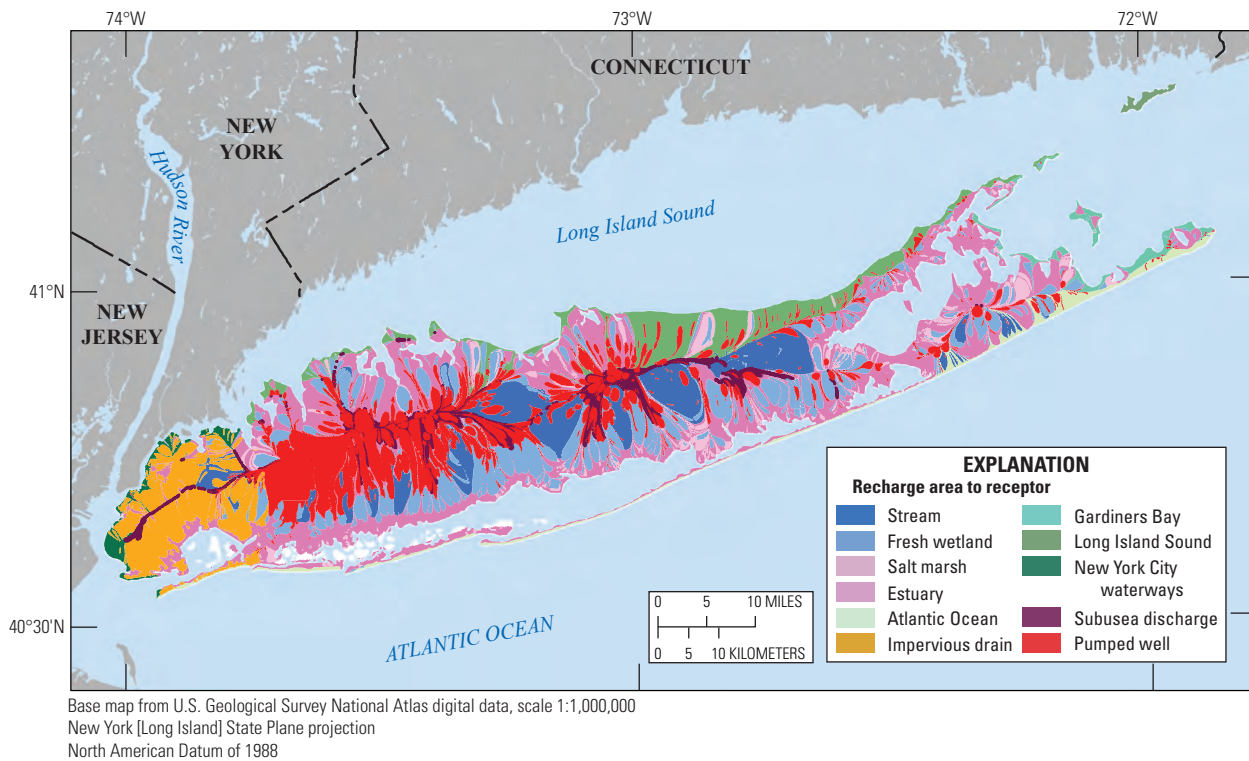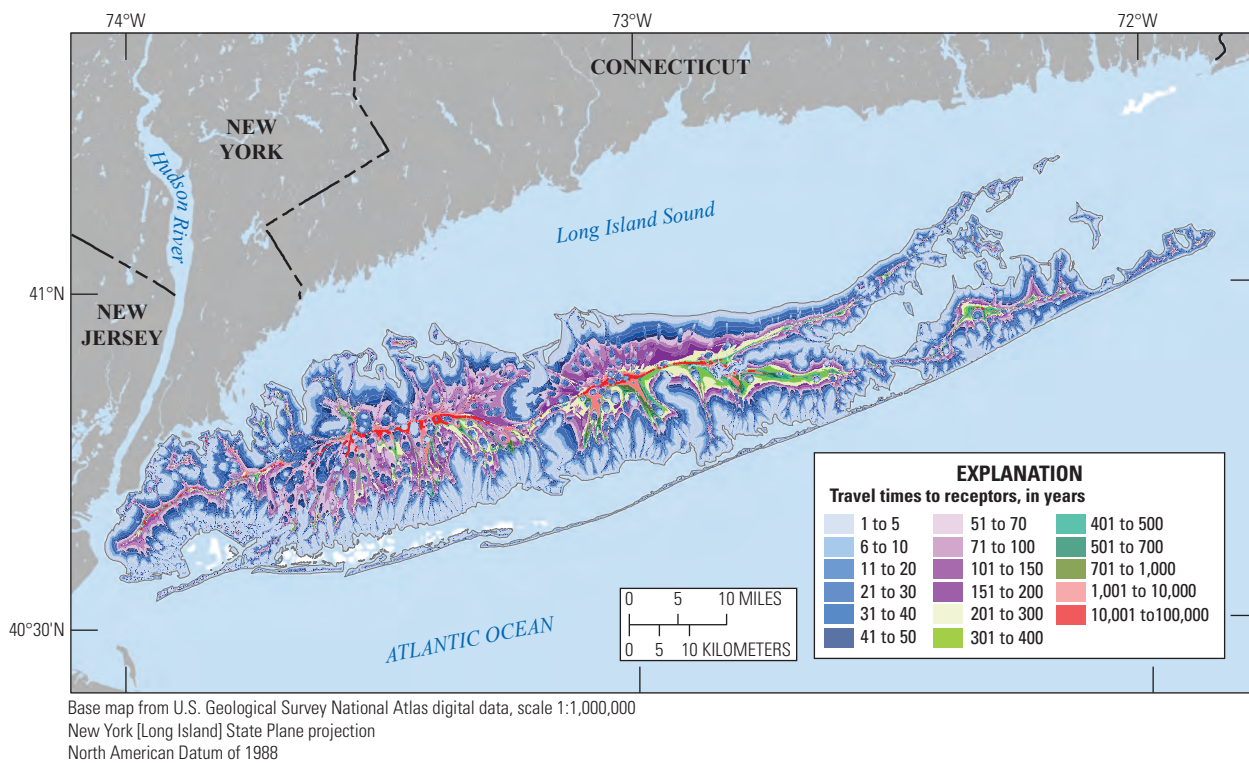
Figure 37.   Map showing *A*, recharge areas and *B*, travel times to hydrologic receptors under current conditions for 2005–15 on Long Island, New York.

Under predevelopment conditions, about 610 mi^2 of the land-surface area above the water table (or 43 percent of the total about 1,400 mi^2 area) contributed groundwater to freshwater streams and wetlands; about 33 percent of the area (466 mi^2) contributed water to estuarine embayments (fig. 38*A*). About 16 percent of the area (220 mi^2) contributed water to open coastal waters, including the Atlantic Ocean, Long Island Sound, Gardiners Bay, and coastal waters surrounding New York City. Only about 2 percent of the area (38 mi^2) discharged from confined aquifers into salty groundwater (subsea discharge). The percentages of recharge areas to all freshwater and saltwater receptors were 43 and 57 percent, respectively, and are like the proportionality of flows to those receptors (table 2).

The elapsed time between water recharging the aquifer system at the water table and discharging to a hydrologic receptor, referred to as travel time, generally is a function of the hydraulic gradient and the length of a flow path between the water table and the terminal receptor. The length of flow paths and, therefore, travel times are a function of hydrologic position as approximated by the relative distance of a given location from groundwater divides and discharge receptors (figs. 36*B* and 37*B*). Simulated groundwater travel times in the Long Island aquifer system range from essentially zero in areas adjacent to receptors to more than 10,000 years in areas near regional groundwater divides (fig. 36*B*).

Median values are used to summarize travel times to receptors because of the potential influence of large travel times on estimated mean values. The smallest travel times under predevelopment conditions generally were for open coastal waters (the Atlantic Ocean. Gardiners Bay, and waters in New York City) where median travel times are less than 10 years (fig. 37*B*). Median travel times to Long Island Sound are larger—about 29 years (fig. 33). Overall, the median travel time to freshwaters receptors—streams and wetlands—is about 18 years. Major streams and wetlands had median travel times of 27 and 15 years, respectively (fig. 37*B*). Median

travel times to inshore estuaries and salt marshes were similar, about 12 and 14 years, respectively. The largest median travel time of about 1,200 years was for subsea discharge from deep, confined aquifers.

Current hydrologic conditions are typified by large withdrawals of groundwater from wells and the interception of recharge by subterranean infrastructure in highly urbanized areas. About 290 mi^2 of the land-surface area above the water table contributes water to pumped wells (fig. 38*A*). This results in smaller recharge areas to natural receptors. The largest decrease in recharge areas resulting from pumping was to freshwater receptors (fig. 37*A*). The land-surface area above the water table contributing recharge to freshwater receptors (streams and wetlands) decreased by about 210 mi^2 (about 35 percent). Recharge areas to inshore estuaries decreased by about 125 mi^2 (or about 26 percent; fig. 38*A*). Recharge from an area of about 110 mi^2 is intercepted by subterranean infrastructure in urbanized areas, as simulated in the model; recharge areas to coastal waters surrounding New York City decreased by about 60 percent.

Current pumping stresses for 2005–15 substantially changed the distribution of travel times, particularly in western and central Long Island (figs. 36*B* and 37*B*). The drawdown of water to pumped wells resulted in isolated and disconnected areas of small travel times to these receptors in interior parts of the island (fig. 37*B*). Median travel times to pumped wells was about 50 years, substantially longer than those to freshwater receptors and coastal waters (fig. 38*B*). Much of the pumping is in deep portions of the aquifer system causing increased vertical hydraulic gradients and the interception of older water that generally resulted in shorter travel times to other receptors. The largest decrease in median travel times was about 11 years for discharge to large streams; travel times to other receptors decreased by about 6 years or less. Travel times to coastal waters in New York City increased slightly (by about 3 years) under hydrologic conditions for 2005–15.

A. **Recharge area**
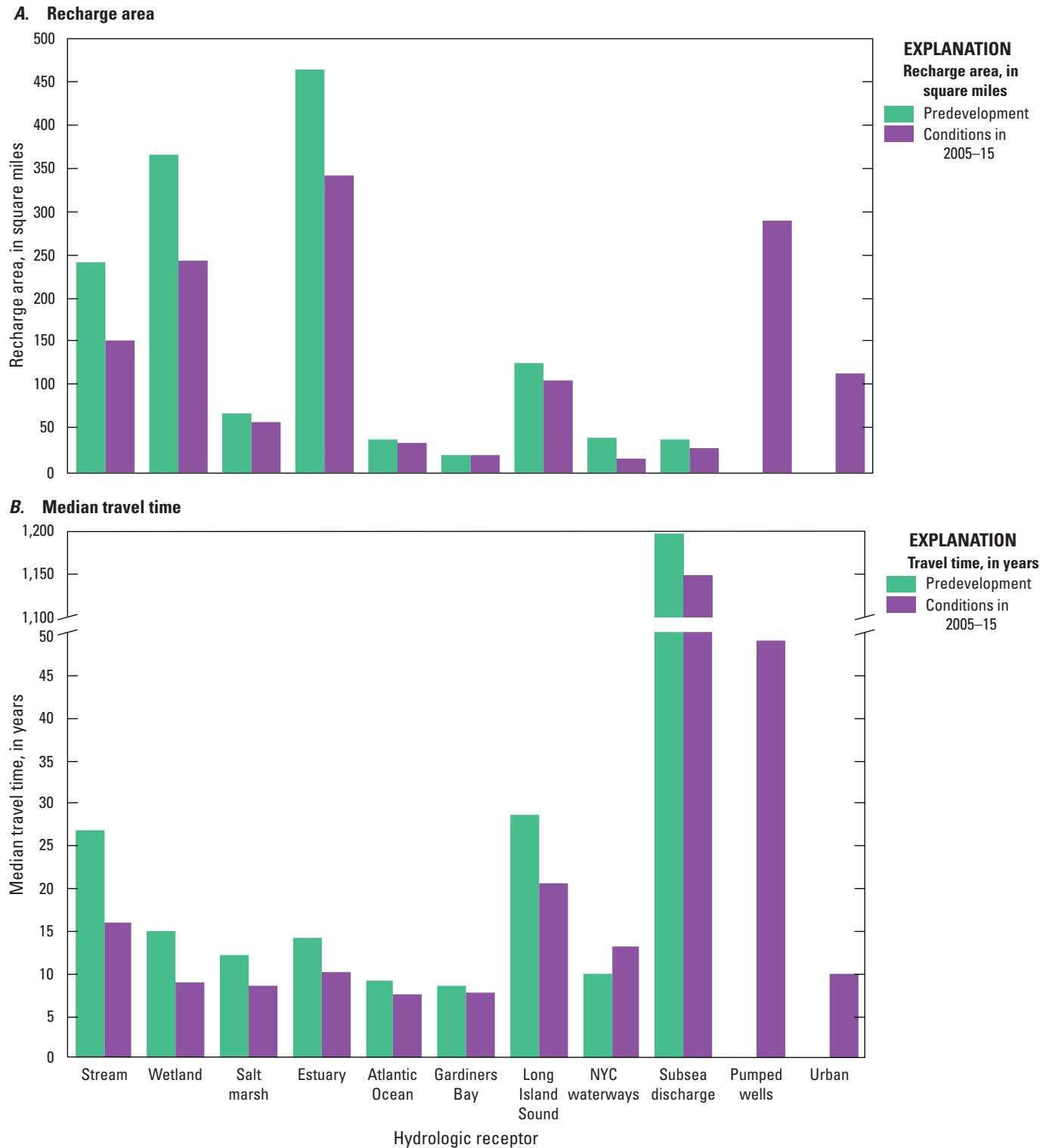

B. **Median travel time**

Figure 38. Graphs showing *A*, areal extents of recharge areas and *B*, median travel times to hydrologic receptors under predevelopment and current conditions on Long Island, New York, for 2005–15.

Limitations of Analysis

The use of numerical models to simulate regional ground-water flow systems such as the Long Island aquifer system has inherent limitations; however, a proper model design to address scale-appropriate questions can help minimize these limitations. Some of the primary limitations of a numerical model include (1) the simplifying assumptions inherent in the conceptual model underlying those numerical models, (2) the assumption of steady-state conditions, (3) model discretization and the representation of hydrologic boundaries, (4) representation of hydraulic stresses and intrinsic aquifer properties, (5) model fit to observed hydrologic conditions, and (6) the accuracy of aquifer properties estimated from model calibration.

The calibration period [2005–15] was assumed to represent average hydrologic conditions. Observed water levels and streamflows during this period generally are similar to long-term average conditions. Average recharge for 2005–15, as estimated using the SWB model, is similar to that estimated since the early 1980s, and estimated total water use is similar to average water use since the early 1990s. Measurements of water levels and streamflows for the calibration period [2005–15] also were similar to measurements over longer-term periods of record. However, the assumption of steady-state conditions could affect estimated recharge areas and travel times because it does not account for the effects of time-varying pumping stresses on advective transport, particularly in interior parts of the island with large historical withdrawals and larger travel times.

The discretization of a model is determined to be the minimum cell size needed to reasonably represent the hydrologic system at a spatial scale appropriate for the analysis, while maintaining a tractable model size given current computational resources. The Long Island regional model has a uniform horizontal discretization of 500 ft on a side and is appropriate for regional-scale analyses, including simulation of water levels, streamflows, recharge areas, and travel times.

This regional model is not appropriate for local-scale analyses in which more detailed information is required, but it can provide boundary conditions for inset models when a finer discretization appropriate for such analyses is needed. The implicit representation of streams and coastal waters as head-dependent flux boundaries is also considered appropriate as these hydrologic features generally are areas of groundwater discharge where the volume of discharge is proportional to hydrologic gradients at those features.

Numerical models ideally are based on independent data that can be adjusted, to an expected degree, during model calibration to achieve a fit within established parameters to observed hydrologic conditions. Aquifer recharge, as represented in the model, was estimated from land use, soil characteristics, and climatological data by use of an SWB model (Misut and others, 2020). The hydraulic conductivities of aquifer sediments in the island's principal aquifers (the upper glacial and Magothy aquifers) were derived from a quasi-three-dimensional lithologic texture model based on a large database of lithology from boreholes and aquifer tests (Walter and Finkelstein, 2020). Although these represent generally reliable initial values for the numerical models, both the modeled estimates and uncertainties associated with those underlying models also could contribute to some uncertainty in model inputs for the Long Island regional model.

These initial values of hydraulic conductivity were adjusted during model calibration using inverse methods; these methods use a Gauss-Newton formulation of the Levenberg-Marquardt nonlinear regression to estimate a set of model inputs that best fit observed hydrologic conditions. The results of a regression are a function of the relative weights of the hydrologic observations, which are subjective and reflect the relative importance of different types of observations to model predictions. Observations of long-term average streamflow were assumed to be better indicators of long-term average hydrologic conditions and were given higher weights than were observations of water levels.

Changing the relative weights of the hydrologic observations will result in a different set of model inputs and could result in different model predictions. Even though the calibrated model has a degree of misfit (or error) that varies spatially, the model produced simulated water levels and streamflows that generally were in good agreement to observed values. The degree of misfit contributes to uncertainty in model predictions; model-prediction uncertainties would be expected to be higher in areas of greater misfit or in areas with fewer weighted observations.

The most reliable initial aquifer properties and weighted water-level observations are within the upper glacial aquifer and within the Magothy and contiguous aquifers, which are the region's principal aquifers and of greatest importance to local stakeholders. Fewer data are available in the underlying Raritan confining unit and Lloyd aquifers. The former is important as a control on deep groundwater flow and the position of the freshwater/saltwater interface in the underlying Lloyd aquifer. Few data are available on the surface altitude, thickness, and hydraulic characteristics of the Raritan confining unit, particularly in the central and eastern parts of Long Island. Representation of the Raritan confining unit in the model is generally based on available information regarding the hydraulic properties, geometry, and extent of the unit. Based on the limited data available, the unit is assumed to be continuous across the island and absent only along the northern shore of the island. The unit also is assumed to consist primarily of clay with a low horizontal and vertical hydraulic conductivity of about 1 and 0.001 ft/d, respectively.

Changing the representation of the Raritan confining unit (thickness, continuity, and hydraulic conductivity) could affect hydrologic predictions, including the degree of confinement and position of the freshwater/saltwater interface in the Lloyd aquifer along the southern shore of the island and the recharge area to the Lloyd aquifer. The current representation of the Raritan confining unit results in a simulated recharge area to the Lloyd aquifer of about 16 mi^2 (or about 1.3 percent of

the total island-wide recharge area). Increasing the horizontal hydraulic conductivity of the Raritan confining unit to 10 ft/d (from 1 ft/d) and vertical hydraulic conductivity to 0.1 ft/d (from 0.001 ft/d) results in a recharge area of about 52 mi^2 (or about 4 percent of the island's recharge area). Further increasing the horizontal and vertical hydraulic conductivity to 30 and 1 ft/d, respectively, consistent with fine-grained silty sand, increases the recharge area to a total of about 60 mi^2 (or about 4.7 percent of the overall recharge area).

This sensitivity analysis suggests that the recharge area to the Lloyd aquifer likely is relatively small—less than 5 percent of the total—over a wide range of possible hydraulic conductivity values. Although this representation of the Raritan confining unit may not affect the extent of the recharge area to the Lloyd aquifer, representation of the unit as discontinuous, particularly in interior parts of the island, could affect the degree of confinement of the Lloyd aquifer and the position of the freshwater/saltwater interface in the Lloyd aquifer along the southern shore.

The regional model represents the freshwater/saltwater interface as a static no-flow boundary that is decoupled from the numerical model solution. The position of the interface in areas where the principal aquifers are unconfined was estimated using water-table altitudes and a saltwater-to-freshwater density ratio of 40:1. Salinities (and densities) likely are lower in some brackish water estuaries; however, a density ratio assumption of 40:1 would overestimate the aquifer thickness, which was considered to be preferable. The interface position in the Lloyd aquifer and in confined parts of the Magothy aquifer and contiguous units was estimated from isochlors determined from borehole and surface geophysical data (Stumm and others, 2020). These data are limited in most areas, and the location of the interface is largely unknown.

Groundwater discharge from confined aquifers was simulated at head-dependent flux boundaries that specify freshwater-equivalent heads computed from mapped geologic surfaces. This implicit, static representation of what in reality is a dynamic interface may result in imbalances between the onshore groundwater flow field, the simulated offshore discharge boundaries, and the specified location of the no-flow interface. This representation of the freshwater/saltwater interface may result in simulated (saltwater) inflow from offshore boundaries in some areas; these inflows are balanced by outflows in other, nearby boundaries, forming localized recirculation patterns of water in adjacent model cells. These recirculation patterns are largely considered numerical artifacts that are virtually nonexistent in the real flow system, they are limited primarily to offshore areas of the Lloyd aquifer in the model and generally are small, less than 1 percent of the hydrologic budget. The implicit representation of the interface does not affect model predictions of hydrologic responses to changing stresses and the resulting recharge areas and travel times. However, this limitation does not allow for the use of this model to explicitly simulate the movement of the interface in response to groundwater withdrawals.

Summary

The hydrologic system underlying Long Island, New York, is a sole-source aquifer system that supplies water to about 2.9 million people. The aquifer system also supports freshwater and marine aquatic ecosystems that are important recreational and economic resources. Anthropogenic activities have affected the quantity and quality of groundwater, owing to Long Island's large population and the generally unconfined conditions prevalent across the aquifer system. Large withdrawals of groundwater and urbanization in the western part of Long Island have resulted in large drawdowns and the intrusion of salty groundwater into the aquifer. Wastewater disposal and agricultural discharge have resulted in a large reservoir of nutrients in the aquifer system and increases in nitrogen loads to ecologically sensitive aquatic ecosystems. Subsurface contamination also emanates from numerous sources associated with industrial sites and adversely affects water supplies.

In 2016, the U.S. Geological Survey (USGS) began a series of hydrologic analyses and the development of a regional-scale numerical model of the Long Island aquifer system. The broad objective of the program was to assess the vulnerability of the Nation's water supply to contamination from anthropogenic and natural compounds. The numerical model was developed to simulate groundwater ages in the aquifer system; groundwater age has been shown to be an important predictor of water-quality characteristics. The model could also be used to evaluate water-quality and water-quantity issues of importance to local stakeholders.

The regional, three-dimensional numerical model of Long Island is a synthesis of a diverse set of data on the physiography, geology, and hydrology of the island. These include data regarding (1) the physiography of Long Island, (2) the regional hydrogeologic framework, (3) the hydraulic properties of aquifers and confining units, (4) the extent of salty groundwater in the aquifer, (5) natural and anthropogenic recharge, (6) groundwater withdrawals, and (7) current hydrologic conditions in the aquifer system. These data compilation and analysis efforts are summarized below:

- The altitude of land surface and seabed bathymetry were estimated from a 1-meter (m; 3.3 foot [ft]) topobathymetric elevation model of coastal areas of the northeastern United States. This seamless mosaic of data was derived from light detection and ranging (lidar), side-scan sonar, and hydrographic surveys. The 1-m data were aggregated and mapped to the numerical model grid to define the top altitudes of the model. The locations of hydrologic boundaries were determined from georeferenced aerial photographs; streambed and seabed altitudes were derived from the 1-m topobathymetric elevation model.

- Surficial geology and hydrogeologic unit surfaces from previous investigations were assembled and used to develop a three-dimensional representation of the Long Island hydrogeologic framework. A total of nine Pleistocene units and four Cretaceous units are included in the framework. The three-dimensional hydrogeologic framework was mapped to the three-dimensional numerical model grid.

- The current extent of freshwater in the aquifer system was determined from mapped isochlors in the Magothy and Lloyd aquifers. These isochlors were determined from borehole and surface geophysical data and combined to determine the seaward extent of freshwater in confined parts of Cretaceous aquifers and contiguous units along the southern shore of the island. A mapped water table from April to May 2010 was used to estimate the approximate altitude of the freshwater/saltwater interface in unconfined parts of the Magothy and upper glacial aquifers using density ratios as defined by the Ghyben-Herzberg ratio. Estimates of the position of the freshwater/saltwater interface were combined and mapped to the three-dimensional model grid to define the extent of the active modeled area.

- Horizontal and vertical hydraulic conductivities were estimated from a new three-dimensional lithologic texture model. This model represents these properties as determined from previous aquifer-tests results and a database of 1,769 boreholes across the island. More than 36,000 lithologic records were categorized and converted to regular point values over the length of each borehole. These data points were interpolated by use of spherical kriging into a set of data rasters that, when combined, produce a quasi-three-dimensional model of hydraulic conductivity. Values from the lithologic texture model were mapped to the numerical model grid; these mapped values were used as initial values of horizontal and vertical hydraulic conductivity that were adjusted during model calibration.

- Recharge to the aquifer for 2005–15 was estimated by use of a soil-water balance (SWB) model. The method uses a modified Thornthwaite-Mather approach in combination with spatial data—land use and impervious surfaces, available soil-water capacity, soil type—and daily precipitation and temperature data to estimate aquifer recharge. Recharge also was estimated for predevelopment conditions and combined with current recharge to estimate the potential recharge lost to impervious surfaces. Anthropogenic recharge from wastewater return flow was estimated from 2010 population data. Potential recharge from leaky infrastructure was estimated from road lengths within each model cell and distributed county-scale water use. Estimates of these recharge components were mapped to the model grid and adjusted during model calibration.

- Groundwater withdrawals were compiled for 1900–2015 from a variety of sources. Withdrawals from 1,680 wells for 2005–15, which defines current conditions in this analysis, were compiled and mapped to the model grid to define pumping stresses in the model.

- Current hydrologic conditions—water levels and streamflows—were assembled from the USGS National Water Information System database. A total of 24,964 water levels and 65,471 streamflow measurements were compiled and grouped by numbers of observations and periods of record to identify those suitable for representing average conditions for 2005–15. A total of 290 wells and 67 streamflow sites were included in the analysis.

These data were synthesized into a numerical groundwater flow model of the Long Island aquifer system. The model is a steady-state simulation and consists of 25 layers, 348 rows, and 1,309 columns with a uniform horizontal discretization of 500 feet (ft). The simulation period chosen was 2005–15, and the model represents average hydrologic conditions during this period. Initial model inputs were derived from the assembled data. Recharge, hydraulic conductivity, and boundary leakances were adjusted during model calibration using inverse methods followed by postcalibration conditioning. Development and calibration of the numerical model are summarized below.

- The model uses the USGS finite-difference MODFLOW–NWT model. Model layering is based on a three-dimensional hydrogeologic framework developed from mapped surficial geology and hydrogeologic-unit surfaces. The Magothy and upper glacial aquifers—Long Island's principal aquifers—are subdivided to ensure adequate vertical discretization for the hydrologic analyses. Layer thicknesses are variable, but do not exceed 60 ft in the Magothy aquifer. Fresh and salty surface waters are represented as head-dependent flux boundaries. Hydraulic stresses include natural and anthropogenic recharge and pumping and are represented as distributed and point specified flux boundaries, respectively.

- Initial values of recharge and hydraulic conductivity were derived from the SWB model and texture models; both were represented as parameters and varied during calibration. The recharge values as estimated from the SWB model were used as multipliers to which a global parameter was multiplied, allowing total recharge to the system to vary while maintaining the spatial variability as determined from the SWB model. Anthropogenic components of recharge—wastewater return flow, leaky infrastructure, and artificial recharge through recharge basins—also are represented as adjustable multipliers.

- Initial values of horizontal and vertical hydraulic conductivity were derived from the lithologic texture model and were used as a three-dimensional array of base values. Sets of pilot-point parameters within each hydrogeologic unit were used to estimate a three-dimensional array of multipliers that, when multiplied by the array of base values, produced the hydraulic conductivity fields used for input into the model.

- The model was calibrated using highly parameterized, inverse methods, as implemented in the calibration software PEST. Inverse calibration methods determine the model parameters that best fit a given set of observations using an iterative form of a Levenberg-Marquardt formulation of a Gauss-Newton nonlinear regression to minimize an objective function. Regularization was implemented to avoid overfit to observations and to ensure reasonable adherence to prior hydrogeologic knowledge, as represented by initial conditions estimated from the SWB and texture models.

- The inverse calibration reduced misfit in the model and produced a set of model inputs that reasonably matched observations of long-term average water levels and streamflows. Postcalibration conditioning was used to ensure that all model inputs were within a range considered reasonable and to improve local areas of model misfit. The calibration process decreased absolute mean residuals for highly weighted water levels from an initial value of 5.32 ft to 2.68 ft. The initial and calibrated absolute mean residuals for streamflows were 4.41 and 1.30 ft^3/s, (cubic feet per second) respectively.

Predevelopment conditions and current stresses for 2005–15 were simulated to evaluate the effects of pumping, return flow, and changes in land use and impervious surfaces on hydrologic conditions in the aquifer system. Changes in these stresses affect water-table altitudes, streamflows, and recharge areas and travel times to receptors.

- About 2,590 ft^3/s of water recharged the aquifer system under simulated predevelopment conditions, as simulated. Most—about 56 percent—discharged into coastal waters, and about 39 percent discharged into freshwater streams. The remaining 5 percent of recharge ultimately discharged from confined aquifers into salty groundwater (as subsea discharge). Water-table altitudes under predevelopment conditions exceeded 90 ft in western Long Island; the configuration of the water table is a function of coastal geometry and surface-water drainages. A regional groundwater divide trends east-west across the main part of the island and bifurcates onto the North and South Forks on the eastern part of Long Island. Recharge to Cretaceous-age aquifers is in the central part of the island. Recharge to the deepest aquifer—the Lloyd aquifer—is generally in a narrow band along the regional groundwater divide.

- About 656 ft^3/s of water was withdrawn from 2005 to 2015 for water supply, and about 349 ft^3/s of water recharged the aquifer from return flow and leaky infrastructure. Parts of New York City have large drawdowns, resulting in water-table altitudes that are as much as 25 ft lower in some areas, primarily as a result of urbanization and associated large decreases in recharge rates. Drawdowns over large areas in the Nassau and western Suffolk Counties have resulted in water tables lowered by more than 10 ft, mostly from large groundwater withdrawals and sewering; sewering largely eliminates recharge from wastewater return flow. Water-table altitudes in eastern parts of the island increased by more than 2 ft in some areas as a result of wastewater return flow in unsewered areas and changes in land use; changes in streamflows show a similar pattern. Streamflow generally decreased in western parts of the island where there were large drawdowns and increased in eastern parts of the island where water-table altitudes increased.

- Recharge areas to major receptors generally reflected the proportionality of those receptors. About 43 and 57 percent of the land-surface area above the water table, respectively, contributes water to freshwater and saltwater receptors. The median travel time to all receptors is about 16 years. Median travel times to individual receptor types, as delineated in these analyses, range from about 8 years for Gardiners Bay to about 28 years for Long Island Sound. Groundwater withdrawals change the recharge areas at the water table that contribute water to receptors and the travel times to those receptors. Most pumping was in the interior parts of the island; about 20 percent of the water table contributed water to wells. The recharge areas at the water table that contributed water to other receptors decreased as a result; the largest decrease in recharge areas was for freshwater streams and wetlands.

- Groundwater withdrawals in interior parts of the island generally captured old water from deep parts of the aquifer; median travel times to wells is about 50 years, more than that for natural freshwater and saltwater receptors. Median travel times to these other receptors decreased as a result of pumping. The median travel time to large streams decreased by about 11 years.

Selected References

Arihood, L.D., 2008, Processing, analysis, and general evaluation of well-driller logs for estimating hydrogeologic parameters of the glacial sediments in a ground-water flow model of the Lake Michigan basin: U.S. Geological Survey Scientific Investigations Report 2008–5184, 26 p. [Also available at https://doi.org/10.3133/sir20085184.]

Barlow, P.M., 1989, Determination of aquifer properties from a thermal tracer experiment—Eos, American Geophysical Union: Transactions, v. 70, no. 15, p. 137.

Barlow, P.M., and Hess, K.M., 1993, Simulated hydrologic responses of the Quashnet River stream-aquifer system to proposed ground-water withdrawals: U.S. Geological Survey Water-Resources Investigations Report 93–4064, 52 p. [Also available at https://doi.org/10.3133/wri934064.]

Buxton, H.T., and Shernoff, P.K., 1999, Ground-water resources of Kings and Queens Counties, Long Island, New York: U.S. Geological Survey Water-Supply Paper 2498, 113 p., 7 pls. [Also available at https://doi.org/10.3133/wsp2498.]

Buxton, H.T., and Smolensky, D.A., 1999, Simulation analysis of the development of the ground-water flow system of Long Island, New York: U.S. Geological Survey Water-Resources Investigations Report 98–4069, 57 p. [Also available at https://doi.org/10.3133/wri984069.]

Cadwell, D.H., 1989, Surficial geologic map of New York—Lower Hudson sheet: New York State Museum Map and Chart Series 40, 1 sheet, scale 1:250,000. [Also available at http://www.nysm.nysed.gov/research-collections/geology/gis.]

Cadwell, D.H., and Muller, E.H., 1986, Surficial geologic map of New York: New York Museum data, accessed August 4, 2019, at http://www.nysm.nysed.gov/research-collections/geology/gis.

Charles, E.G., 2016, Regional chloride distribution in the Northern Atlantic Coastal Plain aquifer system from Long Island, New York, to North Carolina: U.S. Geological Survey Scientific Investigations Report 2016–5034, 37 p., apps., accessed June 15, 2020, at https://doi.org/10.3133/sir20165034.

Como, M.D., Zuck, M.A., and Stumm, F., 2020, Time domain electromagnetic surveys collected to estimate the extent of saltwater intrusion in Nassau and Queens County, New York, October–November 2017: U.S. Geological Survey data release, https://doi.org/10.5066/P90B6OTX.

Danielson, J.J., and Haines, J., 2017, Hurricane Sandy region—Topobathymetric elevation model of New England: U.S. Geological Survey web page, accessed October 5, 2019, at https://www.usgs.gov/land-resources/eros/coned/science/topobathymetric-elevation-models.

Doherty, J., 2003, Ground water model calibration using pilot points and regularization: Ground Water, v. 41, no. 2, p. 170–177. [Also available at https://doi.org/10.1111/j.1745-6584.2003.tb02580.x.]

Doherty, J., 2010, PEST—Model independent parameter estimation—User documentation: Watermark Numerical Computation website, accessed 2015 at http://www.pesthomepage.org/.

Doherty, J.E., and Hunt, R.J., 2010, Approaches to highly parameterized inversion—A guide to using PEST for groundwater-model calibration: U.S. Geological Survey Scientific Investigations Report 2010–5169, 59 p. [Also available at https://doi.org/10.3133/sir20105169.]

Doherty, J., and Welter, D., 2010, A short exploration of structural noise: Water Resources Research, v. 46, no. 5, W05525, 14 p. [Also available at https://doi.org/10.1029/2009WR008377.]

Doriski, T.P., and Wilde-Katz, F., 1982, Geology of the "20-foot" clay and Gardiners clay in southern Nassau and southwestern Suffolk counties, Long Island, New York: U.S. Geological Survey Water-Resources Investigations Report 82–4056, 21 p. [Also available at https://doi.org/10.3133/wri824056.]

Farnsworth, R.K., Thompson, E.S., and Peck, E.L., 1982, Evaporation atlas for the contiguous 48 United States: National Oceanic and Atmospheric Administration Technical Report NWS 33, 26 p. [Also available at https://www.nws.noaa.gov/oh/hdsc/Technical_reports/TR33.pdf.]

Faunt, C.C., Belitz, K., and Hanson, R.T., 2010, Development of a three-dimensional model of sedimentary texture in valley-fill deposits of Central Valley, California, USA: Hydrogeology Journal, v. 18, no. 3, p. 625–649. [Also available at https://doi.org/10.1007/s10040-009-0539-7.]

Fienen, M.N., 2013, We speak for the data: Ground Water, v. 51, no. 2, p. 157. [Also available at https://doi.org/10.1111/gwat.12018.]

Fienen, M.N., Masterson, J.P., Plant, N.G., Gutierrez, B.T., and Thieler, R.E., 2013, Bridging groundwater models and decision support with a Bayesian network: Ground Water, v. 49, no. 10, p. 6459–6473. [Also available at https://doi.org/10.1002/wrcr.20496.]

Finkelstein, J.S., and Walter, D.A., 2020, Aquifer texture data describing the Long Island aquifer system: U.S. Geological Survey data release, https://doi.org/10.5066/P954DLLC.

Franke, O.L., and Cohen, P., 1972, Regional rates of ground-water movement on Long Island, New York, *in* Geological survey research 1972: U.S. Geological Survey Professional Paper 800–C, p. C271–277. [Also available at https://doi.org/10.3133/pp800C.]

Franke, O.L., and Getzen, R.T., 1976, Evaluation of hydrologic properties of the Long Island ground-water reservoir using cross-sectional analog models: U.S. Geological Survey Open-File Report 75–679, 80 p. [Also available at https://doi.org/10.3133/ofr75679.]

Fuller, M.L., 1914, The geology of Long Island: U.S. Geological Survey Professional Paper 82, 233 p. [Also available at https://doi.org/10.3133/pp82.]

Garabedian, S.P., Gelhar, L.W., and Celia, M.A., 1988, Large-scale dispersive transport in aquifers—Field experiments and reactive transport theory: Cambridge, Massachusetts Institute of Technology Department of Civil Engineering, Ralph M. Parsons Laboratory Report 315, 291 p. [Also available at https://www.nrc.gov/docs/ML0331/ML033160542.pdf.]

Guswa, J.H., and LeBlanc, D.R., 1985, Digital flow models of ground-water flow in the Cape Cod aquifer system, Massachusetts: U.S. Geological Survey Water-Supply Paper 2209, 112 p. [Also available at https://doi.org/10.3133/wsp2209.]

Guswa, J.H., and Londquist, C.J., 1976, Potential for development of ground water at a test site near Truro, Massachusetts: U.S. Geological Survey Open-File Report 76–614, 38 p. [Also available at https://doi.org/10.3133/ofr76614.]

Harbaugh, A.W., 2005, MODFLOW–2005, the U.S. Geological Survey modular ground-water model; the ground-water flow process: U.S. Geological Survey Techniques and Methods, book 6, chap. A16, 253 p. [Also available at https://doi.org/10.3133/tm6A16.]

Konikow, L.F., and Reilly, T.E., 1998, Groundwater modeling, chap. 20 *of* Delleur, J.W., ed., The handbook of groundwater engineering: Boca Raton, Fla., CRC Press, p. 20–1—20–40. [Also available at https://doi.org/10.1201/9781420048582.ch20.]

Kontis, A.L., 1999, Simulation of freshwater-saltwater interfaces in the Brooklyn-Queens aquifer system: U.S. Geological Survey Water-Resources Investigations Report 98–4067, 26 p. [Also available at https://doi.org/10.3133/wri984067.]

Krulikas, R.K., and Koszalka, E.J., 1982, Geologic reconnaissance of an extensive clay unit in north-central Suffolk County, Long Island, New York: U.S. Geological Survey Water-Resources Investigations Report 82–4075, 9 p., 1 pl. [Also available at https://doi.org/10.3133/wri824075.]

LeBlanc, D.R., Guswa, J.H., Frimpter, M.H., and Londquist, C.J., 1986, Ground-water resources of Cape Cod, Massachusetts: U.S. Geological Survey Hydrologic Atlas 692, 4 pls. [Also available at https://doi.org/10.3133/ha692.]

Levenberg, K., 1944, A method for the solution of certain non-linear problems in least squares: Quarterly of Applied Mathematics, v. 2, no. 2, p. 164–168. [Also available at https://doi.org/10.1090/qam/10666.]

Lindner, J.B., and Reilly, T.E., 1983, Analysis of three tests of the unconfined aquifer in southern Nassau County, Long Island, New York: U.S. Geological Survey Water-Resources Investigations Report 82–4021, 52 p. [Also available at https://doi.org/10.3133/wri824021.]

Marquardt, D.W., 1963, An algorithm for least squares estimation of nonlinear parameters: Journal of the Society for Industrial and Applied Mathematics, v. 11, no. 2, p. 431–441. [Also available at https://doi.org/10.1137/0111030.]

Masterson, J.P., and Barlow, P.M., 1997, Effects of simulated ground-water pumping and recharge on ground-water flow in Cape Cod, Martha's Vineyard, and Nantucket Island basins, Massachusetts: U.S. Geological Survey Water-Supply Paper 2447, 78 p., 1 pl. [Also available at https://doi.org/10.3133/wsp2447.]

Masterson, J.P., Pope, J.P., Fienen, M.N., Monti, J., Jr., Nardi, M.R., and Finkelstein, J.S., 2016, Assessment of groundwater availability in the Northern Atlantic Coastal Plain aquifer system from Long Island, New York, to North Carolina: U.S. Geological Survey Professional Paper 1829, 76 p., accessed June 15, 2020, at https://doi.org/10.3133/pp1829.

Masterson, J.P., Walter, D.A., and Savoie, J., 1998, Use of particle-tracking to improve numerical model calibration and to analyze ground-water flow and contaminant migration, Massachusetts Military Reservation, western Cape Cod, Massachusetts: U.S. Geological Survey Water-Supply Paper 2482, 50 p. [Also available at https://doi.org/10.3133/wsp2482.]

McClymonds, N.E., and Franke, O.L., 1972, Water-transmitting properties of aquifers on Long Island, N.Y: U.S. Geological Survey Professional Paper 627–E, 24 p. [Also available at https://doi.org/10.3133/pp627E.]

McDonald, M.G., and Harbaugh, A.W., 1988, A modular three-dimensional finite-difference groundwater flow model: U.S. Geological Survey Techniques of Water-Resources Investigations, book 6, chap. A1, 586 p. [Also available at https://doi.org/10.3133/twri06A1.]

Misut, P.E., and Monti, J., Jr., 1999, Simulation of ground-water flow and pumpage in Kings and Queens Counties, Long Island, New York: U.S. Geological Survey Water-Resources Investigations Report 98–4071, 50 p. [Also available at https://doi.org/10.3133/wri984071.]

Misut, P.E., Schubert, C.E., Bova, R.G., and Colabufo, S.R., 2004, Simulated effects of pumping and drought on ground-water levels and the freshwater-saltwater interface on the north fork of Long Island, New York: U.S. Geological Survey Water-Resources Investigations Report 2003–4184, 58 p. [Also available at https://doi.org/10.3133/wri20034184.]

Misut, P.E., Walter, D.A., Schubert, C.E., and Dressler, S., 2020, Analysis of remedial scenarios affecting plume movement through a sole-source aquifer system in southeastern Nassau County, New York: U.S. Geological Survey Scientific Investigations Report 2020–5090, https://doi.org/10.3133/sir20205090.

Moench, A.F., LeBlanc, D.R., and Garabedian, S.P., 1996, Preliminary type-curve analysis of a pump test in an unconfined sand and gravel aquifer, Cape Cod, Massachusetts, *in* Morganwalp, D.W., and Aronson, D.A., 1994, U.S. Geological Survey Toxic Substances Hydrology Program—Proceedings of the technical meeting, Colorado Springs, Colorado, September 20–24, 1993: U.S. Geological Survey Water-Resources Investigations Report 94–4015, p. 273–281. [Also available at https://doi.org/10.3133/wri944015.]

Monti, J., Jr., Como, M.D., and Busciolano, R.J., 2013, Water-table and potentiometric surface altitudes in the upper glacial, Magothy, and Lloyd aquifers beneath Long Island, New York, April–May 2010: U.S. Geological Survey Scientific Investigations Map 3270, 5 pls. [Also available at https://doi.org/10.3133/sim3270.]

Monti, J., Jr., Misut, P.E., and Busciolano, R.J., 2009, Simulation of variable-density ground-water flow and saltwater intrusion beneath Manhasset Neck, Nassau County, New York, 1905–2005: U.S. Geological Survey Scientific Investigations Report 2008–5166, 69 p. [Also available at https://doi.org/10.3133/sir20085166.]

National Historical Geographic Information System, [undated] a, Source of water, 1990, table NH23 *of* STF3 dataset: National Historical Information System database, accessed June 8, 2011, at https://data2.nhgis.org/main. [Filter for dataset 1990_STF3 and Water, Plumbing, and Sewage in the Resources and Amenities category under Housing.]

National Historical Geographic Information System, [undated] b, Total persons, 1990, table NP1 *of* STF1 dataset: National Historical Information System database, accessed June 8, 2011, at https://data2.nhgis.org/main. [Filter for dataset 1990_STF1.]

New York State Department of Environmental Conservation, 2020, Water withdrawals by facility—Beginning 2009: New York State Department of Environmental Conservation data, accessed June 15, 2020, at https://data.ny.gov/Energy-Environment/Water-Withdrawals-by-Facility-Beginning-2009/94ue-tysy.

Niswonger, R.G., Panday, S., and Ibaraki, M., 2011, MODFLOW–NWT, a Newton formulation for MODFLOW–2005: U.S. Geological Survey Techniques and Methods, book 6, chap. A37, 44 p., accessed June 15, 2020, at https://doi.org/10.3133/tm6A37.

Oliver, M.A., and Webster, R., 1990, Kriging—A method of interpolation for geographical information systems: International Journal of Geographical Information Systems, v. 4, no. 3, p. 313–332. [Also available at https://doi.org/10.1080/02693799008941549.]

Pollock, D.W., 2012, User guide for MODPATH version 6—A particle-tracking model for MODFLOW: U.S. Geological Survey Techniques and Methods, book 6, chap. A41, 58 p., accessed June 15, 2020, at https://doi.org/10.3133/tm6A41.

Prince, K.R., and Schneider, B.J., 1989, Estimation of hydraulic characteristics of the upper glacial and Magothy aquifers at East Meadow, New York, by use of aquifer tests: U.S. Geological Survey Water-Resources Investigations Report 87–4211, 43 p. [Also available at https://doi.org/10.3133/wri874211.]

Reilly, T.E., 2001, System and boundary conceptualization in ground-water flow simulation: U.S. Geological Survey Techniques of Water-Resources Investigations, book 3, chap. B8, 29 p. [Also available at https://doi.org/10.3133/twri03B8.]

Reilly, T.E., Buxton, H.T., Franke, O.L., and Wait, R.L., 1983, Effects of sanitary sewers on ground-water levels and streams in Nassau and Suffolk Counties, New York, Part 1; Geohydrology, modeling strategy, and regional evaluation: U.S. Geological Survey Water-Resources Investigations Report 82–4045, 45 p. [Also available at https://doi.org/10.3133/wri824045.]

Schubert, C.E., Bova, R.G., and Misut, P.E., 2004, Hydrogeologic framework of the North Fork and surrounding areas, Long Island, New York: U.S. Geological Survey Water-Resources Investigations Report 02–4284, 24 p., 4 pls., scale 1:120,000. [Also available at https://doi.org/10.3133/wri024284.]

Shaffer, K.H., and Runkle, D.L., 2007, Consumptive water-use coefficients for the Great Lakes basin and climatically similar areas: U.S. Geological Survey Scientific Investigations Report 2007–5197, 191 p., accessed June 15, 2020, at https://doi.org/10.3133/sir20075197.

Smolensky, D.A., Buxton, H.T., and Shernoff, P.K., 1989, Hydrogeologic framework of Long Island, New York: U.S. Geological Survey Hydrologic Atlas 709, 3 sheets. [Also available at https://doi.org/10.3133/ha709.]

Stumm, F., 2001, Hydrogeology and extent of saltwater intrusion of the Great Neck peninsula, Great Neck, Long Island, New York: U.S. Geological Survey Water-Resources Investigations Report 99–4280, 41 p. [Also available at https://doi.org/10.3133/wri994280.]

Stumm, F., and Como, M.D., 2017, Delineation of salt water intrusion through use of electromagnetic-induction logging—A case study in southern Manhattan Island: Water (Basel), v. 9, no. 9, p. 631. [Also available at https://doi.org/10.3390/w9090631.]

Stumm, F., Como, M.D., and Zuck, M.A., 2020, Use of time domain electromagnetic soundings and borehole elec-tromagnetic induction logs to delineate the freshwater/saltwater interface on southwestern Long Island, New York, 2015–17: U.S. Geological Survey Open-File Report 2020–1093, https://doi.org/10.3133/ofr20201093.

Stumm, F., Lange, A.D., and Candela, J.L., 2002, Hydrogeology and extent of saltwater intru-sion on Manhasset Neck, Nassau County, New York: U.S. Geological Survey Water-Resources Investigations Report 00–4193, 42 p. [Also available at https://doi.org/10.3133/wri004193.]

Stumm, F., Lange, A.D., and Candela, J.L., 2004, Hydrogeology and extent of saltwater intrusion in the northern part of the town of Oyster Bay, Nassau County, New York: U.S. Geological Survey Water-Resources Investigations Report 03–4288, 55 p. [Also available at https://doi.org/10.3133/wri034288.]

Terraciano, S.A., 1996, Position of the freshwater/saltwater interface in southeastern Queens and southwestern Nassau counties, Long Island, New York, 1987–88: U.S. Geological Survey Open-File Report 96–456, 17 p. [Also available at https://doi.org/10.3133/ofr96456.]

Thornthwaite, C.W., and Mather, J.R., 1957, Instructions and tables for computing potential evapotranspiration and the water balance: Centerton, N.J., Drexel Institute of Technology Laboratory of Climatology, 129 p.

Tonkin, M.J., and Doherty, J., 2005, A hybrid regularized inversion methodology for highly parameter-ized environmental models: Water Resources Research, v. 41, no. 10, W10412, 16 p., accessed January 23, 2019, at https://doi.org/10.1029/2005WR003995.

U.S. Census Bureau, 2018, QuickFacts, United States: U.S. Census Bureau data, accessed October 9, 2018, at https://www.census.gov/quickfacts.

U.S. Geological Survey, 2004, User's manual for the National Water Information System of the U.S. Geological Survey Ground-Water Site Inventory System: U.S. Geological Survey Open-File Report 2004–1238, 262 p., accessed January 23, 2018, at https://doi.org/10.3133/ofr20041238.

U.S. Geological Survey, 2018, USGS water data for the nation: U.S. Geological Survey data release, accessed June 13, 2018, at https://doi.org/10.5066/F7P55KJN.

U.S. Geological Survey, 2020, US topo—Maps for America: U.S. Geological Survey National Geospatial Program web site, accessed May 7, 2020, at https://www.usgs.gov/core-science-systems/national-geospatial-program/us-topo-maps-america.

Walter, D.A., and Finkelstein, J.S., 2020, Distribution of selected hydrogeologic characteristics of the upper glacial and Magothy aquifer, Long Island, New York: U.S. Geological Survey Scientific Investigations Report 2020–5023, 21 p., accessed September 9, 2020, at https://doi.org/10.3133/sir20205023.

Walter, D.A., Masterson, J.P., and Barlow, P.M., 1996, Hydrogeology and analysis of ground-water-flow system, Sagamore marsh area, southeastern Massachusetts: U.S. Geological Survey Water-Resources Investigations Report 96–4200, 41 p. [Also available at https://doi.org/10.3133/wri964200.]

Walter, D.A., McCobb, T.D., and Fienen, M.N., 2018, Use of a numerical model to simulate the hydrologic system and transport of contaminants near Joint Base Cape Cod, western Cape Cod, Massachusetts: U.S. Geological Survey Scientific Investigations Report 2018–5139, 98 p., accessed June 14, 2019, at https://doi.org/10.3133/sir20185139.

Walter, D.A., Masterson, J.P., Finkelstein, J.S., Monti, J., Jr., Misut, P.E., and Fienen, M.N., 2020, MODFLOW–NWT and MODPATH6 used to simulate groundwater flow in the regional aquifer system on Long Island, New York, for pumping and recharge conditions in 2005–15: U.S. Geological Survey data release, https://doi.org/10.5066/P9KWQSEJ.

Westenbroek, S.M., Kelson, V.A., Dripps, W.R., Hunt, R.J., and Bradbury, K.R., 2010, SWB—A modified Thornthwaite-Mather soil-water-balance code for esti-mating groundwater recharge [revised March 14, 2012]: U.S. Geological Survey Techniques and Methods, book 6, chap. A31, 60 p., accessed March 11, 2013, at https://doi.org/10.3133/tm6A31.

Yang, Q., Tian, H., Li, X., Tao, B., Ren, W., Chen, G., Lu, C., Yang, J., Pan, S., Banger, K., and Zhang, B., 2015, Spatiotemporal patters of evapotranspiration along the North American east coast as influenced by multiple envi-ronmental changes: Ecohydrology, v. 8, no. 4, p. 714–725, accessed January 23, 2019, at https://doi.org/10.1002/eco.1538.